SYNCHRONIZATION OF ULTRASOUND IMAGING WITH HEMODYNAMIC WAVEFORMS

- Master's Thesis -

Femke Dieneke Bosman

Student number : 5658012

15th August 2025

Thesis in partial fulfilment of the requirements for the joint degree of Master of Science in

Technical Medicine

Leiden University ; Delft University of Technology ; Erasmus University Rotterdam

Master thesis project (TM30004 ; 35 ECTS)

Dept. of Intensive Care & Anesthesiology,
Catharina Hospital Eindhoven
10th February 2025 – 15th August 2025

Supervisor(s):

Dr. A.J.R. (Ashley) de Bie Dekker
ir. I.W.F. (Igor) Paulussen
Prof. dr. R. A. (Arthur) Bouwman
Prof. dr. D.J. (David) van Westerloo

Thesis committee members:

Prof. dr. D.J. van Westerloo, LUMC (Chair)
Dr. A.J.R. de Bie Dekker, Catharina Ziekenhuis
Dr. ir. F.J.H. Gijsen, Technische Universiteit Delft
ir. I.W.F. Paulussen, TU/e & Catharina Ziekenhuis

Universiteit Leiden

TU Delft Delft University of Technology

Erasmus Universiteit Rotterdam

1 Preface

This master's thesis was completed as part of the Technical Medicine program, a joint degree between TU Delft, Erasmus MC and LUMC. The research took place at the Department of Intensive Care and Anesthesiology at Catharina Hospital in Eindhoven.

Prior to this thesis, a literature review was conducted on the use of carotid ultrasound for predicting fluid responsiveness. This study is included in Appendix 8.1.

This thesis focused on two main objectives. Firstly, exploring methods to synchronize ultrasound imaging with hemodynamic parameters. Secondly, developing a study protocol for a medical ethics committee (METC) application to compare invasive and non-invasive techniques for assessing respiratory effort in ICU patients weaning from mechanical ventilation.

Contents

2 Abbreviations

ABP	Arterial Blood Pressure
AWF	AirWay Flow
AWP	AirWay Pressure
AWV	AirWay Volume
BPC	Binned Peak Correlation
DTF	Diaphragm Thickening Fraction
DWC	Data Warehouse Connect
E_{di}	diaphragm Electrical activity
ECG	ElectroCardioGram
ICU	Intensive Care Unit
MM	Moving Mean
NK	NeuroKit
OR	Operating Room
P_{di}	trandiaphragmatic Pressure
P_{es}	esophageal Pressure
P_{ga}	gastric Pressure
P_{occ}	occlusion Pressure
POCUS	Point-Of-Care UltraSound
P-SILI	Patient Self-Inflicted Lung Injury
PTP_{es}	Pressure Time Product
RRIC	R-R Interval Correlation
ROI	Region-Of-Interest
SV	Stroke Volume
TEE	TransEsophageal Echocardiography
US	UltraSound

3

Introduction

Point-Of-Care UltraSound (POCUS) has become an increasingly accessible tool in Intensive Care Units (ICUs), enhancing the physical examination and facilitating real-time clinical decision-making [1]. Advances in technology, particularly the development of handheld ultrasound devices, have significantly improved POCUS availability and its integration into everyday critical care practices [2]. These innovations have also opened up new opportunities for POCUS, expanding its role beyond just a diagnostic tool to one that supports ongoing patient monitoring. Research has shown an average of 0.55 POCUS procedures per patient per day in ICUs, highlighting its growing role in patient management [3]. POCUS is now employed for diagnostics, procedural guidance, and continuous monitoring of patients' conditions [4]. This study specifically examines its use in hemodynamic and respiratory monitoring.

3.1 Hemodynamic monitoring

Patients admitted to the ICU often suffer from, or are at risk of, organ failure, commonly following major surgery or trauma. A key contributor to organ dysfunction is hemodynamic instability, a mismatch between oxygen delivery and demand, caused by factors such as reduced circulating volume, impaired cardiac function, or altered vascular tone (e.g. septic shock) [5]. This is monitored through hemodynamic assessment of key vital signs, including heart rate, blood pressure, central venous pressure, oxygen saturation (both peripheral and central), respiratory parameters, and urine output. When these parameters are inadequate, more advanced monitoring may be necessary. This includes measurements like cardiac output, pulmonary arterial occlusion pressure, pulmonary arterial pressure, mixed venous oxygen saturation, and stroke volume variation, all of which help guide fluid management and the use of vasopressors or inotropic support [5]. POCUS can assist in hemodynamic monitoring by evaluating a patient's fluid status, enabling evaluation of physiological and hemodynamic parameters related to volume status, fluid responsiveness, and fluid tolerance. When combined with other clinical indicators, POCUS of the heart, lungs, and vasculature supports the management of complex volume-related challenges [1]. In particular, carotid Doppler ultrasound has shown potential as a non-invasive technique for hemodynamic monitoring [6]. Based on these findings, a literature review on using carotid ultrasound to predict

patients' fluid responsiveness was conducted as part of preparation for this thesis (see *Appendix 8.1*).

3.2 Respiratory monitoring

On average, patients admitted to the ICU require mechanical ventilation for 9.6 hours per admission, providing respiratory support [7]. To guide and evaluate mechanical ventilation, accurate respiratory monitoring is essential. POCUS of the thorax can detect pulmonary edema, pneumothorax, pleural effusion, atelectasis and pneumonia, with proven higher diagnostic accuracy than standard chest radiography [8, 9]. In addition to anatomical imaging, assessing respiratory effort is essential during ventilation. Respiratory effort is the pressure generated by the respiratory muscles, mainly the diaphragm, in response to neural signals from the brainstem respiratory centers (respiratory drive). It is essential to understand how support settings impact the drive–effort relationship, as mismatches between neural demand and mechanical assistance may cause clinically important conditions such as over-assistance or under-assistance, potentially resulting in diaphragm atrophy and prolonged ICU stays, or Patient Self-Inflicted Lung Injury (P-SILI), respectively. This highlights the importance of accurately assessing both respiratory drive and effort to optimize respiratory management in mechanically ventilated ICU patients [10]. Additionally, during the weaning phase, the process of discontinuing mechanical ventilation and removing the endotracheal tube, close monitoring of respiratory effort is essential as well [11]. Diaphragm electrical activity (E_{di}) and transdiaphragm pressure (P_{di}) are considered reference methods for assessing respiratory effort, however diaphragm examination with POCUS offers a non-invasive alternative [10, 12, 13, 14]. A study protocol will be developed to assess the relationship between invasive reference measures of respiratory effort (E_{di} & P_{di}) and non-invasive techniques such as diaphragm assessment using POCUS in ICU patients weaning from mechanical ventilation.

3.3 Study proposal

The diagnostic value of POCUS is closely linked to patient-specific physiological characteristics. If relevant anatomical or hemodynamic factors are not taken into account, this can lead to misinterpretations [1]. When applied in complementary manner, POCUS and hemodynamic parameters provide synergistic insights: POCUS delivers real-time, direct visualization of cardiac anatomy and filling dynamics, whereas hemodynamic parameters provides continuous data on physiologic trends [15]. By combining these modalities, clinicians gain a more comprehensive understanding of the patient's status, merging structural imaging with functional hemodynamic insights [1]. Consequently, synchronizing ultrasound imaging with hemodynamic parameters offers a promising approach to optimize data interpretation, improve personalized patient assessment and support clinical decision-making.

Specifically in the fields of hemodynamic and respiratory monitoring, the alignment of POCUS with hemodynamic parameters is of particular interest. In hemodynamic monitoring, POCUS serves as a valuable adjunct to conventional methods by providing real-time visualization of cardiac function and vascular status. Synchronizing these ultrasound findings with hemodynamic parameters is essential for accurate data interpretation.
In respiratory monitoring, POCUS offers a non-invasive alternative to gold standard techniques, such as E_{di} and P_{di}, for assessing respiratory effort. This is especially relevant during weaning from mechanical ventilation, where it can provide clinically important information on diaphragm function and effort, the primary respiratory muscle, helping guide ventilator support and prevent complications such as diaphragm atrophy or P-SILI [10]. The practical feasibility of studying POCUS for respiratory effort, for which a protocol is developed in this thesis, depends on the precise alignment of POCUS and hemodynamic parameters to ensure accurate analysis.

Accordingly, this thesis investigates the technical feasibility of aligning these two modalities, both to facilitate their complementary clinical application and to enable the practical execution of the respiratory effort study.

The core objectives of this thesis can be summarized in three points:

1. Assessing the technical feasibility of synchronizing ultrasound imaging with hemodynamic waveforms for integrated patient monitoring, as addressed in *Chapter 4*.

2. Investigating the use of ultrasound to quantify respiratory effort in patients weaning from mechanical ventilation, as discussed in *Chapter 5*.

3. Exploring the potential of carotid ultrasound to predict patients' fluid responsiveness, as outlined in the literature review in *Appendix 8.1*.

4

Synchronization of Ultrasound Imaging with Hemodynamic Waveforms

Point-Of-Care UltraSound (POCUS) and hemodynamic parameters serve as complementary tools for patient monitoring in the ICU, as discussed in *Chapter 3*. This chapter explores the technical feasibility of aligning ultrasound imaging with hemodynamic parameters. The situation is illustrated in *Figure 1*.

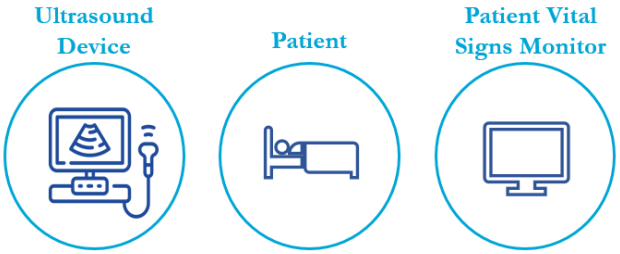

Figure 1: Illustration of an ultrasound system performing POCUS (left) examination on a patient (middle), alongside the bedside vital signs monitor (right) displaying the patient's hemodynamic parameters.

Figure 1 illustrates the ultrasound system used for the POCUS examination of the patient, alongside the bedside monitor displaying the patient's hemodynamic parameters. Both modalities, as applied in the ICU and Operating Room (OR), are described below.

4.1 Bedside vital signs monitor

The hemodynamic parameters monitored in the ICU and OR are displayed on the bedside vital signs monitor (MX750, Philips). Patients are connected to this monitor via ECG cables, oxygen saturation sensors, and pressure lines, depending on which vital parameters are relevant for monitoring the patient (see Chapter 3).

Starting from July 2024, all high-resolution monitoring data available from the bedside monitors in the ICU and OR are stored in Philips Data Warehouse Connect (DWC). This data included patient demographics, high frequency vital sign waveforms, tabular trend data, and alarm events. Medical devices, such as ventilators and saturation measurement devices, generate physiological data that is displayed on different monitors at the bedside. These devices are connected to the monitors either directly or via a bridge module, and the monitors forward the data to a central station for real-time patient monitoring. Using Philips DWC, the data is automatically stored on the DWC server and subsequently archived in the hospital's high-resolution monitoring database. From this archive, data can be made available to researchers through the hospital's AI Expertise Centre. This development opens up research opportunities, as data can be accessed retrospectively. The data flow is illustrated in *Figure 2*.

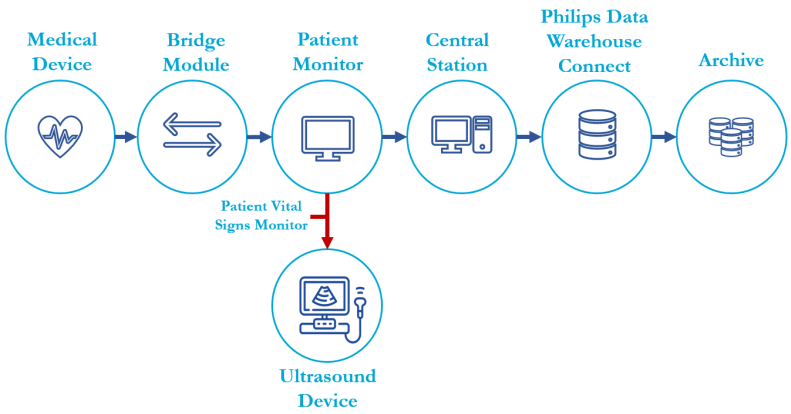

Figure 2: Data flow in the Intensive Care Units at Catharina Hospital Eindhoven. Medical devices connect to monitors directly or via a bridging module. Data is transmitted to a central station, stored on the Philips Data Warehouse Connect server, and archived. Additionally, the ultrasound device receives ECG data from the patient's vital signs monitor (red arrow).

Hemodynamic waveforms can be requested by specifying the patient, the desired parameters, and time window. The data are provided in CSV format, with each file containing a single parameter. The CSV files include columns for the WaveID, SequenceNumber, Timestamp, and the corresponding waveform values, structured as $WaveID, SequenceNumber, TimeStamp, v0, v1, v2, \ldots, vN$. Each row represents an individual waveforms, starting at the specified timestamp. Each waveform has a fixed duration of 5.12 seconds. Since the parameters were sampled at varying frequencies, the number of values within each waveform depends on its specific

sampling frequency. *Table 1* provides an overview of the waveform parameters included in this study, listing their DWC label, parameter description, unit, sampling period, sampling frequency, and the number of samples per waveform.

Table 1: Overview of hemodynamic waveform parameters extracted from Data Warehouse Connect (DWC), including their DWC label, parameter description, unit, sampling period, sampling frequency, and the number of samples per waveform.

DWC-label	Parameter description	Unit	Sampling period (ms)	Sampling frequency (Hz)	Number of samples
ABP	Arterial Blood Pressure	mmHg	8	125	640
AWF	Airway Flow	L/min	8	125	640
AWP	Airway Pressure	cmH_2O	8	125	640
AWV	Airway Volume	mL	8	125	640
CO_2	Expired CO_2 concentration	%	16	62.5	320
CVD	Central Venous Pressure	mmHg	8	125	640
Edi	Diaphragm electrical activity	µV	8	125	640
II	ECG Lead II	mV	2	500	2560
Pleth	Plethysmography waveform	–	8	125	640
Resp	Respiratory waveform	cmH_2O*s/L	16	62.5	320

In practice, the actual sampling periods can be slightly longer than the specified nominal values. This discrepancy is largely due to the functioning of crystal oscillators used in the monitoring hardware. These oscillators serve as the time reference for signal acquisition, generating highly stable clock signals. Nonetheless, due to manufacturing tolerances, temperature variations, and inherent physical limitations, the actual clock frequency can deviate slightly from its specified ideal value. For example, while the ECG signal nominally samples at 2 ms intervals, the effective sampling period may be slightly longer (e.g., 2 ms plus approximately 0.9 nanoseconds). To account for such deviations and ensure better temporal alignment, a sampling period of 3 ms is sometimes used instead of 2 ms during data processing.

4.2 Ultrasound System

POCUS in the ICU department of Catharina Hospital Eindhoven is performed using the Philips Affiniti 70 system [16]. In the operating room, the Philips EPIQ CVx is used [17]. The EPIQ CVx provides more advanced cardiac imaging capabilities and is primarily used by anesthesiologists for TransEsophageal Echocardiography (TEE). In contrast, the Affiniti system is more broadly applied for general POCUS examinations within the ICU setting.

The ultrasound device receives ECG data via a cable linking the patient's vital signs monitor to the ultrasound system, enabling real-time display of the ECG alongside ultrasound images, see *Figure 2*.

The ECG-signal is acquired directly from the patient via electrodes connected by cables, allowing it to be transmitted and displayed on the patient vital sign monitor. The same ECG signal is also routed via a cable from this monitor to the ultrasound system, where it is displayed as a green waveform at the bottom of the ultrasound image, as outlined in *Figure 3*.

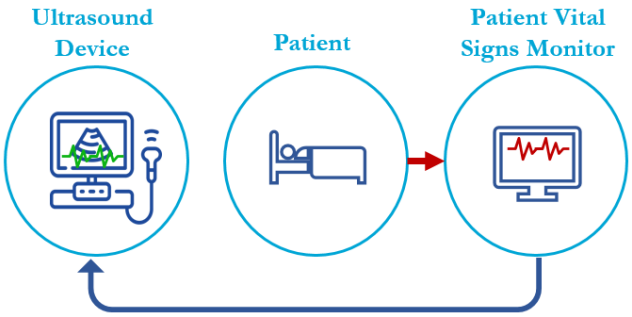

Figure 3: Illustration of the ECG electrodes connecting the patient to the patient vital signs monitor (red), the ECG signal transmitted from this monitor to the ultrasound device (blue), and the ECG waveform displayed in the ultrasound image (green).

4.3 Time-Based Synchronization

To synchronize the POCUS imaging with the hemodynamic waveforms, a logical first step is to examine the timestamps associated with both signals. These timestamps provide an initial temporal reference that can be used to align the datasets.

The hemodynamic waveforms stored in Philips Data Warehouse Connect (DWC) are synchronized with the hospital's central time server. The integration of data flow with DWC is illustrated in *Figure 2*. Bedside monitoring devices inherit their time settings from the central station upon connection and maintain their own internal clocks thereafter. The monitor's clock is continuously compared with the central station's time, and is automatically reset if a difference of 30 seconds or more is detected. The same synchronization process applies to the DWC server, ensuring consistent timestamps within the DWC database. However, between these automatic corrections, a small time drift may occur.

Analysis of the ultrasound system's timestamps revealed that its internal clock often deviates unpredictably from the time on the patient's vital signs monitor. This drift is primarily due to the limited accuracy of the system's crystal oscillator, which causes the clock to gradually shift over time rather than from manual adjustments by users. To further examine this discrepancy, the clinical physics department was consulted. This led to a meeting with a hospital ICT staff member, who reviewed the current ultrasound configuration. It was found that while the device was connected to the hospital network, it was not synchronized with the hospital's central time server. Following this discovery, the device was reconfigured to use the hospital's central time server by configuring the *Network Time Source* setting, as illustrated in *Figure 4*.

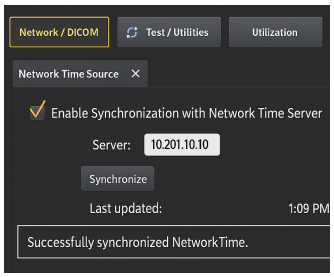

Figure 4: Configuration interface showing the ultrasound device set to synchronize its internal clock with the hospital's central time server configuring the *Network Time Source* setting.

As a result, the ultrasound system is now synchronized with the hospital's central time server, as is the patient vital signs monitor. Synchronization between ultrasound images and hemodynamic waveforms is now achievable with minute-level accuracy. Since visual comparison of timestamps on the ultrasound and monitor was not feasible at the second level, and, as mentioned earlier, waveform timestamps could drift but were adjusted whenever differences exceeded 30 seconds. Although this adjustment was minor, it greatly enhances synchronization.

4.4 ECG-Based Synchronization

After time-based synchronization, the two modalities can be aligned with an accuracy of up to one minute. However, further refinement is needed to achieve more precise alignment. Since both modalities contain the ECG signal (see *Figure 3*), the feasibility of ECG-based synchronization is now being explored.

The ECG signal from the ultrasound (ECG_{us}) has the same duration as the ultrasound recording itself, typically ranging from 2 to 10 seconds. This ECG segment needs to be matched within the longer ECG signal available from DWC (ECG_{dwc}). Since both devices now share a clock synchronized to within one minute, the corresponding segment can be searched for within a time window spanning one minute before the ultrasound start time to one minute after its end time, as illustrated in *Figure 5*.

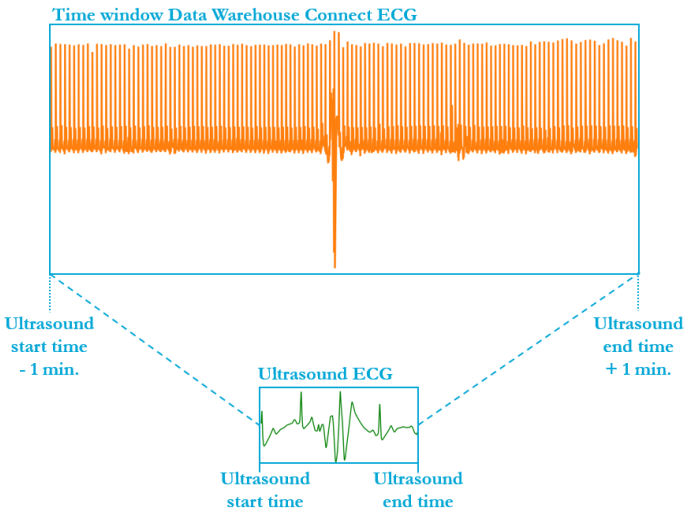

Figure 5: Illustration of the ECG segment from ultrasound (green) alongside the time window used to search for the corresponding ECG segment within the Data Warehouse Connect (DWC) ECG data (orange). The DWC time window is defined as the period from one minute before the ultrasound start time and one minute after the ultrasound end time.

The ECG_{dwc} can be retrieved from the AI Expertise Centre, and ideally, the ECG_{us} signal would also be available as raw signal data within the DICOM file. Although the ECG_{us} signal is visible on the screen, it could not be found in the DICOM file. The clinical physics department was consulted and contacted Philips, but no clarity was provided on whether the ECG_{us} is available as raw data or how it could potentially be obtained. Therefore, a method was developed to extract the ECG_{us} signal from the green pixels representing the waveform in the ultrasound image.

4.5 ECG-Signal Extraction From Ultrasound

The ECG in the DICOM files is stored as part of the ultrasound image, where it is represented by green pixels. A previous project by a fellow student focused on extracting the ECG by detecting these green pixels, which represent the ECG waveform, using MATLAB. Since Python is a more accessible and widely used programming language than MATLAB, the code was translated into Python. This process involved identifying and implementing appropriate Python equivalents for MATLAB-specific functions. Additionally, the code was enhanced to improve its robustness, as the previous version was designed for a specific ultrasound setup. Several factors can vary between ultrasound settings, such as the image size (rows and columns) and the location of the ECG signal (center or bottom). The method was enhanced to ensure robustness against these variations. Detailed improvements are described in the comprehensive explanation of the green pixel extraction mechanism below.

The code splits the image into the three RGB color channels. A binary mask is then created by applying a filter to isolate green pixels, defined by the condition: red channel ≤ 140, green channel ≥ 200, and blue channel ≤ 140. *Figure 6A* shows the original frame, and *Figure 6B* displays the frame after applying the green channel filter. At the beginning, the ECG signal fills the width of the screen and continuously overwrites itself at the location of a visible black sweeping line moving across the display. This black sweeping line is also visible in *Figure 6A* and *Figure 6B*, where it appears as a discontinuity in the signal. The ECG signal is extracted from frames in which a complete new segment of the ECG waveform is visible, these are referred to as the frames to analyze. The frames to analyze are identified by detecting the black sweeping line within the region-of-interest (ROI) at the left edge of the ECG signal, see *Figure 6C* and *Figure 6D*.
This ROI was adjusted from its original definition. Initially, it was set between the minimum and maximum rows containing green pixels, and from the minimum column containing green pixels plus 7. However, it was observed that the black sweeping line sometimes fell just outside this ROI, so the region was expanded by selecting plus 14 instead of 7 to ensure its detection.

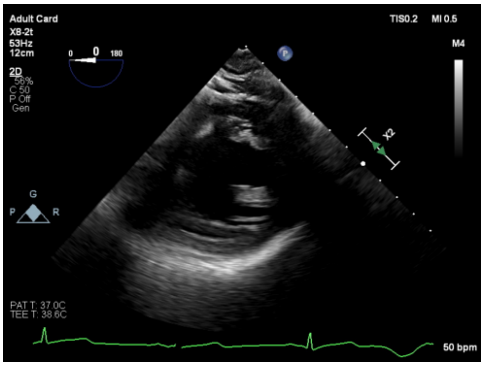

(A) Original ultrasound image of the last frame.

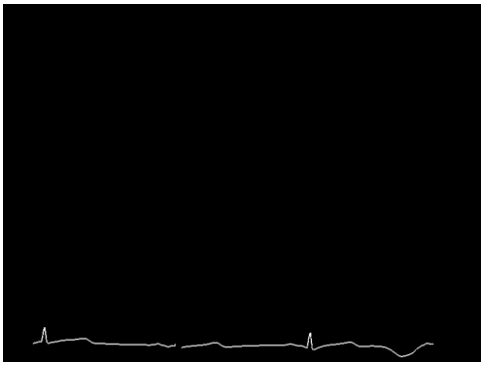

(B) Last frame after green-channel filtering.

(C) Detected ECG signal with indicated ROI.

(D) Zoomed view of the ROI.

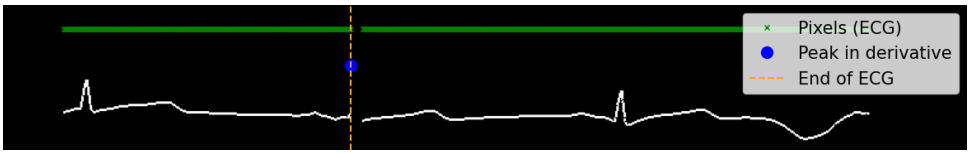

(E) ECG signal visible in the last frame with the black sweeping line marking the end.

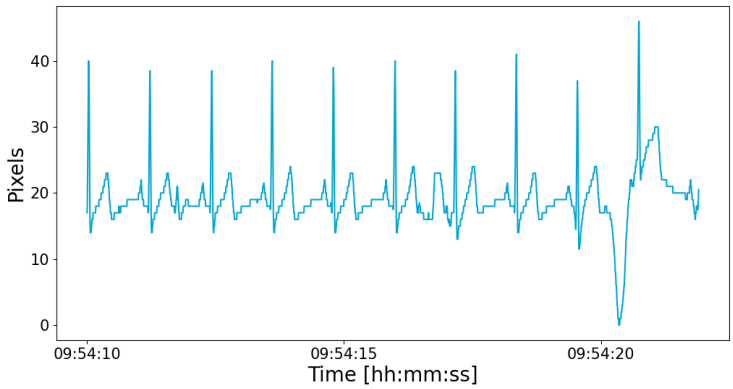

(F) Final extracted ECG signal.

Figure 6: Overview of the ECG extraction process. (A) Original ultrasound image of the last frame; (B) Last frame after green-channel filtering; (C) Detected ECG signal with indicated ROI; (D) Zoomed view of the ROI; (E) ECG signal visible in the final frame with the black sweeping line marking the end; (F) Final extracted ECG signal.

The code iterates over all frames in the binary green-filtered image. When the pixel values within the ROI fall below a threshold, it can be assumed that the black sweeping line is present, meaning a complete ECG cycle has been captured. The frame numbers corresponding to these complete ECG signals are saved as the frames to analyze. To extract the ECG trace, each frame is split into a left and right section, with a correction applied to the frame numbers in frames to analyze to prevent the black sweeping line from interrupting the signal. To ensure the final portion of the ECG segment is not missed, the last frame is always included in the analysis, as it is not automatically selected due to the absence of a sweeping line within the region of interest. For the final segment, in the last frame, the portion to the left of the sweeping line must be extracted. This is achieved by analyzing the derivative of the green pixel positions to identify the largest discontinuity, which corresponds to the location of the sweeping line, see *Figure 6E*. The ECG waveform to the left of this point is then extracted as the final part of the signal. Finally, all extracted ECG segments are concatenated to reconstruct the full ECG signal.

Extracting the green pixels also results in missing values when the ECG signal falls outside the visible range or when dashed lines or annotations on the ultrasound image disrupt the continuity of the green ECG waveform. This issue can be addressed in two ways: by leaving the missing values as NaNs or by applying interpolation. Since different synchronization methods will be compared later in this study, both approaches are implemented, resulting in two distinct versions of the ECG signal (ECG_{us}). The first version, denoted as $ECG_{us,nan}$, retains the original signal including any missing values (NaNs). The second version, $ECG_{us,int}$, is created by filling these gaps using linear interpolation via the *interp1d* function from the *scipy.interpolate* module. Both signals are shown in *Appendix 8.2.1*.

This results in a signal with x- and y-values corresponding to row and column indices. To synchronize this signal with the ultrasound acquisition timing, a time axis is constructed starting from the acquisition timestamp stored in the DICOM-info as *AcquisitionDateTime*. The frame rate (*CineRate*) is also retrieved from the DICOM-info, allowing calculation of the time per frame as $\frac{1}{\text{CineRate}}$. The total acquisition duration is then calculated by multiplying the time per frame with the total number of frames. To synchronize the time axis with the extracted ECG signal, the total acquisition time is divided by the number of ECG data points, resulting in the time duration per ECG pixel. Finally, a list of time points is created, starting from the acquisition timestamp and increasing by this time interval for each ECG data point, thereby assigning each ECG pixel to a moment in time, see *Figure 6F*.

Now that the ECG signal has been extracted from the ultrasound image, both the ultrasound and monitor ECG signals are available, ECG_{us} & ECG_{dwc}, retrospectively. This enables investigation into the most effective methods for aligning these two ECG signals.

4.6 Methods - ECG-Based Synchronization

This section presents an exploratory study on ECG-based synchronization of ultrasound imaging with hemodynamic waveforms, covering the data, preprocessing, synchronization and peak detection methods, and results.

4.6.1 Data collection

For this study, data were retrospectively collected from the anesthesiology and intensive care departments of Catharina Hospital in Eindhoven. Ultrasound recordings were originally acquired for clinical purposes. Recordings from the anesthesiology department within the Operating Room (OR) were obtained using Trans-Esophageal Echocardiography (TEE) during cardiac surgery for intraoperative monitoring. Recordings from the ICU were acquired to monitor patients' respiratory function using Point-of-Care UltraSound (POCUS). Inclusion was performed randomly, given the exploratory nature of the study. Four patients, POR_01, POR_02, POR_03, and POR_04, were selected from the anesthesiology department, and three patients, PIC_01, PIC_02, and PIC_03, were selected from the ICU. The primary inclusion criterion was that each ultrasound recording contained an ECG signal embedded within the image, enabling ECG-based synchronization.

Various settings can be configured when making ultrasound recordings. The duration can be set either as a specific time in seconds or as a number of heartbeats. It can be reasoned that a longer recording also includes a longer ECG signal, which may facilitate synchronization with hemodynamic waveforms by providing more data.

Furthermore, artefacts in the ECG may arise from disturbances to the electrodes caused by for example patient positioning. By manipulating an electrode, an artefact can be created, serving as a visual reference point within the ECG signal. To assess the feasibility of synchronizing different ultrasound recordings with their corresponding ECG signals, a distinction is made between short and long ECG segments, as well as recordings containing artefacts. First, it was determined whether a recording contained artefacts. Recordings with artefacts were manually identified by the presence of sinus rhythm disturbances, increased fluctuations, irregular oscillations, or spike-like patterns, characteristics linked to signal interference rather than patient-related hemodynamic factors. The remaining recordings were then categorized by length: short recordings contained 3 or 4 heartbeats, while long recordings consisted of 9 or 10 heartbeats.

4.6.2 Preprocessing

The ECG was extracted from the ultrasound images by isolating green pixels using a green filter, producing two versions of the ECG_{us} signal: $ECG_{us,nan}$, retaining missing values, and $ECG_{us,int}$, containing an interpolated signal. Both were extracted in terms of row-height and column-width within the DICOM frame, with pixel count as its unit of measurement, see *Appendix 8.2.1*. Before this signal was visualized on the ultrasound screen, it had already undergone certain preprocessing steps. In contrast the ECG_{dwc} represents the raw ECG-signal prior to any preprocessing.

To allow for a valid comparison between ECG_{us} and ECG_{dwc}, both signals require equivalent preprocessing as outlined below.

Resampling

All signals were standardized to a sampling rate of 500 Hz, corresponding to a sample every 2 ms. The ECG_{dwc} signal already had this rate and required no changes, whereas the ultrasound-derived signals ($ECG_{us,nan}$ and $ECG_{us,int}$) were resampled to 500 Hz after determining their original sampling rates from the recordings.

Flatline artefacts

If the ECG signal displayed in the ultrasound image extends beyond the actual acquisition window of the ECG data, the resulting segments are incomplete. These appear as gaps at the signal's minimum values or as flat (horizontal) lines at its maximum. The horizontal segments do not represent valid data but are instead indicative of missing data. An example of an ECG signal exhibiting such a artefact is provided in Appendix 8.2.2. To address this, $ECG_{us,nan}$ is corrected by detecting stretches where more than two consecutive samples equal the signal's maximum value, these are then marked as missing (NaN). The $ECG_{us,int}$ signal remains unchanged.

Cleaning ECG

`Ecg_clean` from the NeuroKit2 library was applied to $ECG_{us,nan}$, $ECG_{us,int}$ and ECG_{dwc}-signals. A brief description of NeuroKit2 is provided in *Appendix 8.3.1*. An ECG signal can exhibit gradual shifts in its baseline level, meaning that the isoelectric line drifts upward or downward over time. This phenomenon, often caused by factors such as breathing or patient movement, was corrected using detrending by `ecg_clean`. Furthermore, this function reduces high frequency noise and improves peak detection accuracy [18]. An example of baseline drift and high frequency noise is provided in *Appendix 8.3.2*.

It is important to note that the ECG_{us} signals may have undergone some preprocessing, such as correction for baseline drift, before being displayed in the ultrasound images, whereas the ECG_{dwc} signals represent unprocessed, raw data.

Since the `ecg_clean`-function cannot handle NaNs in the $ECG_{us,nan}$ signal, a mask was applied to exclude the NaN values, and `ecg_clean` was applied only to the valid (non-NaN) segments.

Normalization

Normalization ensures that both ECG signals have a mean of 0 and a standard deviation of 1, making them more comparable for synchronization purposes. Normalization of the cleaned ECG signals was performed using the following formula:

$$\text{signal}_{\text{normalized}} = \frac{\text{signal}_{\text{cleaned}} - \text{mean}(\text{signal}_{\text{cleaned}})}{\text{std}(\text{signal}_{\text{cleaned}})}$$

4.6.3 Synchronization

Time window of ECG_{dwc}

For synchronization, the ECG_{us} signal was searched within a defined time window of the ECG_{dwc} signal, as outlined in *Table 2*. For patients POR_03, POR_04, and PIC_03, the ultrasound system was already synchronized with the hospital's central time server at the moment of the measurement. Enabling the alignment process within a time window of 2 minutes, ranging from one minute before the ultrasound start time to one minute after its end time (*Figure 5*).

For patients POR_01, POR_02, PIC_01, and PIC_02, the ultrasound system was not synchronized with the hospital's central time server. In these cases, the times of the ultrasound and monitor recordings were noted manually during the measurement, enabling the calculation of the time difference between the two modalities. The ultrasound start and end times were used as reference points. The DWC signal window was then determined by subtracting the calculated time difference from the ultrasound start time and adding it to the ultrasound end time. Additionally, this interval was extended by one minute on both sides, resulting in an approximate two-minute time window for the alignment process.

Table 2: Per patient, indication of whether the ultrasound was synchronized with the hospital's central time server, the calculated time difference between the ultrasound system and the monitor (a positive value indicates the DWC timestamp occurs after the ultrasound timestamp, while a negative value indicates the opposite), and the time windows within the DWC signal used for synchronization with the ultrasound signal.

Patient	Network Time Source Synchronized	Time difference (min)	Time window (min)
POR_01	no	+7	$t_{us,start}$ +6 — $t_{us,end}$ +8
POR_02	no	+69	$t_{us,start}$ +68 — $t_{us,end}$ +70
POR_03	yes	<1	$t_{us,start}$ -1 — $t_{us,end}$ +1
POR_04	yes	<1	$t_{us,start}$ -1 — $t_{us,end}$ +1
PIC_01	no	+76	$t_{us,start}$ +75 — $t_{us,end}$ +77
PIC_02	no	+76	$t_{us,start}$ +75 — $t_{us,end}$ +77
PIC_03	yes	<1	$t_{us,start}$ -1 — $t_{us,end}$ +1

Pearson correlation of the full ECG-signal

To precisely align the ECG_{us} and ECG_{dwc} signals, a sliding template correlation approach was employed. ECG_{dwc} served as the template, against which $ECG_{us,nan}$ was matched. Pearson correlation was used to quantify the similarity between the two signals. The $ECG_{us,nan}$ was shifted sample by sample across the template, and at each position, the correlation coefficient was computed between the $ECG_{us,nan}$ and the corresponding window in the ECG_{dwc}. To ensure accurate comparison despite missing values, a masked correlation function was used that ignored NaNs. As the $ECG_{us,int}$ signal contains interpolated (and thus artificial) values, only the original $ECG_{us,nan}$ signal was used for this comparison. The timeshift corresponding to the highest correlation was selected as the optimal synchronization offset.

Peak based synchronization

To enable synchronization based on peaks, peak detection was performed on the preprocessed ECG_{us} and ECG_{dwc} signals. Since the detection algorithms did not perform reliably in the presence of missing values, as is in $ECG_{us,nan}$, peak detection was performed only on the interpolated ultrasound ECG signal ($ECG_{us,int}$). Since this study includes ECG segments containing artefacts, two peak detection algorithms were employed: NeuroKit to detect true R-peaks in clean segments, and the Moving Mean method to detect peaks in segments containing artefacts (these peaks do not necessarily correspond to true R-peaks). Both algorithms are described below.

Peak Detection with NeuroKit (NK)

The NeuroKit2 library enables automatic R-peak detection in ECG signals [18]. QRS-complexes are detected based on the steepness of the absolute gradient of the ECG signal, after which R-peaks are identified as local maxima within these complexes. NeuroKit2 provides several detection algorithms, which were compared in Appendix 8.3.3. Based on this comparison, the default NeuroKit method was selected as the most suitable. It was observed that R-peaks near the beginning and end of the signal were not reliably detected. This is likely due to insufficient data available for NeuroKit in these regions. To address this, 2 seconds of data from the end of the signal were appended to the beginning, and 2 seconds from the beginning were appended to the end. This extension allowed for more reliable detection of peaks at the signal boundaries. To avoid false positives introduced by this artificial extension, any peaks detected exactly at the original signal boundaries were automatically discarded.

Peak Detection with Moving Mean (MM)

The moving mean peak detection method uses a moving average, which means it calculates the average signal value over a sliding time window [19]. In this study, a window length of 0.25 times the sampling rate was used, equivalent to 125 samples, or 0.25 seconds. This means that for each point in the signal, the average is calculated over a window including 62 samples before, the point itself, and 62 samples after. Near the start and end of the signal, the full window may not fit due to limited data. In those cases, the moving average is calculated using only the available samples within the window, effectively shortening it at the edges. To adjust the sensitivity of peak detection, two approaches were implemented by adding a fixed offset of either 0.2 or 1 to the moving mean signal. This resulted in two distinct moving mean–based detection methods. The resulting value acts as a threshold: when the signal exceeds this threshold, peaks can be detected.

Figure 7 presents an example of peak detection applied to an $ECG_{us,int}$ signal using both the NeuroKit and Moving Mean methods.

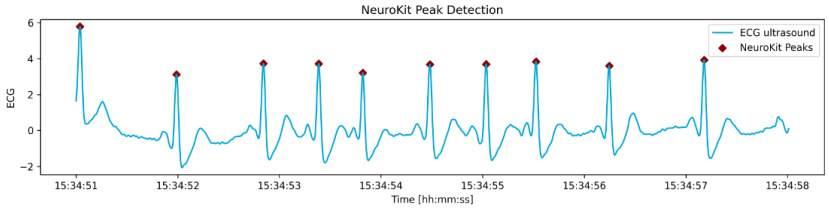

(A) NeuroKit

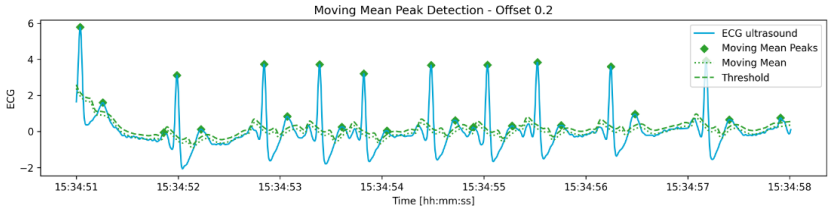

(B) Moving Mean offset 0.2

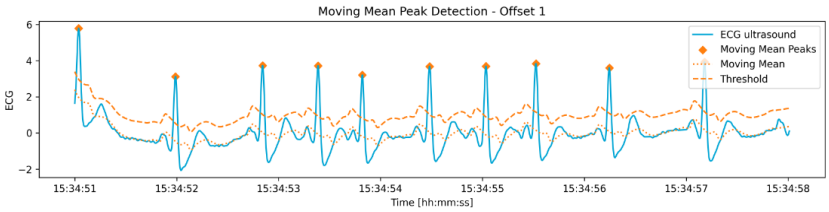

(C) Moving Mean offset 1

Figure 7: Illustration of peak detection methods applied to the $ECG_{us,int}$-signal. **(A)** R-peak detection using NeuroKit; **(B)** Moving Mean with an offset 0.2; **(C)** Moving Mean with an offset 1.

R-R Interval Correlation (RRIC)

From the detected R-peaks using both the NeuroKit and Moving Mean methods in the $ECG_{us,int}$ and ECG_{dwc} signals, the R-R intervals (i.e., the distances between consecutive R-peaks) can be used for synchronization [20]. The ECG_{dwc} signal had a duration of just over two minutes, for an average resting heartrate (60-80 bpm) this means 120-160 beats. The ECG_{us} signal contains only 3 to 10 heartbeats, comparable to 2 to 3 seconds for 3 beats, and 7 to 10 seconds for 10 beats. The ECG_{dwc} signal was treated as a reference template, while the $ECG_{us,int}$ signal was shifted over it peak by peak. At each position, the corresponding R-R intervals were compared using Pearson correlation. This sliding procedure was repeated across the two minute DWC signal, and the timeshift corresponding to the highest correlation value was selected as the optimal alignment.

Binned Peak Correlation (BPC)

For this method, the ECG signals are divided into 100 ms bins, with each bin marked as 1 if a peak is present and 0 if absent, an example of binned signal is shown in *Figure 8* [20]. The resulting binned peak data are then compared using Pearson's correlation coefficient. A high correlation indicates that peaks largely occur in the same bins, reflecting strong synchronization between the two datasets. Conversely, a low correlation suggests that peaks rarely coincide in the same or adjacent bins, demonstrating poor alignment within the given time window.

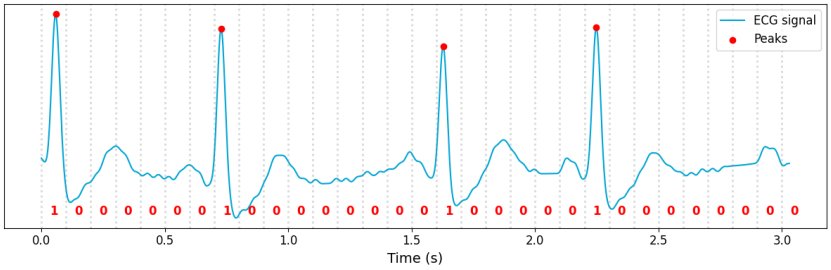

Figure 8: Illustration of an ECG signal segmented into 100 ms bins, with each bin labeled as 1 or 0 depending on whether a peak is present or not.

The Pearson correlation between the full signals shifts the ECG_{us} relative to the ECG_{dwc} sample by sample, for the RRIC method peak by peak, and for the BPD method bin by bin. The RRIC is sensitive to missing peaks because the absence of a single peak disrupts the R-R intervals, making comparison difficult. In contrast, the BPC is more robust in this regard, as it evaluates individual peaks independently rather than relying on their intervals.

The following seven synchronization methods will be evaluated:

1. Pearson correlation of the full ECG-signal
2. R-R Interval Correlation (RRIC) using Pearson with peaks detected with:
   a NeuroKit (RRIC - NK)
   b Moving Mean with an offset of 0.2 (RRIC - MM0.2)
   c Moving Mean with an offset of 1 (RRIC - MM1)
3. Binned Peak Correlation (BPC) using peaks detected with:
   a NeuroKit (BPC - NK)
   b Moving Mean with an offset of 0.2 (BPC - MM0.2)
   c Moving Mean with an offset of 1 (BPC - MM1)

For all these methods, the timeshift required to align the ultrasound data with the hemodynamic waveforms is calculated in both seconds and minutes. A negative value indicates that ECG_{us} must be shifted backward in time, while a positive value indicates a forward shift to align with ECG_{dwc}. Additionally, the Pearson correlation coefficient is determined.

4.7 Results - ECG-Based Synchronization

4.7.1 Data collection

For this study, ultrasound images were retrospectively collected at Catharina Hospital Eindhoven, specifically from the intensive care and anesthesiology departments. Four recordings were obtained from the anesthesiology department (POR_01, POR_02, POR_03, and POR_04), and three from the ICU (PIC_01, PIC_02, and PIC_03). Patient PIC_03 was monitored on three separate days, resulting in recordings labeled as PIC_03_1, PIC_03_2, and PIC_03_3. Recordings were categorized as short (3 or 4 beats), long (9 or 10 beats), or containing artefacts. Ultrasound recordings that did not contain artefacts but also did not meet the criteria for either short or long were excluded from analysis. *Table 3* provides an overview of the data collection with the number of recordings per patient and per category.

Table 3: Overview of the data collection, showing for each patient the number of ultrasound recordings in each category: short (3–4 beats), long (9–10 beats), artefact-containing, or excluded if not fitting these categories.

Patient	Short	Long	Artefact	Excluded
POR_01	1	2	0	56
POR_02	1	1	5	48
POR_03	0	0	2	37
POR_04	2	1	2	29
PIC_01	2	0	0	0
PIC_02	1	4	0	0
PIC_03_1	5	10	3	5
PIC_03_2	6	14	3	3
PIC_03_3	14	9	0	1
Total	**32**	**41**	**15**	**179**

As shown in *Table 3*, a total of 32 ultrasound recordings were classified as short, 41 as long, 15 contained artefacts, and 179 were excluded from analysis. The high number of 179 excluded recordings mainly originated from patients included from the anesthesiology department, as these studies contained many recordings of only a single heartbeat. The distribution of recordings across the different categories also varied between patients. Not all patients had ultrasound recordings containing artefacts, which can make it more difficult to determine the correct timeshift, as clear markers in the ECG signal may be absent to validate the identified timeshifts.

4.7.2 Preprocessing

The ECG signal was extracted from the ultrasound images by isolating the green pixels. The duration of each ultrasound recording, the original sampling frequency of ECG_{us} before resampling to 500 Hz, and the percentage of missing values in $ECG_{us,nan}$ are presented in *Table 4*.

Table 4: Descriptive statistics (mean ± SD) of ultrasound features for each measurement type: short (3 or 4 beats), long (9 or 10 beats), and artefact-containing recordings.

Statistic	Short	Long	Artefact
Duration of ECG_{us} (s)	2.14 ± 0.52	6.57 ± 1.64	5.66 ± 2.25
Sample frequency ECG_{us} (Hz)	264.32 ± 73.94	241.99 ± 52.65	211.77 ± 52.08
Missing values in $ECG_{us,nan}$ (%)	9.20 ± 10.90	10.85 ± 10.88	25.86 ± 12.90

As shown in *Table 4*, the distribution of ultrasound recording durations corresponds to expectations for short, long, and artefact-containing recordings. Since artefacts introduce additional peaks, and the ultrasound system was set to record for the duration of 10 peaks, recordings with artefacts are shorter than typical 10-beat recordings. Furthermore, a higher percentage of missing values was observed in $ECG_{us,nan}$ signals containing artefacts. This happens when the ECG signal shifts outside the visible range of the ultrasound screen due to an artefact, causing the signal to disappear at minimal values and appear as a flatline at maximum values, an example is provided in *Appendix 8.2.2*. Missing values also resulted from annotations or scale markings in the ultrasound image, which disrupted the continuity of the green ECG waveform, an example is provided in *Appendix 8.2.3*.

All collected ECG_{dwc}-signals had already a sampling frequency of 500 Hz. Both the ECG_{us}-signals were resampled to 500 Hz. In the $ECG_{us,nan}$ signal, flatline artefacts were detected and replaced with missing values (NaNs). The `ecg_clean`-function from the NeuroKit2 library was applied to the ECG_{dwc}, and resampled ECG_{us}-signals, after which the signals were normalized to have a mean of 0 and a standard deviation of 1. An example of a raw, cleaned, and normalized signal of ECG_{dwc}, $ECG_{us,nan}$, and $ECG_{us,int}$ is shown in *Figure 9* for a recording containing an artefact.

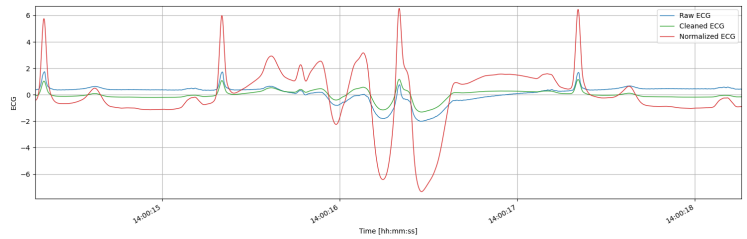

(A) ECG_{dwc}

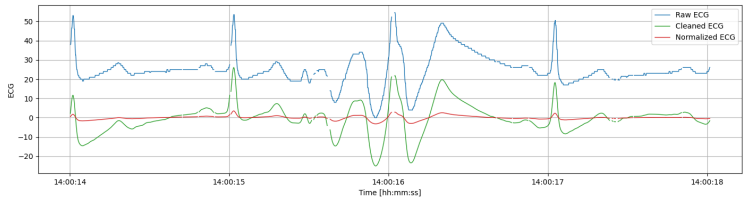

(B) $ECG_{us,nan}$

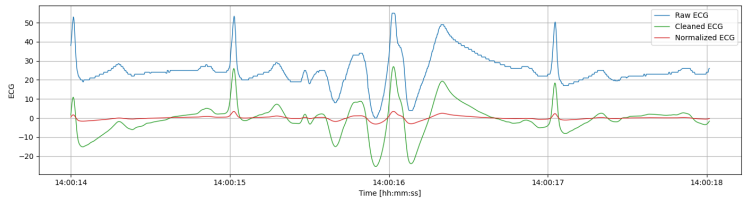

(C) $ECG_{us,int}$

Figure 9: Overview of the preprocessing steps, in an example containing an artefact, for the three ECG signals. Each subplot shows a signal after resampling (blue), cleaning using `ecg_clean` (green), and normalization (red). **(A)** ECG_{dwc} from Data Warehouse Connect, shown as a cropped segment; **(B)** $ECG_{us,nan}$ with missing values preserved; **(C)** $ECG_{us,int}$ with interpolated values.

Figure 9 shows that the ECG_{us} signals have relatively high values prior to normalization. This is because they were extracted from ultrasound images and are expressed in terms of row height. Furthermore, missing values or gaps in the ECG signal are only present in $ECG_{us,nan}$. Since this example includes an artefact, it is easy to observe that both the DWC and US signals represent the same segment of the ECG, however, with different timestamps and a timeshift of approximately one-third of a second.

4.7.3 Synchronization

Peaks in the $ECG_{us,int}$-signal were detected using NeuroKit and the Moving Mean methods. The number of identified peaks is summarized in *Table 5*.

Table 5: The number of peaks in $ECG_{us,int}$ found per peak detection method for each category: short (3 or 4 beats), long (9 or 10 beats), and artefact-containing recordings. **NK**: NeuroKit; **MM0.2**: Moving Mean with an offset of 0.2; **MM1**: Moving Mean with an offset of 1.

Peak Detection Method	Short	Long	Artefact
NK	3.44 ± 0.50	9.95 ± 0.22	6.27 ± 2.69
MM0.2	9.84 ± 1.72	28.80 ± 2.76	19.20 ± 8.14
MM1	4.50 ± 1.27	13.90 ± 4.04	9.53 ± 3.11

The number of peaks detected with NeuroKit falls within the expected range for both short (3–4 beats) and long (9–10 beats) recordings, which were differentiated based on this criterion. Recordings containing artefacts show intermediate values, as artefacts introduce peaks that do not correspond to true R-peaks, they are not always detected with NeuroKit. Additionally, Moving Mean with an offset of 0.2 (MM0.2) detected more peaks than Moving Mean with an offset of 1 (MM1), which is expected due to the smaller offset.

Seven different synchronization methods were applied, Pearson correlation of the full ECG signals, R-R Interval Correlation (RRIC), and Binned Peak Correlation (BPC), using peaks detected with three methods: NeuroKit (NK), Moving Mean with an offset of 0.2 (MM0.2), and Moving Mean with an offset of 1 (MM1). The identified timeshifts were recorded in seconds, and their corresponding correlation values were calculated. Each timeshift calculated to align the ECG_{us} signal with the ECG_{dwc} signal was manually classified as correct or incorrect based on visual inspection. *Figure 10* provides an overview of the data collection (including *Table 3*), the categorization, and the synchronization results for each method, showing the correctly and incorrectly identified timeshifts by category (short, long, and artefact). An overview of the determined timeshifts and corresponding correlation values for each patient and synchronization method is provided in *Appendix 8.4*.

Patient	Short	Long	Artefact	Excluded
POR_01	1	2	0	56
POR_02	1	1	5	48
POR_03	0	0	2	37
POR_04	2	1	2	29
PIC_01	2	0	0	0
PIC_02	1	4	0	0
PIC_03_1	5	10	3	5
PIC_03_2	6	14	3	3
PIC_03_3	14	9	0	1
Total	32	41	15	179

Figure 10: Overview of the data collection, showing for each patient the number of ultrasound recordings in each category: short (3–4 beats), long (9–10 beats), artefact-containing, or excluded if not fitting these categories. For each category, the number of included ultrasound recordings is indicated, along with the number of unvalidated recordings for which synchronization could not be confirmed. Visualization of the results of the seven synchronization processes per category, with correct synchronizations in green, incorrect in red, and the percentage of correct synchronizations per method.
RRIC: R-R Interval Correlation; **BPC**: Binned Peak Correlation; **NK**: NeuroKit; **MM0.2**: Moving Mean with an offset of 0.2; **MM1**: Moving Mean with an offset of 1.

As shown in *Figure 10*, the timeshifts determined by the synchronization processes could not be validated for 29 short and 37 long recordings. All recordings containing artefacts allowed for validation of the timeshifts.

For only three short recordings, verification of the determined timeshifts was possible, an example is provided in *Appendix 8.6.1*. Given this low number, it is difficult to draw definitive conclusions. Short segments contain less data, resulting in fewer identified peaks compared with the categories long and artefact (see *Table 5*). Therefore, it is not surprising that synchronization using Pearson correlation over the full signal performs better compared with the peak-based RRIC and BPC methods.

For only four long recordings, verification of the determined timeshifts was possible, an example is provided in *Appendix 8.6.2*. All four of these long recordings originate from patient PIC_02. Validation was not possible for the other long recordings, as visual confirmation of synchronization could not be achieved. A possible explanation for this is the variation in R–R intervals. For patients with a regular heart rate, the R–R intervals show little variation, making it difficult to distinguish between different ECG segments. *Table 6* presents the heart rate variability for all patients during the periods corresponding to the included ultrasound segments.

Table 6: Heart rate variability, expressed as median (IQR) heart rate measured by ECG, for each patient over the entire duration of the ECG_{dwc} time windows in which synchronization with the ECG_{us} segments was searched.

Patient	Heart Rate (bpm)	Duration DWC Window (min)
POR_01	46.50 (45.50-47.75)	5.5
POR_02	60.00 (50.00-71.00)	115.4
POR_03	54.00 (50.75-63.00)	10.8
POR_04	60.00 (59.00-61.00)	8.5
PIC_01	115.50 (114.75-116.25)	2.1
PIC_02	91.00 (87.00-96.00)	20.3
PIC_03_1	90.00 (90.00-91.00)	15.9
PIC_03_2	97.00 (96.00-97.00)	21
PIC_03_3	115.00 (114.00-115.00)	84.5

Table 6 shows that PIC_02 exhibits high variability in heart rate, resulting in fluctuations in R-R intervals that support synchronization based on the R-peaks, as this variation makes it easier to distinguish individual segments. Looking at *Figure 10*, long segments exhibit comparable performance across the seven synchronization methods, with the exception of the RRIC & BPC approach using peaks detected by the Moving Mean with an offset of 0.2. Due to the lower offset, this method identified more peaks compared with NeuroKit and the Moving Mean with an offset of 1 (see Table 5), making it more sensitive to noise. This increased sensitivity can result in discrepancies in peak identification between the ECG_{dwc} and $ECG_{us,int}$ signals, and difficulty in determining the correct timeshift.

All recordings containing artefacts allowed for validation of the correct timeshifts, as these artefacts were prominent in the ECG signal, making it easy to visually verify whether the determined timeshift was correct. An example is provided in *Appendix 8.6.3*. As shown in *Figure 10*, the RRIC method shows the lowest performance. Compared to short and long segments, artefacts cause greater discrepancies in peak detection between the ECG_{dwc} and $ECG_{us,int}$ signals, even a single missed peak in one of the signals leads to a complete shift in the R-R interval alignment. For the BPC method, peak detection using NeuroKit performs the worst, as NeuroKit detects R-peaks, while artefacts in the ECG signal introduce additional peaks that are not hemodynamic or patient-related. Not all segments containing artefacts could be successfully synchronized. In particular, timeshifts were not found for PIC_03_3. For PIC_03_2, a low performance was found, the three corresponding ECG_{us} segments, along with two other artefact-containing segments used for comparison, are provided in *Appendix 8.5*. Artefacts in PIC_03_2 resulted in the ECG moving out of the visible range in the ultrasound, resulting in flatline artefacts and missing data, which complicates peak detection and synchronization. This emphasizes that the nature of the artefact can critically affect the ability to detect peaks and achieve accurate synchronization. Artefacts characterized by a higher peak frequency were easier to synchronize.

In conclusion, a large number of the included ECG segments could not be validated, as it was not possible to confirm whether the identified timeshift was correct. A contributing factor for this was the absence of a ground truth, as no correct synchronization could be achieved using an artefact-containing segment from the same patient, underscoring the need for a suitable reference segment. For short recordings, the Pearson algorithm achieved the best performance (100%). For long recordings, the Pearson (100%) and the RRIC & BPC with NeuroKit (100% & 100%) and Moving Mean with an offset of 1 (75% & 100%) worked best, Moving Mean with an offset of 0.2 showed a poor performance (0% & 0%). For segments containing artefacts, Pearson (40%), BPC MM0.2 (33%), and MM1 (33%) showed the best performance, with performance expected to improve in the presence of high peak frequency artefacts compared to flatline artefacts.

4.8 Discussion

This study aimed to achieve synchronization between ultrasound imaging and hemodynamic waveforms. As with any research, certain limitations and considerations have emerged throughout the process. These are discussed below to provide context for the findings and to highlight areas for future improvement.

4.8.1 Time-based synchronization

A key challenge in achieving synchronization was that the internal clock of the ultrasound system frequently deviated, often unpredictably, from the time used by the patient monitor. This issue was partially mitigated by synchronizing the ultrasound system with the hospital's central time server by configuring the Network Time Source setting on the ultrasound system, allowing both systems to be aligned on a minute level. However, insights from clinical physics suggest that data recorded on patient monitors, including those saved in DWC, may gradually drift in timing, requiring periodic resets to maintain acceptable synchronization. Despite recent changes to the internal clock settings, the long-term stability and consistency of the synchronization with the hospital's central time server remain uncertain, possibly requiring manual updates to the Network Time Source setting.

Furthermore, the synchronization relies on the ECG signal available on both devices. The ECG signal is transmitted via a cable from the monitor to the ultrasound system, where it is displayed in green pixels at the bottom of the ultrasound screen (*Figure 3*). It is possible that there is a delay in the signal path, causing the ECG to appear slightly later on the ultrasound display than on the monitor, a factor that is currently not accounted for in the synchronization process. As a result, the two ECG signals may appear synchronized, while in reality, the ECG was not originally aligned with the ultrasound image.

4.8.2 ECG extraction from ultrasound

The ECG was extracted from the ultrasound images by isolating green pixels using a green filter. In certain ultrasound imaging settings, a green box appeared in the image when the ultrasound system was set to measure in 3D mode. This introduced complications for ECG extraction based on green pixel detection. An example of such a green 3D box can be found in *Appendix 8.2.4*. For these cases, the rows of interest were not selected from the minimum row containing green pixels to the last row of the image. Instead, the selection started from the lowest row containing green pixels that was at least located beyond half the image height, up to the last row of the image, to excluded the green box.

To determine the end of the ECG in the final frame, the derivative of the signal was calculated to detect sharp changes, which likely corresponded to the position of the black sweeping line. However, in cases of artefacts or missing data, the maximum derivative value did not align with the actual end of the ECG, but instead with noise or gaps in the data. The process of marking the ECG endpoint is illustrated

in *Appendix 8.2.5*. The derivative value at the location of the black sweeping line varied between patients, ranging from 9 to 12 pixels, making it impossible to define a single standard value. Moreover, a standard value could coincide with the maximum derivative caused by an artefact. In cases where the automatic detection failed, the endpoint index was manually adjusted to correctly indicate the end of the ECG (*Appendix 8.2.5*).

Although the ECG signal was extracted from the green pixel values in the image, it is not the original raw ECG signal. Prior to display, the signal undergoes preprocessing to ensure it fits within the visible range of the screen. For example, baseline drifts are corrected to prevent the waveform from exceeding the display boundaries, and signal peaks are scaled accordingly. However, some peaks still fall outside the visible ECG range on the screen, resulting in missing data and making it impossible to accurately determine their precise peak location, this was particularly the case for ultrasound recordings containing artefacts. This highlights the limitation of working with extracted ECG data obtained by filtering the green pixels, rather than using the raw ECG signal from the ultrasound.

4.8.3 Preprocessing

The extracted ECG signal from the ultrasound image was represented in row height, whereas the ECG data from the DWC system was recorded in millivolts and reflects the unprocessed, raw signal. The pixel-based extraction resulted in an ECG signal with an average sampling frequency of around 250 Hz, whereas the raw ECG data from the DWC system was sampled at 500 Hz. To enable synchronization, resampling the ECG_{us}-signals to 500 Hz was beneficial. Furthermore, the ECG_{dwc}, $ECG_{us,nan}$, and $ECG_{us,int}$ signals were cleaned using the `ecg_clean` function from the NeuroKit2 toolbox. While ECG_{dwc} represented the raw signal, containing baseline drift and high frequency noise (*Appendix 8.3.2*), which was resolved by `ecg_clean`, the ECG_{us} signals had already undergone some unspecified preprocessing steps before their visualization in the ultrasound image. Subsequently, all three signals were normalized to have a mean of 0 and a standard deviation of 1. It is important to note that normalization for ECG_{dwc} was performed over a longer time period (2 minutes) compared to a maximum of 10 seconds for the ECG_{us} signals. Consequently, the normalization of ECG_{dwc} was more affected by noise and outliers, which in turn influenced peak detection.

4.8.4 Synchronization

The synchronization approach which determines the timeshift based on the highest Pearson correlation between the full signals, is highly dependent on the signals' sampling rates. Higher sampling rates improve temporal resolution, whereas lower rates, or resampling, as applied to the $ECG_{us,nan}$ signal can reduce precision due to small shifts or smoothing of peaks introduced during interpolation. Furthermore, the preprocessing steps can affect the shape and timing of the signals, with outliers, particularly in the longer ECG_{dwc} segment.

Peak based synchronization, R-R Interval Correlation (RRIC) and Binned Peak Correlation (BPC), used peaks detected in the $ECG_{us,int}$ and ECG_{dwc} signals by NeuroKit and the Moving Mean with an offset of 0.2 and 1. RRIC is highly sensitive to discrepancies in peak detection. If even a single R-peak is missing in one of the two signals, the sequences of R-R intervals become misaligned. As a result, all subsequent R-R intervals shift, leading to a sharp drop in correlation, even if the rest of the peaks are accurately detected. As demonstrated in the results, the BPC method proved to be more robust, which aligns with the findings of previous research [20].

Artefacts were manually introduced into the ECG by physically interacting with the electrodes, providing clear visual markers for verifying alignment. As shown in *Appendix 8.5*, these artefacts varied in form. Some resulted in missing data as it was not visible in the ultrasound image, while other artefacts had a high peak frequency facilitating alignment with visual confirmation. Highlighting the need to consider the form of the artefact. Furthermore, during the ultrasound measurements, multiple artefacts were generated over subsequent recordings. As the timewindow of the ECG_{dwc} was 2 minutes, multiple artefacts were present within this timewindow. This made distinguishing between the different artefacts more challenging. Moreover, ECG artefacts can arise from patient positioning during surgery or patient positioning to enable ultrasound examination, they can appear within the 2-minute time window of ECG_{dwc}, complicating the identification of the artefact corresponding to the ultrasound measurement.

To use more data for detecting a timeshift, an attempt was made to concatenate individual ECG_{us} segments from different ultrasound recordings of the same patient for synchronization, with their original timestamps. However, this approach did not work, as timedrifting occurred within the ECG_{us}-signal, causing one ultrasound segment to align better than another at the same timeshift. Ultimately, when synchronizing the individual ultrasound segments, it was also found that the determined timeshift between ultrasound recordings varies within a single patient.

As observed in the results, the patient's level of heart rate variability has a significant impact on synchronization performance. *Table 6* shows that PIC_02 exhibits high variability in heart rate, leading to variation in R–R intervals, which facilitated synchronization based on the R-peaks. POR_02 and POR_03 also display considerable variation, but were not found validated (*Figure 10*). However, in the long segment included for POR_02, the R–R intervals were relatively regular, and no recording for POR_03 was classified as long. More data from various patients is needed to draw conclusions from the influence of the heart rate variability on the synchronization performance.

A large number of the included ECG segments could not be validated, as it was not possible to confirm whether the identified timeshift was correct. A contributing factor for this was the absence of a ground truth, as no correct synchronization could be achieved using an artefact-containing segment from the same patient, underscoring the need for a suitable reference segment. In particular, many recordings from PIC_03 could not be validated, partly due to the type of artefacts resulting in missing data and preventing synchronization. Additionally, this patient exhibited low heart rate variability, as shown in *Table 6*, and was receiving veno-arterial ECMO support. Furthermore, comparison of the ECG_{dwc} and ECG_{us} signals from PIC_03 revealed differences in R-peak morphology, which may be attributed to preprocessing steps applied to the signals. An example of these differences is provided in *Appendix 8.7*.

Synchronization was performed using the ECG_{us} signal extracted from the green pixels in the ultrasound image. Resampling and preprocessing steps were applied to make the two originally identical signals more comparable. Ideally, access to the raw ECG_{us} signal would significantly improve synchronization accuracy, as peaks would be detected at precisely the same locations, and artefact induced missing data in ECG_{us} would no longer be a problem. Although efforts were made to retrieve this data, they were unsuccessful. Further discussions with Philips, the manufacturer of the ultrasound systems used in this study, are recommended to explore possibilities for accessing raw ECG input and thereby enhancing the robustness of the synchronization process.

4.9 Conclusion

This master's thesis explored a method to synchronize ultrasound imaging with hemodynamic waveform data, using the available ECG signals as a reference. Synchronization is both essential and challenging, requiring consideration of multiple factors. One of the key elements is ensuring that all systems operate in alignment with the same (internal) clock. In this study, the ultrasound system was synchronized with the hospital's central time server, eliminating the need to manually determine the time offset between the ultrasound system and the vital signs monitor. This enabled the use of ultrasound timestamps to define an automatic and accurate time window within the hemodynamic waveforms for synchronization.

For synchronization, it is recommended to use Pearson correlation over the full ECG signals to determine the correct timeshift. When using peak-based synchronization methods, NeuroKit peak detection performs best in segments without artefacts, whereas the Moving Mean with an offset of 1 is more robust in segments containing artefacts. Among the evaluated approaches, the Binned Peak Correlation (BPC) method proved to be more resilient to discrepancies in peak detection compared to R-R Interval Correlation (RRIC), making it the preferred method. To visually validate synchronization, introducing an artefact with a high peak frequency is essential, as artefacts causing flatlines or signal dropout (e.g., due to the ECG line moving out of view) result in missing data and complicate validation.

Future research should include a larger cohort of patients with varying heart rate variability, and incorporate artefacts with high peak frequency to allow visual validation of the determined timeshifts, enabling more robust conclusions.

4.9.1 Future Research

A major limitation was the lack of access to raw ECG data from the ultrasound recordings. The ECG_{us} segments were extracted by isolating green pixels from the ultrasound screen. Future research should focus on obtaining raw ECG output directly from the ultrasound device. This would likely improve synchronization accuracy and reduce the need for artificial artefacts, enhancing both clinical applicability and automation potential. Moreover, it is worth investigating whether the visualization of the ECG displayed on the ultrasound image is identical to the visualization of the ECG on the vital signs monitor. It is possible that the preprocessing as observed on the ultrasound screen (as compared with the raw ECG obtained from Data Warehouse Connect (DWC)) was not performed by the ultrasound system itself, but had already been applied by the vital signs monitor before the signal was transmitted via the connecting cable. Instead of extracting the raw signal from the ultrasound for comparison with the raw DWC signal, an alternative approach could be to compare the visualized signal on the vital signs monitor with that displayed on the ultrasound device.

Future research should focus on inducing artefacts with a high peak frequency. Once the timeshift of the corresponding ECG segment is determined, it can be used to narrow the ECG_{dwc} timewindow for synchronizing subsequent ultrasound recordings from the same patient, potentially improving synchronization compared with the broader timewindow of 2 minutes. Moreover, developing a method to automatically include one recording in an ultrasound study with a high peak frequency artefact would facilitate clinical integration, as it would eliminate the need for additional manual manipulations to generate artefacts.

In this study, the focus was on detecting R-peaks using NeuroKit. However, additional ECG features, as P, Q, S, and T peaks, onset and offset times, or areas under the curve, could also be extracted. Considering the low variability observed in the signals, incorporating more features may reveal patterns or variations that are not captured by R-peaks alone, offering a richer basis for synchronization or signal analysis in future research. By combining this approach with a narrower timewindow enabled by synchronization to the artefact-containing segment, it is expected that including additional features will further improve synchronization.

4.10 Clinical usecases

There are numerous potential scenarios where synchronization of ultrasound with hemodynamic parameters can provide significant benefits, such as achieving more accurate beat-to-beat synchronization with ultrasound recordings. Two examples, one related to respiratory function and one to cardiac function, are outlined below, though many more could be identified. However, exploring all possible applications extends beyond the scope of this thesis.

4.10.1 Diaphragm Thickening Fraction

As highlighted in *Chapter 3.2* monitoring a patients respiratory effort during mechanical ventilation is essential. One promising non-invasive method for assessing respiratory effort is ultrasound evaluation of the diaphragm. The Diaphragm Thickening Fraction (DTF), measured in M-mode, quantifies the change in diaphragm thickness between inspiration and expiration [13, 14]. The DTF can be calculated using the following formula:

$$\text{DTF} = \frac{T_{\text{PI}} - T_{\text{EE}}}{T_{\text{EE}}} \times 100\%$$

where T_{PI} is the diaphragm Thickness at Peak Inspiration and T_{EE} is the Thickness at End Expiration. In clinical practice, the exact moments to determine T_{PI} and T_{EE} are difficult to pinpoint. Synchronizing ultrasound imaging with hemodynamic waveforms enables the identification of specific timepoints, which helps reduce one source of uncertainty. Currently, healthcare professionals must manually estimate when peak inspiration begins and when end expiration occurs. This uncertainty can be eliminated by synchronizing with the CO_2 curve. By examining the CO_2 curve, T_{PI} and T_{EE} can be accurately identified, allowing diaphragm thickness to be measured at these precise timepoints, as illustrated in *Figure 11*.

From *Figure 11*, a diaphragm thickness at T_{PI} of 2.41 mm and at T_{EE} of 1.96 mm were determined. Using these values, the DTF was calculated as

$$\text{DTF} = \frac{T_{\text{PI}} - T_{\text{EE}}}{T_{\text{EE}}} \times 100\% = \frac{2.41 - 1.96}{1.96} \times 100\% \approx 23\%.$$

Using this approach, a more structured and standardized protocol can be developed, eliminating assumptions regarding the timing and location of thickness measurements.

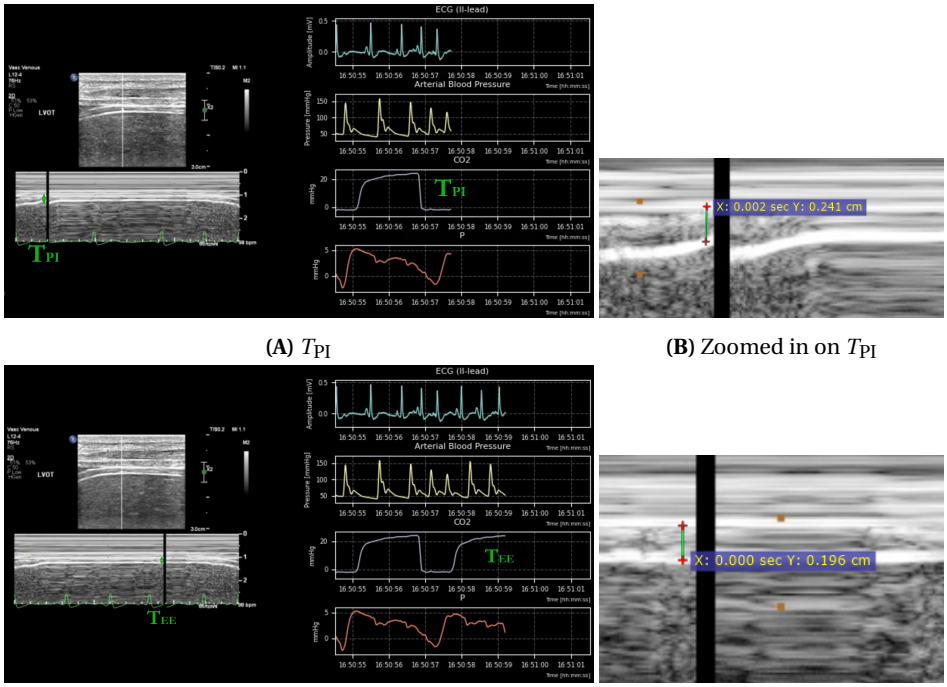

(A) T_{PI} **(B)** Zoomed in on T_{PI}

(C) T_{EE} **(D)** Zoomed in on T_{EE}

Figure 11: Measurement of diaphragm thickness using M-mode ultrasound synchronized with the CO_2 curve, enabling accurate assessment of the Diaphragm Thickening Fraction. **(A)** T_{PI}: diaphragm Thickness at Peak Inspiration; **(B)** zoomed view of T_{PI}; **(C)** T_{EE}: diaphragm Thickness at End Expiration; **(D)** zoomed view of T_{EE}.

4.10.2 Assessment of Stroke Volume

Synchronization of ultrasound imaging with hemodynamic waveforms can facilitate the calibration of Stroke Volume (SV) on a beat-to-beat level. When SV is determined using TransEsophageal Echocardiography (TEE), this can be used to calibrate with the area under the Arterial Blood Pressure (ABP) curve. The area from the start of systole to the dicrotic notch can be compared with the SV determined using TEE, resulting in a factor $k = \frac{SV}{\text{Area}}$. Once this factor is determined, the SV for subsequent heartbeats can be derived from the specified area under the ABP-curve. This could potentially reduce the need for invasive techniques (Swan-Ganz catheter) post-surgery for a limited period (under similar conditions). Estimating SV from the ABP curve can help a clinician easily assess cardiac output without using invasive techniques. However, many factors may influence this, and a detailed discussion is beyond the scope of this thesis.

An example is provided below illustrating the estimation of SV with the ABP-area. Synchronized ultrasound imaging with hemodynamic waveforms enables calibration at the level of individual heartbeats. This usecase was developed following the synchronization, as shown in *Figure 12A*, assessing the second heartbeat within the ultrasound recording for calibration. The area under the ABP-curve was determined, as illustrated in *Figure 12B*. SV can be calculated using the following formula [4]:

$$\text{Stroke Volume} = \left(\pi \left(\frac{\text{Diameter}_{\text{LVOT}}}{2}\right)^2 \times \text{VTI}_{\text{LVOT}}\right)$$

with the diameter of the Left Ventricular Outflow Tract (LVOT) measured using the parasternal long axis view, see *Figure 12C*, and the LVOT Velocity Time Integral (VTI) obtained from the apical 5-chamber or apical 3-chamber view as the area under the Pulse Wave, see *Figure 12D*.

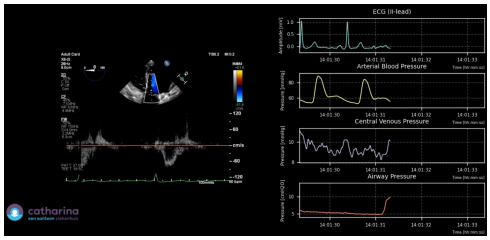

(A) Printscreen of synchronized ultrasound imaging with hemodynamic waveforms.

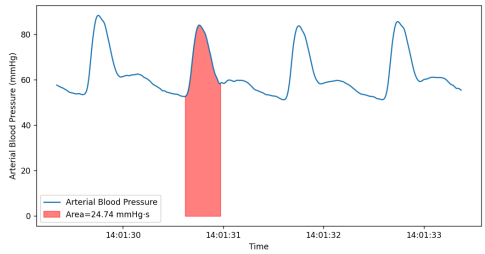

(B) Area ABP = 24.74 mmHg*s

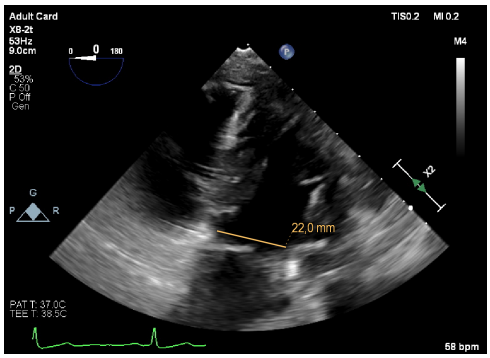

(C) Diameter LVOT = 22.0 mm

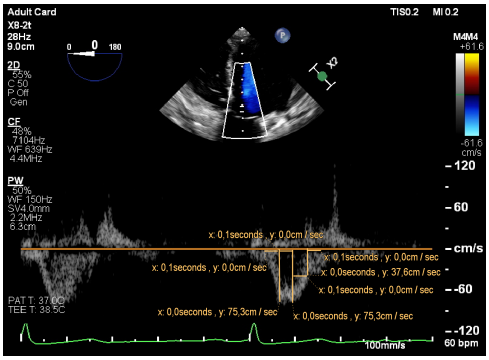

(D) VTI = 18.82 cm; calculated using the trapezium rule: (0.5 × 0.1 s × 75.3 cm/s) + (0.1 s × 75.3 cm/s) + (0.1 s × 37.6 cm/s) + (0.5 × 0.1 s × 37.7 cm/s) + (0.5 × 0.1 s × 37.6 cm/s).

Figure 12: Usecase with **(A)** synchronized ultrasound imaging and hemodynamic waveforms from which the second heartbeat is used for calibration; **(B)** the area under the Arterial Blood Pressure (ABP) curve; **(C)** the measurement of the diameter of the Left Ventricular Outflow Tract (LVOT); **(D)** the calculation of the Velocity Time Integral (VTI) from Pulse Wave Doppler.

The area under the ABP curve was 24.74 mmHg·s. With an LVOT diameter of 22.0 mm and a VTI of 18.82 cm, the stroke volume was calculated as 71.5 mL using the formula. From this, the scaling factor $k = \frac{SV}{\text{Area}}$ was determined as 2.89 mL·s/mmHg.

Using this approach, SV can be calibrated with the ABP area on a beat-to-beat basis, allowing estimation of SV for subsequent heartbeats from the ABP curve.

4.11 Implementation in clinical practice

To improve the accessibility and clinical usability of ultrasound review in combination with hemodynamic waveforms, synchronized integration is necessary. Ideally, this integration should occur within existing clinical review systems, rather than by introducing a separate platform. Therefore, it is recommended to implement this functionality directly into currently used hospital software. An example of such an implementation within the electronic health record system Hix is illustrated in *Figure 13*. The current radiology module and existing ultrasound review interface are shown. A proposed enhancement demonstrates how waveform data, such as hemodynamic or respiratory signals, could be displayed alongside the ultrasound image, with the ability to select relevant parameters. This layout is intended to support real-time clinical interpretation and streamline the workflow for healthcare professionals.

Synchronized visualization of ultrasound and waveform data offers several clinical advantages. It enables more accurate and efficient interpretation of anatomical images by correlating it with the synchronized hemodynamic waveforms. Furthermore, this beat-to-beat synchronization enables the standardization of protocols. For example, the timing of diaphragm thickness measurements can be aligned with the synchronized CO_2 curve, as outlined in *Chapter 4.10.1*, and the calibration of Stroke Volume (SV) with the area under the Arterial Blood Pressure (ABP) curve, for subsequent SV estimation based on the ABP curve, as illustrated in *Chapter 4.10.2*. Synchronization enables to structure and standardize such protocols.

Some implementation steps are still required. Currently, the monitoring data is sent to the database only every 12 to 24 hours. The data management process needs to be optimized to shorten this delay. Additionally, a connection between Hix and Data Warehouse Connect is necessary to integrate the waveforms with ultrasound review in Hix's radiology module.

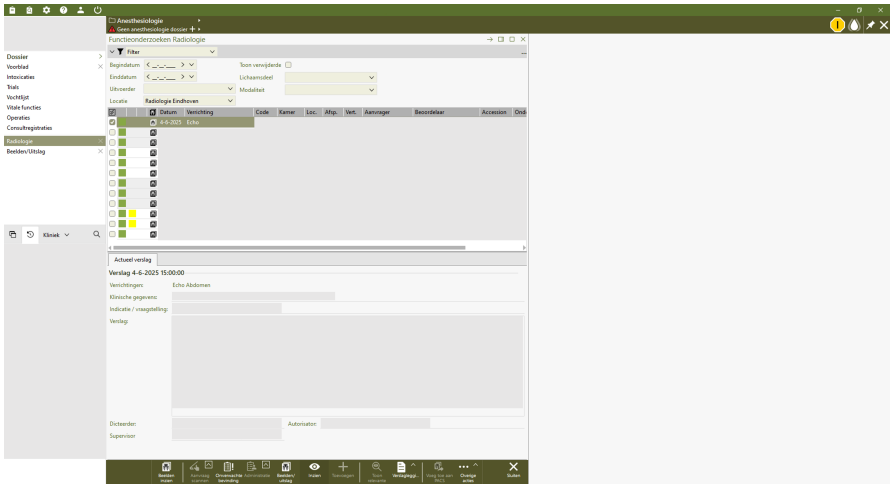

(A) Radiology module interface in Hix.

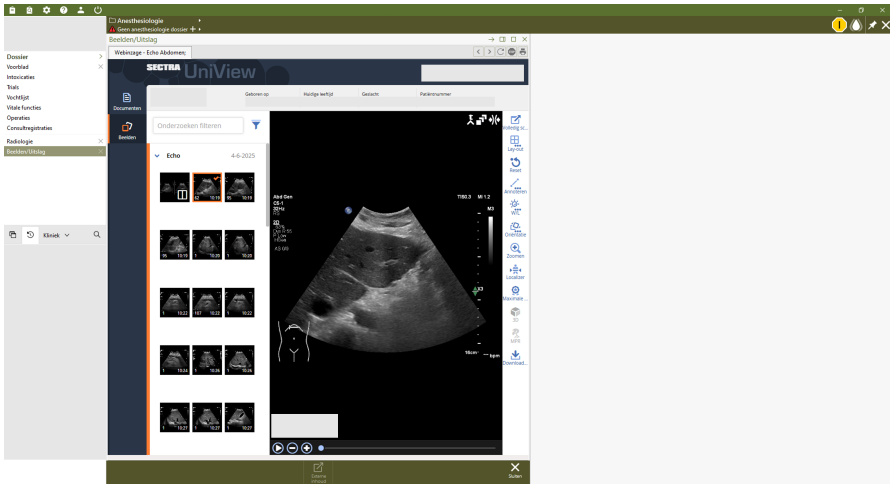

(B) Current ultrasound viewing options within Hix.

(C) Proposed integration of waveform data alongside ultrasound imaging, offering the ability to select from a range of hemodynamic parameters.

Figure 13: Overview of the current and proposed implementation of ultrasound and waveform integration within the Hix system.

5

Respiratory effort

Study on assessing respiratory effort in patients weaning from mechanical ventilation.

As part of this master's thesis project, a research protocol was developed to apply for ethical approval to compare different methods of measuring respiratory effort in patients undergoing weaning from mechanical ventilation, the complete protocol is included in *Appendix 8.8*.

5.1 Introduction / rationale protocol

In 2024, there were 70,108 admissions to Intensive Care Units (ICUs) in the Netherlands. On average, patients required mechanical ventilation for 9.6 hours per admission [7]. Mechanical ventilation is a critical component in the treatment of critically ill ICU patients, ensuring adequate respiratory support during episodes of severe illness and acute respiratory failure. However, prolonged mechanical ventilation can result in diaphragm dysfunction caused by both insufficient and excessive respiratory effort. This dysfunction complicates the weaning process and is associated with adverse clinical outcomes, including increased mortality and the risk of Patient Self-Inflicted Lung Injury (P-SILI) [21, 22]. Weaning is the process of gradually discontinuing mechanical ventilatory support and removing the endotracheal tube. Typically, this process begins with a Spontaneous Breathing Trial (SBT) to assess the patient's readiness for weaning [11]. The patient's readiness for weaning can be evaluated by measuring respiratory effort, which can be assessed using various methods.

Transdiaphragmatic pressure

The measurement of transdiaphragmatic Pressure (P_{di}) via an esophageal catheter is considered the reference standard [23]. P_{di} is calculated as the difference between gastric Pressure (P_{ga}) and esophageal Pressure (P_{es}), requiring the placement of a catheter capable of measuring both pressures. Limitations of assessing the pressure swings is the neglect of contraction duration and frequency, lack of correction for chest wall recoil pressure, and its weak association with energy expenditure [24]. The Pressure-Time Product (PTP_{es}) represents the area under the inspiration curve of the respiratory muscles Pressure (P_{mus}) during the inspiration phase, providing

an integrated measure of inspiratory effort [25, 26]. Compared to P_{di}, PTP_{es} better reflects muscle activity and energy expenditure [24]. A significant limitation of both P_{di} and PTP_{es} is the invasive approach.

Diaphragm electrical activity

An alternative catheter-based method to assess respiratory effort is the measurement of diaphragm Electrical activity (E_{di}) through a nasogastric (feeding) catheter. E_{di} provides a reliable estimate of respiratory drive by measuring neuromuscular transmission and has shown good correlation with P_{di} [27]. Some limitations of E_{di} include its inability to reflect the activation of accessory respiratory muscles, which reduces its suitability for assessing breathing effort at high workloads. Additionally, E_{di} measures neural drive rather than direct breathing effort, and it remains an invasive technique [24].

Diaphragm ultrasound

One promising non-invasive method for assessing respiratory effort is ultrasound evaluation of the diaphragm. The Diaphragm Thickening Fraction (DTF), measured in M-mode, quantifies the change in diaphragm thickness between inspiration and expiration. It has demonstrated a strong correlation with E_{di} [13]. However, its accuracy decreases in patients with diaphragmatic dysfunction, and it does not capture the duration or frequency of diaphragm excursions [14]. Despite these limitations, it remains a valuable non-invasive tool.

Occlusion pressures

Lastly, occlusion Pressure measurements from modern ventilators, obtained through an end-expiratory occlusion maneuver, provide another method for evaluating respiratory effort. P_{occ} represents the swing in airway Pressure (P_{aw}) generated by respiratory muscle effort when the airway is briefly occluded, while $P_{0.1}$ reflects the drop in P_{aw} during the first 100 milliseconds of an occluded breath [25]. However, this technique lacks standardization across ventilator models, with some providing an estimate of $P_{0.1}$ without requiring a maneuver. Furthermore, $P_{0.1}$ tends to underestimate respiratory drive, particularly in patients with high levels of effort [27].

To our knowledge, no study to date has evaluated all of these methods and their interrelationships in assessing respiratory effort in patients weaning from mechanical ventilation:

1. P_{di} & PTP_{es}
2. E_{di}
3. DTF
4. $P_{0.1}$ & P_{occ}

While previous studies have largely examined individual techniques in isolation, there is still a lack of systematic comparison, especially between invasive and

non-invasive methods. No clear consensus has emerged on the most accurate or practical approach. Understanding how these methods correlate may help determine whether certain non-invasive techniques, either alone or in combination, could serve as reliable surrogates for more invasive measurements. This could lay the foundation for developing a standardized, clinically feasible strategy for monitoring respiratory effort. Ultimately, such standardization could lead to more personalized weaning protocols based on patient-specific respiratory effort.

The selection of the study population aims to assess respiratory effort in a real-world ICU setting, using two distinct cohorts. The inclusion of post-operative cardiac surgery patients allows for the quantification of respiratory effort during weaning from mechanical ventilation following general anesthesia in a homogeneous group, free from known underlying respiratory complications. Additionally, the inclusion of ICU patients who have been on mechanical ventilation for more than 24 hours ensures a diverse representation of individuals at risk for diaphragm dysfunction.

By exploring the relationships between different respiratory effort parameters, including both invasive and non-invasive techniques, this study could provide evidence to support more individualized weaning and ventilation strategies. If non-invasive techniques, alone or combined, can reliably serve as alternatives to invasive standards, it could streamline monitoring practices. The findings may contribute to refining clinical guidelines, reducing diaphragm dysfunction, and ultimately improving weaning outcomes for ICU patients.

The complete research protocol can be found in *Appendix 8.8*

5.2 Discussion and Future Research

For this protocol, specific choices were made to enable a comparison between invasive and non-invasive respiratory effort measurement techniques. Since the non-invasive diaphragm ultrasound primarily reflects diaphragmatic activity, the double-balloon NutriVent catheter was selected. This catheter measures both gastric Pressure (P_{ga}) and esophageal Pressure (P_{es}), allowing the calculation of transdiaphragmatic Pressure (P_{di}). However, a new catheter is now available that enables the measurement of P_{es} in a steady state, eliminating the need for calibration and thereby improving ease of use. Nevertheless, the Nutrivent double balloon catheter was chosen to measure P_{di}, as its relationship with ultrasound-derived diaphragm parameters is under investigation, and P_{di} provides a more specific reflection of diaphragmatic activity, whereas P_{es} reflects the effort of all inspiratory muscles [28].

The ultrasound-derived parameter investigated is the Diaphragm Thickening Fraction (DTF). However, there is disagreement regarding its correlation with respiratory effort [29, 13, 14]. An emerging and promising ultrasound-derived parameter can

be obtained using speckle tracking software, which allows for the assessment of deformation (strain) and deformation velocity (strain rate) [12]. The DTF needs to be assessed in M-mode in order to determine the expansion of the diaphragm, where the speckle tracking software works in B-mode. In speckle tracking software, gray dots (speckles) are identified and tracked within the diaphragm. Strain (ε) represents the relative change in length between an initial reference state (L_0) and the compressed/shortened state (L). It is conventionally defined as: $\varepsilon = \frac{L-L_0}{L_0}$, where positive strain indicates stretching, and negative strain indicates shortening. Strain rate (ε") reflects the speed at which the deformation occurs and is defined as the time derivative of strain: $\varepsilon" = \frac{d\varepsilon}{dt}$. Unlike strain, strain rate reflects the instantaneous speed of deformation and does not require reference to an initial length [12].
In literature, the EchoPac Q-analysis tool from GE Healthcare is commonly used. However, no license for this software is currently available at Catharina Hospital Eindhoven. At the cardiology department, TomTec software from Philips is used for automated strain analysis of the heart muscle. It remains uncertain whether this tool can also be applied for speckle tracking of the diaphragm, but this represents an interesting direction for future research.
In practice, measuring both DTF and strain/strain rate is more complex, as they are acquired in different modes, M-mode and B-mode, respectively. This increases measurement time, and because these parameters must be correlated with other respiratory effort measures, it is preferable to narrow the ultrasound measurement time window.

6

Acknowledgements

This master's thesis originated from a spontaneous and unexpected conversation between Sander (my partner), and Arthur Bouwman at the Catharina Hospital, during which it came up that I was looking for a graduation internship. This led to a meeting with Arthur Bouwman, Ashley de Bie, and Igor Paulussen, and later with Frederique de Raat and Esmee de Boer. During these two meetings, their enthusiasm and support convinced me to conduct my graduation project at the Catharina Hospital in Eindhoven within the departments of Intensive Care and Anesthesiology.

Ashley de Bie supported me throughout the entire project. During our meetings a lot of new ideas were brought up and there was always time to dive deeper into the clinical relevance. I also learned a lot from the feedback sessions. I want to thank Ashley for his involvement, interest, and enthusiasm during this project.

Igor Paulussen was my daily supervisor and always easy to approach with questions. Time was always made to offer help or provide extra feedback when needed, which I really appreciated. I want to thank Igor for his interest, commitment, and enthusiasm throughout the project.

Arthur Bouwman always showed interest, was approachable for questions, and open to share new ideas. I would like to thank Arthur for that.

Frederique de Raat helped me find my way within Catharina. Sharing ideas about Technical Medicine in professional practice was very valuable. Help was always there whenever needed, and I would like to thank Frederique for that.

David van Westerloo (LUMC) was involved as a remote supervisor, from the LDE alliance (Leiden, Delft, and Erasmus), to ensure alignment with the Technical Medicine master's program. I would like to thank David for his interest and enthusiasm throughout this project.

Frank Gijsen (TU Delft) has joined the graduation committee as an independent member. I would like to thank Frank for the time he has dedicated to this role.

7

References

[1] J. Y. Kan, S. Arishenkoff, and K. Wiskar. "Demystifying Volume Status: An Ultrasound-Guided Physiologic Framework". In: *Chest* 167.6 (2025), pp. 1667–1683. DOI: 10.1016/j.chest.2024.12.026. URL: https://doi.org/10.1016/j.chest.2024.12.026.

[2] Frederique Maria de Raat et al. "Comparison between Handheld Echocardiography and Cardiac Magnetic Resonance for Stroke Volume and Left Ventricular Ejection Fraction Quantification". In: *Journal of Medical Ultrasound* 32.3 (July 2024), pp. 215–220. DOI: 10.4103/jmu.jmu_52_23. URL: https://doi.org/10.4103/jmu.jmu_52_23.

[3] L. Zieleskiewicz et al. "Point-of-care ultrasound in intensive care units: assessment of 1073 procedures in a multicentric, prospective, observational study". In: *Intensive Care Medicine* 41.9 (2015), pp. 1638–1647. DOI: 10.1007/s00134-015-3952-5. URL: https://doi.org/10.1007/s00134-015-3952-5.

[4] K. Guevarra and Y. Greenstein. "Ultrasonography in the Critical Care Unit". In: *Current Cardiology Reports* 22.11 (2020), p. 145. DOI: 10.1007/s11886-020-01393-z. URL: https://doi.org/10.1007/s11886-020-01393-z.

[5] Jeroen Huygh et al. "Hemodynamic monitoring in the critically ill: an overview of current cardiac output monitoring methods". In: *F1000Research* 5 (2016), F1000 Faculty Rev–2855. DOI: 10.12688/f1000research.8991.1. URL: https://doi.org/10.12688/f1000research.8991.1.

[6] I. Suriani et al. "Carotid Doppler ultrasound for non-invasive haemodynamic monitoring: a narrative review". In: *Physiological Measurement* 43.10 (2023). DOI: 10.1088/1361-6579/ac96cb. URL: https://doi.org/10.1088/1361-6579/ac96cb.

[7] Stichting NICE. *Basisgegevens IC-units 2024*. https://www.stichting-nice.nl/datainbeeld/public?year=2024&subject=BASIC&

hospital= - 1 & icno = 0. [Dataset]. Data in Beeld. Retrieved July 16, 2025. 2024.

[8] S. Sartini et al. "The Role of POCUS in Acute Respiratory Failure: A Narrative Review on Airway and Breathing Assessment". In: *Journal of Clinical Medicine* 13.3 (2024), p. 750. DOI: 10.3390/jcm13030750. URL: https://doi.org/10.3390/jcm13030750.

[9] M. Beshara et al. "Nuts and bolts of lung ultrasound: utility, scanning techniques, protocols, and findings in common pathologies". In: *Critical Care* 28.1 (2024), p. 328. DOI: 10.1186/s13054-024-05102-y. URL: https://doi.org/10.1186/s13054-024-05102-y.

[10] R. Tonelli et al. "Assessing inspiratory drive and effort in critically ill patients at the bedside". In: *Critical Care (London, England)* 29.1 (2025), p. 339. DOI: 10.1186/s13054-025-05526-0. URL: https://doi.org/10.1186/s13054-025-05526-0.

[11] J. M. Boles et al. "Weaning from mechanical ventilation". In: *The European Respiratory Journal* 29.5 (2007), pp. 1033–1056. DOI: 10.1183/09031936.00010206.

[12] E. Oppersma et al. "Functional assessment of the diaphragm by speckle tracking ultrasound during inspiratory loading". In: *Journal of Applied Physiology* 123.5 (2017), pp. 1063–1070. DOI: 10.1152/japplphysiol.00095.2017.

[13] Michael C. Sklar, Fabiana Madotto, Andre H. Jonkman, et al. "Duration of diaphragmatic inactivity after endotracheal intubation of critically ill patients". In: *Critical Care* 25.1 (2021), p. 26. DOI: 10.1186/s13054-020-03435-y. URL: https://doi.org/10.1186/s13054-020-03435-y.

[14] Michele Umbrello et al. "Oesophageal pressure and respiratory muscle ultrasonographic measurements indicate inspiratory effort during pressure support ventilation". In: *British Journal of Anaesthesia* 125.1 (2020), e148–e157. DOI: 10.1016/j.bja.2020.02.026. URL: https://doi.org/10.1016/j.bja.2020.02.026.

[15] A. Noor et al. "Point-of-Care Ultrasound Use in Hemodynamic Assessment". In: *Biomedicines* 13.6 (2025), p. 1426. DOI: 10.3390/biomedicines13061426.

[16] Philips Healthcare. *Affiniti 70 Ultrasound System*. Accessed: 2025-08-02. 2025. URL: https://www.philips.nl/healthcare/product/HC795210/affiniti-70-ultrasound-system#galleryTab=CLI.

[17] Philips Healthcare. *EPIQ CVx – Premium Cardiology Ultrasound System*. Accessed: 2025-08-02. 2025. URL: https://www.philips.nl/healthcare/

product / HC795231 / epiq - cvx - premium - cardiology - ultrasound-system.

[18] Dominique Makowski et al. "NeuroKit2: A Python toolbox for neurophysiological signal processing". In: *Behavior Research Methods* 53.4 (2021). Accessed on July 16, 2025, pp. 1689–1696. DOI: 10.3758/s13428-020-01516-y. URL: https://neuropsychology.github.io/NeuroKit/functions/ecg.html#neurokit2.ecg.ecg_clean.

[19] T. Nguyen et al. "Low Resource Complexity R-peak Detection Based on Triangle Template Matching and Moving Average Filter". In: *Sensors (Basel, Switzerland)* 19.18 (2019), p. 3997. DOI: 10.3390/s19183997. URL: https://doi.org/10.3390/s19183997.

[20] M. Alhaskir et al. "ECG Matching: An Approach to Synchronize ECG Datasets for Data Quality Comparisons". In: *Studies in Health Technology and Informatics* 307 (2023), pp. 225–232. DOI: 10.3233/SHTI230718. URL: https://doi.org/10.3233/SHTI230718.

[21] E. C. Goligher et al. "Mechanical Ventilation-induced Diaphragm Atrophy Strongly Impacts Clinical Outcomes". In: *American Journal of Respiratory and Critical Care Medicine* 197.2 (2018), pp. 204–213.

[22] M. Dres et al. "Coexistence and Impact of Limb Muscle and Diaphragm Weakness at Time of Liberation from Mechanical Ventilation in Medical Intensive Care Unit Patients". In: *American Journal of Respiratory and Critical Care Medicine* 195.1 (2017), pp. 57–66. DOI: 10.1164/rccm.201602-0367OC.

[23] A. H. Jonkman et al. "The oesophageal balloon for respiratory monitoring in ventilated patients: updated clinical review and practical aspects". In: *European Respiratory Review* 32.168 (2023), p. 220186. DOI: 10.1183/16000617.0186-2022.

[24] H. de Vries et al. "Assessing breathing effort in mechanical ventilation: physiology and clinical implications". In: *Annals of Translational Medicine* 6.19 (2018), p. 387. DOI: 10.21037/atm.2018.05.53.

[25] R. Cornejo, I. Telias, and L. Brochard. "Measuring patient's effort on the ventilator". In: *Intensive Care Medicine* 50.4 (2024), pp. 573–576. DOI: 10.1007/s00134-024-07352-4.

[26] T. Mauri et al. "Esophageal and transpulmonary pressure in the clinical setting: meaning, usefulness and perspectives". In: *Intensive Care Medicine* 42.9 (2016), pp. 1360–1373. DOI: 10.1007/s00134-016-4400-x.

[27] A. H. Jonkman, H. J. de Vries, and L. M. A. Heunks. "Physiology of the Respiratory Drive in

ICU Patients: Implications for Diagnosis and Treatment". In: *Critical Care* 24.1 (2020), p. 104. DOI: 10.1186/s13054-020-2776-z.

[28] Julien P van Oosten et al. "Solid-state esophageal pressure sensor for the estimation of pleural pressure: a bench and first-in-human validation study". In: *Critical Care* 29.1 (2025), p. 47.

[29] T. Poulard et al. "Poor Correlation between Diaphragm Thickening Fraction and Transdiaphragmatic Pressure in Mechanically Ventilated Patients and Healthy Subjects". In: *Anesthesiology* 136.1 (2022), pp. 162–175. DOI: 10.1097/ALN.0000000000004042.

8 Appendix

8.1 Appendix – Literature Study

Master Technical Medicine
Leiden, Delft & Rotterdam - the Netherlands

&

Catharina Ziekenhuis, Department of Intensive Care & Anesthesia
Eindhoven - the Netherlands

Literature Study: Carotid ultrasound for fluid responsiveness assessment in mechanically ventilated patients.

February 7, 2025

Femke Bosman (5658012)
Literature Study Master Thesis
Period = 16/12/2024 - 07/02/2025
Track Imaging and Intervention

Supervised by:
Medical supervisor
Ashley de Bie Dekker, Internist-Intensivist, Catharina Ziekenhuis
LDE-supervisor
David van Westerloo, Internist-Intensivist, LUMC
Daily supervisor
Frederique de Raat, PhD-Candidate, Catharina Ziekenhuis

Arthur Bouwman, Anesthesiologist & Professor, Catharina Ziekenhuis
Igor Paulussen, Research Coördinator & PA, Catharina Ziekenhuis

1 Introduction

In critically ill patients, fluid administration is often required to stabilize circulation during hemodynamic instability. However, only 50% of hemodynamically unstable patients are fluid responsive, meaning their cardiac output (CO) increases following a fluid challenge. The Frank-Starling curve describes the relationship between cardiac preload and stroke volume (SV) [1, 2, 3]. Its shape depends on the patient's ventricular systolic function, meaning a fluid challenge can either significantly or negligible increase SV and CO [4]. While insufficient volume is harmful, excessive fluid administration will cause tissue edema, leading to compartment syndromes and reduced oxygen delivery, which in turn increases mortality [5, 6]. Therefore, it is essential to evaluate a patient's fluid responsiveness (FR) prior to fluid administration. Fluid responsiveness assessment is particularly complex in mechanically ventilated patients, as positive pressure ventilation influences preload and cardiac function [4]. Various methods are available to assess fluid responsiveness in mechanically ventilated patients.

Stroke volume variation (SVV) and pulse pressure variation (PPV) are dynamic indices that reflect cyclic intrathoracic pressure changes during positive pressure ventilation. These changes influence venous return and cardiac preload, leading to fluctuations in SV and arterial pulse pressure. By analyzing these variations, SVV and PPV provide a bedside tool for evaluating preload responsiveness. However, they are unreliable in spontaneously breathing patients (also while intubated), and patients with cardiac arrhythmias [4].

While the SVV & PPV make use of the positive pressure ventilation, the passive leg raise (PLR) serves as an alternative method to assess fluid responsiveness. The PLR is a reversible maneuver that simulates a fluid challenge of around 300 mL blood without the infusion of any fluid. Continuous and real time cardiac output (CO) monitoring is essential to assess the effects of PLR. This can be done invasively using pulse contour analysis, such as PiCCO, or non-invasively through echocardiographic measurements of PLR-induced changes in the velocity time integral (VTI) of the left ventricular outflow tract, both of which are reliable indicators. Due to the need for real-time monitoring, intermittent CO measurements with thermodilution are unsuitable, and the accuracy of CO measurements by bioreactance has been questioned [4, 7, 8].

Cardiac output measurements with PiCCO and echocardiography can also be used to assess fluid responsiveness during a fluid challenge with fluid administration. However, unlike PLR, this method requires the actual infusion of fluids, which is a form of treatment itself and can therefore be considered a disadvantage [4].

In summary, fluid responsiveness can be assessed through different methods, either relying on pressure variation during mechanical ventilation or a fluid challenge. The choice of method depends on the patient's condition and the monitoring tools available.

Ideally, a test to differentiate fluid responders (FR+) from non-responders (FR-) should be accurate, non-invasive, readily available, rapid, reproducible, and require minimal training. However, existing methods have notable limitations. PiCCO requires both an arterial and a central venous catheter, making it minimally invasive, while VTI assessment with echocardiography, requires extensive experience. These drawbacks highlight the need for an alternative approach. Point-of-care ultrasound (POCUS) is a widely available bedside monitoring technique [9]. Combined with the superficial and easily accessible carotid artery, carotid ultrasound emerges as a promising tool for assessing fluid responsiveness.

The aim of this study was to review existing literature to determine the accuracy and reliability of carotid ultrasound measures to assess fluid responsiveness, compared with reference standards, in mechanically ventilated patients.

2 Methods

2.1 Search Strategy & Study Selection Process

The literature search was performed in *PubMed* with the following search term: [(doppler ultrasound imaging[MeSH Terms]) OR (echography[MeSH Terms])] AND [(carotid arteries[MeSH Terms])] AND [(fluid ther-

apy[MeSH Terms]) OR (stroke volume[MeSH Terms]) OR (cardiac output[MeSH Terms])]. The search was saved in *PubMed* under the 'Collections' section, and the identified articles were then exported to *EndNote*. *EndNote* was used as a tool to manage and monitor the inclusion process. Articles were included if they utilized carotid ultrasound to differentiate between fluid responders (FR+) and non-responders (FR-). Exclusion criteria were: studies involving patients who were not mechanically ventilated, age <18 years, pregnancy, non-human studies, single case reports, systematic reviews and non-English articles. The inclusion and exclusion criteria were initially applied by one reviewer during the abstract screening process. Following this, the full texts of the selected articles were reviewed in detail to make the final selection for the literature review.

2.2 Comparison of results

To compare the studies, the following details were identified and summarized in a table: publication year, location, article type, setting, number of patients included, type of participants, percentage & type of mechanical ventilation, percentage of fluid responsiveness, reference standard for fluid responsiveness, performed fluid challenge, carotid measures, and results. To ensure an accurate comparison, the identified carotid measurements were systematically listed alongside their corresponding area under the receiver operating characteristic (ROC) curve (AUC), sensitivity, and specificity for fluid responsiveness assessment. These values were then directly compared to the reference standards for fluid responsiveness assessment, as presented in Table 1. The reference standards include PPV [10] and SVV [11], measured under mechanical ventilation with preload variation between inspiration and expiration, as well as PLR maneuver combined with CO monitoring using bioreactance [12], PiCCO[12], TTE[13], and VTI[14].

3 Results

3.1 Selection Process

The search was performed on PubMed on January 7, 2025, yielding 127 results. Following the selection process, 10 articles were included in the literature review with a total of 418 patients [15, 16, 17, 18, 19, 20, 21, 22, 23, 24]. Eight of these articles were identified directly through the PubMed search, while two were obtained from a systematic review included in the search results [25]. The inclusion process is illustrated in *Figure 1*, and *Table 2* provides details of the included articles.

Table 1: The area under the receiver operating characteristic curve (AUC), sensitivity & specificity for reference standards in assessing fluid responsiveness, the values in brackets [] represent the 95% Confidence Interval (when available) [10, 11, 12, 13, 14]. **PPV**: Pulse pressure variation; **SVV**: Stroke volume variation; **TTE**: Transthoracic echocardiography; **VTI**: Velocity time integral.

Fluid challenge	Reference standard	AUC	Sensitivity	Specificity
Mechanical ventilation	PPV	94% [91-95]	88% [81-92]	89% [84-92]
	SSV	93% [90.7-94.5]	81% [77-85]	80% [70-88]
Passive leg raise	Bioreactance	50%	/	/
	PiCCO	87%	84% [60-97]	97% [82-100]
	TTE	94%	86% [79-91]	90% [83-94]
	VTI	91.9% [81.9-97.3]	78.1% [60-90.7]	96.4% [81.7-99.9]

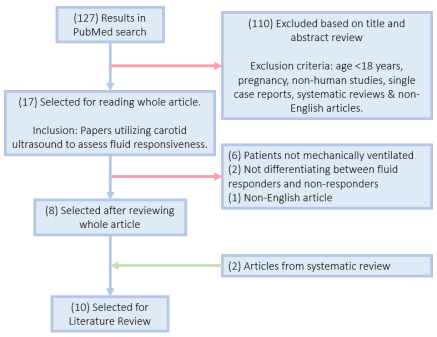

Figure 1: Flow diagram of the inclusion process.

The average fluid responsiveness across all patients was 61%, calculated using the formula $\frac{\sum_{n=1}^{N}(p_n \cdot \%FR_n)}{\sum_{n=1}^{N} p_n} \times 100\%$ where N represents the number of articles, p_n is the number of participants in the n-th article, and $\%FR_n$ is the fluid responsiveness percentage for the n-th article. 87% of the patients were mechanically ventilated, calculated using the same formula, substituting the fluid responsiveness percentage for percentage of mechanically ventilated patients.

In PubMed search	SR Beier	First Author	Year	Location	Article type	Setting	n	Participants	Mechanically ventilated	Fluid Responsive	Reference standard	Fluid Challenge	Carotid Measure	Results
✔	✔	Marik	2013	USA	Evaluation study	ICU	34	Hemodynamically unstable patients	56%, TV: 6-8 ml/kg	53%	≥10% increase in SVI assessed by non-invasive bioreactance	Baseline: 45° semi-recumbent position. PLR: supine with legs raised in 45° (3min) FA: 500 mL of normal saline over 10 min.	CBF & carotid diameter	PLR had a sensitivity of 94% and specificity of 100%. For the mechanically ventilated patients: SVV was 18.0%±5.1% in the FR+ and 14.8%±3.4% in the FR- (p=0.15). CBF increased by 79%±32% after the PLR in the FR+ compared with 0.1±14% in FR- (p<0.001). There was a strong correlation between the percent change in SVI by PLR and the concomitant percent change in CBF (r=0.59, P=0.0003). Using a 20% threshold increase in CBF to predict volume responsiveness, there were two false positives and one false negative, resulting in a sensitivity of 94% and specificity of 86%. A significant increase in the common carotid artery diameter was observed in FR+.
✔	✔	Song	2014	Korea	Clinical trial	OR	40	Undergoing coronary bypass surgery	100%, TV: 8 ml/kg, PEEP: 5 cmH2O	57,50%	≥15% increase in SVI measured with pulmonary artery catheter	FA: 6 mL/kg of 6% hydroxyethyl starch 130/0.4.	ΔCDPV	ΔCDPV showed a significant difference (p<0.001) between FR+ & FR- before VE, 13 (IQR 11-16) & 8 (IQR 7-10), respectively. A significant difference (p<0.001) was found for the FR+ before & after VE, 13 (IQR 11-16) & 6 (IQR 5-8), respectively. AUROC for ΔCDPV was 0.85 (95% CI 0.72–0.97) with cut-off value for FR+ of 11%, with sensitivity and specificity of 0.85 and 0.82, respectively.
✘	✔	Ibarra Estrada	2015	Mexico	Prospective cohort study	ICU	19 patients (59 cases)	Septic shock and lung protective mechanical ventilation	100%, TV: 6 ml/kg	51%	>15% increase in SVI measured with transpulmonary thermodilution	Baseline: 45° semi-recumbent position. PLR: supine with legs raised in 45° (3min). FA: 7 mL/kg normal saline in 30 min.	ΔCDPV	ΔCDPV had an AUROC of 0.88 (95% CI 0.77-0.95); followed by SVV (0.72, 95% CI 0.72, 95% CI 0.63-0.88), PLR (0.69, 95% CI 0.56-0.80), and PPV (0.63, 95% CI 0.49-0.75). The ΔCDPV was a statistically significant superior predictor when compared with the other parameters. Sensitivity (86%), specificity (86%) and positive and negative predictive values were also the highest for ΔCDPV, with an optimal cutoff at 14%. There was good correlation between ΔCDPV and SVI increment after the fluid challenge (r=0.84, p<0.001, 95% CI 0.74-0.90).
✔	✔	Lu	2017	China	Prospective observational study	ICU	49	Septic shock	100%, TV: 8-10 ml/kg, PEEP: 5-12 cmH2O	55%	≥10% increase in cardiac index with cardiac output measured with PiCCO (CI = CO/BSA)	FA: 200 mL normal saline via central venous line in 10 min.	ΔCDPV	ΔCDPV has an r-value and p-value of 0.852 & 0.01, respectively. An optimal cut-off for ΔCDPV was 13% to predict FR+ with AUC of 0.910, 95% CI 0.817-1.0, sensitivity of 78% and specificity of 90% (p<0.001).
✔	✔	Roehrig	2017	Australia	Prospective observational study	OR	33	Patients after coronary bypass surgery	100%, TV: 6-8 ml/kg, PEEP: 5 cmH2O, from volume-controlled to pressure support mode.	60,60%	>10% increase in CO assessed by triplicate bolus thermodilution	Baseline: 30° semi-recumbent position. PLR: supine with legs raised in 30° (5min).	CBF & ΔCDPV	A significant correlation between CBF and CO was shown (r=0.80; 95% CI, 0.61-0.89, p<0.0001), including relative changes after PLR (r=0.79; 95% CI, 0.60-0.89, p<0.0001) that showed a mean difference of 2% with wide limits of agreement (-19%-16%). Changes in CBF after PLR correlated with the baseline arterial resistance but not with compliance or effective elastance. A ΔCDPV >10% before PLR discriminated FR+ to the maneuver with an AUROC of 0.81 (95% CI, 0.55-0.95, p=0.03), with sensitivity and specificity of 83%.

Table 2a: Details of the included studies utilizing carotid ultrasound to assess fluid responsiveness.
BSA: body surface area; **CI**: cardiac index; **CBF**: carotid blood flow; **CO**: cardiac output; **ΔCDPV**: respiratory variation in carotid Doppler peak velocity; **FA**: fluid administration; **FR+**: fluid responders; **FR-**: fluid non-responders; **ICU**: intensive care unit; **MAP**: mean arterial blood pressure; **OR**: operating room; **PLR**: passive leg raise; **PPV**: pulse pressure variation; **ΔPSV**: peak systolic velocities; **SV**: stroke volume; **SVI**: stroke volume index; **SVV**: stroke volume variation; **TV**: tidal volume; **WF+**: subgroup with periodic waveform changes; **WF-**: subgroup without periodic waveform changes.

In PubMed search	SR Beier	First Author	Year	Location	Article type	Setting	n	Participants	Mechanically ventilated	Fluid Responsive	Reference standard	Fluid Challenge	Carotid Measure	Results
✓	✓	Barjaktarevic	2018	USA	Prospective non-interventional study	ICU	77	Patients with new, undifferentiated shock and vasopressor requirements despite fluid resuscitation	Subgroups: 59% mechanical ventilation, 47% passive ventilation (of ventilated group) & PEEP >5 mmHg. No significant difference between subgroups.	70,10%	≥10% increase in SV on bioreactance NICOM (non-invasive cardiac output monitoring)	Baseline: 45° semi-recumbent position (10min). PLR: supine with legs raised in 45° (3min).	ccFT (Wodey's formula)	FR+ had a greater increase in ccFT after PLR than FR- (14.1±19 vs -4.0±8ms, p<0.001). The precentage increase from baseline in ccFT was also higher among FR+ than FR-, 4.8±6.4 vs -1.4±2.9%, p<0.001. Cut-off value of 7msec as a ΔccFT had a specificity of 96%, sensitivity of 68%, AUC of 0.88, predictive value of 97% and accuracy of 82% in detecting FR+ using NICOM.
✗	✓	Girotto	2018	France	Prospective study	ICU	33 patients (39 cases)	Patients with a noninvasive cardiac monitor	94%	93%	≥10% increase in CI measured with PiCCO	PLR (1min) FA: 500 mL normal saline in 10 min.	CBF & ΔPSV	A positive PLR response could not be detected by changes in CBF or carotid ΔPSV (AUROCs: 0.58±0.10 and 0.56±0.09, respectively, all not different from 0.50). The correlations between simultaneous changes in CI & CBF during PLR and volume expansion were not significant (p=0.41).
✓	✓	Jalil	2018	USA	Prospective, cohort study	ICU	22	ICU patients with a noninvasive cardiac monitor requiring a fluid bolus	82%	45%	≥15% increase in SV measured with arterial catheter (FloTrac/Vigileo)	Baseline: 45° semi-recumbent position. PLR: supine with legs 45° raised. (3min with 1min interval for ccFT measurement)	ccFT (Bazett's formula)	Using an increase of ≥24.6% in the ccFT in response to PLR to predict FR+ there was a sensitivity of 60%, specificity of 92%, positive likelihood ratio of 7.2, negative likelihood ratio of 0.4, positive predictive value of 86%, negative predictive value of 73% and receiver operating characteristic of 0.75(95%CI: 0.54-0.96) & 77% accuracy.
✓	✗	Zhang	2021	China	Prospective study	ICU	60	Traumatic shock patients requiring mechanical ventilation	100%, TV: ≥8 mL/kg, PEEP ≤5 mmHg	50%	>15% increase in CO assessed with echocardiography	FA: 250 mL 0.9% saline within 10 min.	ΔCDPV & periodic waveform changes (WF+/WF-)	ΔCDPV of FR+ & FR- was 17.01±11.15 & 4.12±13.27, respectively (p<0.001). AUC 0.803 (95% CI: 0.692-0.914) with cut-off value, sensitivity & specificity of 11.20 cm/s, 70% & 80%, respectively. ΔCDPV in WF+ & WF- was 19.28±10.29 & 13.60±11.96, respectively. When ΔCDPV in WF+ was >12.57%, the velocity waveform or morphology of the CA had significant periodic changes, with sensitivity of 77.8% and specificity of 66.7%. In FR+ 60% and for FR- 13.3% had waveform changes (WF+). Looking at the ROC curve, when the CA waveform showed periodic variation, specificity for indicating FR reached 86.7%.
✓	✗	Zhao	2024	China	Prospective single-center study	ICU	51	VV-ECMO patients with PiCCO and prone ventilation	100%, TV: 4-6 mL/kg	64,70%	≥15% SVI assessed with TTE (SVI = (left ventricular outflow tract area * aortic flow velocity time integral) / BSA)	Baseline: +15° prone position. PLR: Trendelenburg prone position (-15°) (1min) FA: 500 ml crystalloids over 15min	ΔCDPV & ccFT (Wodey's formula)	SVI-trend, ccFT & ΔCDPV demonstrated superior predictive performance of fluid responsiveness. SVI-trend had an AUC of 0.89 (95% CI, 0.80–0.98) with an optimal threshold of 14.5% (95% CI, 12.5-21.5%), with the sensitivity and specificity were 82% (95% CI 66-91%) and 83% (95% CI, 61-94%). ccFT had an AUC of 0.87 (95% CI, 0.76–0.98) with an optimal threshold of 332ms (95% CI, 318-335ms), the sensitivity and specificity were 85% (95% CI, 69–93%) and 83% (95% CI, 61–94%), respectively. ΔCDPV showed an AUC of 0.83 (95% CI, 72–95), with a 10% optimal threshold (95% CI, 9–13%), sensitivity was 82% (95% CI, 66–91%) and specificity 78% (95% CI, 55–91%). SVI-trend, ccFT and ΔCDPV could effectively predict fluid responsiveness in VV-ECMO patients with ARDS in the PP. Compared to SVI-trend and ΔCDPV, ccFT is easier and more direct to acquire, and it does not require Trendelenburg position or VE, making it a more accessible and efficient option for assessing fluid responsiveness.

Table 2b: Details of the included studies utilizing carotid ultrasound to assess fluid responsiveness.
BSA: body surface area; **CI**: cardiac index; **CBF**: carotid blood flow; **CO**: cardiac output; **ΔCDPV**: respiratory variation in carotid Doppler peak velocity; **FA**: fluid administration; **FR+**: fluid responders; **FR-**: fluid non-responders; **ICU**: intensive care unit; **MAP**: mean arterial blood pressure; **OR**: operating room; **PLR**: passive leg raise; **PPV**: pulse pressure variation; **ΔPSV**: peak systolic velocities; **SV**: stroke volume; **SVI**: stroke volume index; **SVV**: stroke volume variation; **TV**: tidal volume; **WF+**: subgroup with periodic waveform changes; **WF-**: subgroup without periodic waveform changes.

3.2 Study methodologies

There was a difference in setting for the studies, 8 studies were conducted at the intensive care unit (ICU) [15, 17, 18, 20, 21, 22, 23, 24] and 2 in the operating room (OR) [16, 19]. To assess fluid responsiveness and perform a fluid challenge, 3 studies did fluid administration [16, 18, 23], 3 used passive leg raise (PLR) [19, 20, 22], and 4 a combination of both [15, 17, 21, 24]. As shown in *Table 2*, the fluid challenges differed across studies. The fluid administration varied in both the type of fluid used and the duration of infusion. The method of performing the PLR varied in terms of both angle and duration. Notably, Zhao et al. [24] used the Trendelenburg maneuver as the patients were in the prone position.

As outlined in *Table 2*, different reference standards were used to determine fluid responsiveness. Cut-off values of either 10 or 15% were used for cardiac output (CO), cardiac index (CI), stroke volume (SV) and stroke volume index (SVI), which are inherently related: $CO = SV \times heartrate$, $CI = \frac{CO}{BSA}$ & $SVI = \frac{CI}{heartrate}$. Additionally, the reference assessment methods varied, including non-invasive techniques such as bioreactance [20, 15], echocardiography [23], and transthoracic echocardiography (TTE) [24], as well as invasive approaches utilizing an arterial catheter with vigilance monitoring [16, 22], thermodilution [17, 19], and PiCCO [21, 18], which requires both a central venous and an arterial catheter.

3.3 Carotid Measures

The following carotid measures, obtained through carotid ultrasound examination, were investigated for their potential in assessing fluid responsiveness: respiratory variation in carotid Doppler peak velocity (ΔCDPV) in 6 studies [16, 17, 18, 19, 23, 24], carotid blood flow (CBF) in 3 studies [15, 19, 21], corrected carotid flow time (ccFT) in 3 studies [20, 22, 24], carotid diameter in 1 study [15], and carotid peak systolic velocity (ΔPSV) in 1 study [21].

The respiratory variation in carotid Doppler peak velocity ΔCDPV was investigated in 6 of the 10 articles [16, 17, 18, 19, 23, 24], and calculated using the following formula: $\Delta CDPV = \frac{\text{Max peak} - \text{Min peak}}{\frac{1}{2} \times (\text{Max peak} + \text{Min peak})} \times 100\%$. In 1 of these articles, the max peak was defined as the end-inspiratory V_{max}, and the min peak as the end-expiratory V_{max} [23]. The results of the receiver operating characteristic curves (ROC) are shown in *Table 3*.

Table 3: Results of the Receiver Operating Characterisctic Curves (ROC) for ΔCDPV from 6 papers. AUC is the area under the ROC curve, and the values in brackets [] represent the 95% Confidence Interval (when available).

Paper	Cut-off value	AUC	Sensitivity	Specificity
Song (2014)	11%	85% [72-97], p<0.001	83%	82%
Ibarra Estrada (2015)	14%	88% [77-95], p<0.001	86% [69-96]	86% [68-96]
Lu (2017)	13%	91.0% [81.7-100], p<0.001	78%	90%
Roehrig (2017)	10%	81% [55-95], p=0.03	83% [52-98]	83% [36-99]
Zhang (2021)	11.20 cm/s	80.3% [69.2-91.4]	70.0%	80.0%
Zhao (2024)	10%	83% [72-95]	82% [66-91]	78% [55-91]

Table 3 showing cut-off values for ΔCDPV between 10-14% and an absolute value of 11.20 cm/s, AUC between 81-91%, sensitivity between 70-86% and specificity between 78-90%.

Carotid blood flow (CBF) to assess fluid responsiveness utilizing a PLR was investigated in 3 papers [15, 19, 21]. Girotto et al.[21] reported that CBF was not effective in detecting a positive PLR, and changes in CBF were not correlated with variations in cardiac index. The retrospective ICU study of Marik et al.[15] found that a 20% increase in CBF following PLR provided a sensitivity of 94% and specificity of 86% for assessing fluid responsiveness. The study also showed that CBF increased by 79% (±32%) in FR+ after PLR, compared to a 0.1% (±14%) increase in FR- ($P < .0001$). Additionally, Roehrig et al.[19] reported a statistically significant correlation (r = 0.79; 95% CI, 0.60–0.89) between CBF and cardiac output following PLR.

The corrected carotid flow time (ccFT) was investigated in 3 papers [20, 22, 24]. This was calculated using either Bazett's formula: $\text{ccFT} = \frac{\text{average flow time (ms)}}{\sqrt{\text{average cycle time (s)}}}$ [22] or Wodey's formula: ccFT =

$FT_{measured} + (1.29 \times (HR - 60))$ [20, 24]. The results of receiver operating characteristic curves (ROC) are shown in *Table 4*.

Table 4: Results of the Receiver Operating Characteristic Curves (ROC) for corrected carotid flow time (ccFT) from 3 papers. AUC is the area under the ROC curve, and the values in brackets [] represent the 95% Confidence Interval (when available).

Paper	Cut-off value	AUC	Sensitivity	Specificity
Barjaktarevic (2018)	ΔccFT = 7 ms	88% [80-96]	68%	96%
Jalil (2018)	24.68% increase	75% [54-96]	60%	92%
Zhao (2024)	332 ms	87% [76-98]	85% [69-93]	83% [61-94]

Table 4 shows three different types of cut-off values; absolute change, percentage change and an absolute cut-off value, with AUC, sensitivity and specificity ranging from 75-88%, 60-85% and 83-96%, respectively. Marik et al. [15] was the only study which investigated the diameter of the carotid artery and found a significant increase in the FR+ group compared to the FR- group post-PLR, with values of 0.11±0.06 and 0.02±0.03, respectively (p=0.01).
The change in peak systolic velocity (ΔPSV) as a measure of assessing fluid responsiveness was investigated only in the study by Girotto et al. [21], who found that the measure was unable to measure a positive PLR, with an AUC of only 0.56±0.09.

4 Discussion

In this literature review, ten articles were selected. Articles that did not differentiate between fluid responders (FR+) and non-responders (FR-) were excluded. One of the 127 search results was a systematic review, which was excluded [25]. By reviewing the systematic review, two additional papers not found in the original search were identified and included [17, 21]. Although a systematic review was already available, this literature study specifically focused on patients who were mechanically ventilated, which is an important factor to consider as fluid responsiveness assessment in this population is particularly challenging as positive pressure ventilation influences preload and cardiac function [4]. Two of the ten included articles had not been reviewed in the available systematic review due to their more recent publication date, highlighting that this literature study serves as an update [23, 24]. Only half of critically ill patients are fluid responsive [1, 2, 3]. In this study, the overall fluid responsiveness was 61%, which is slightly higher, but still in line with findings in literature. It is noteworthy that Girotto et al. [21] reported a fluid responsiveness of 93% in their patient population, which is significantly higher than what is typically reported in literature. This could potentially be explained by the use of a 10% cut-off value (instead of 15%). However, the 10% threshold was also employed in other studies that reported fluid responsiveness rates around 50%. Another possible explanation could be the patient selection criteria. The study included patients with a non-invasive cardiac monitor and a PLR was performed based on a physician's judgment. However, it remains uncertain what this decision was based on and whether it was influenced by the suspicion of hemodynamic instability.

Five distinct carotid measures were investigated in the ten studies. Firstly, the carotid diameter was assessed in only one study, which used bioreactance as a reference standard, a method that is considered unreliable [15, 7, 8]. Similarly, the ΔPSV was evaluated in just one study, which found no significant correlation with the outcome of the PLR test [21]. Furthermore, the studies on carotid blood flow (CBF) presented conflicting results. Girotto et al. [21] did not find a significant correlation. In contrast, Marik et al. [15] demonstrated that changes in carotid blood flow were highly effective in detecting the effects of the PLR maneuver. However, they used bioreactance as the reference method for measuring cardiac output, a technology whose accuracy has been questioned in literature [7, 8]. Roehrig et al. [19] reported a statistically significant correlation between CBF and CO. However, the wide limits of agreement (±20%) in their Bland-Altman analysis suggested that CBF should not be used as a replacement for direct CO monitoring, particularly during the PLR test. In summary, these

findings indicate that carotid diameter, ΔPSV, and CBF are not proven to be reliable measures for assessing fluid responsiveness.

Six studies investigated the potential of ΔCDPV for assessing fluid responsiveness with a fluid challenge. The results are shown in *Table 3*, illustrating that there are 5 percentage change cut-off values between 10-14% and 1 absolute change cut-off value of 11.20 cm/s, the AUC, sensitivity & specificity are slightly lower compared with the reference standards (*Table 1*). The cut-off values indicate that a fluid challenge is needed for assessing fluid responsiveness.

As seen in *Table 4*, there is variability in the cut-off values for corrected carotid flow time (ccFT), which include absolute change, percentage change, and an absolute cut-off value. Due to the difference in reference standards, cut-off value types, and the use of two different formulas (Wodey & Bazett), drawing conclusions is challenging.

However, while the previously discussed carotid measures were evaluated for fluid responsiveness assessment using a fluid challenge, Zhao et al. [24] identified a threshold (absolute cut-off value of 332 ms) for ccFT that allows predicting fluid responsiveness, removing the requirement for a fluid challenge. Similarly, Zhang et al. [23] classified patients based on significant periodic changes in inspiratory and expiratory carotid blood flow waveforms, measured by carotid ultrasound before a fluid challenge, into two groups: subgroup with significant periodic waveform changes (WF+) and without (WF-). These waveform changes were shown to predict fluid responsiveness, eliminating the need for a fluid challenge, much like the ccFT threshold.

The reference standards for assessing fluid responsiveness all require the use of a fluid challenge, as do most of the carotid measures studied. Due to the high heterogeneity among studies, further research is necessary before carotid measures can be considered a reliable alternative to these reference standards. Notably, two carotid measures emerged as potential for predicting fluid responsiveness, ccFT and periodic waveform changes, eliminating the need for a fluid challenge and simplifying the assessment process [23, 24]. Further investigation is needed, as these strategies show potential for predicting fluid responsiveness eliminating the need for a fluid challenge, thereby reducing assessment time and associated risks.

4.1 Limitations

Any literature review carries the possibility that some relevant articles were missed due to the search terms used. However, two additional useful articles were identified through reviewing the systematic review found in the search results. Additionally, the inclusion criterion specified that patients must be mechanically ventilated, as shown in *Table 2*, not all studies included only mechanically ventilated patients. However, since 87% of the patients in these studies were mechanically ventilated, and to avoid excluding potentially relevant papers, it was decided to include studies with a relatively high proportion of mechanically ventilated patients. Finally, there was a high heterogeneity among the studies regarding the reference method used to determine fluid responsiveness, as outlined in *Table 2*. The heterogeneity, combined with the variation in carotid measures and the fact that not all measures were investigated in the same number of studies, further limits the amount of data available, the conclusions that can be drawn, and the ability to perform a meta-analysis.

5 Conclusion

This review explored the available literature on the use of carotid ultrasound for assessing fluid responsiveness in mechanically ventilated patients. The studies showed a high heterogeneity, the carotid measures with most potential as alternative of the current reference standards are ΔCDPV & ccFT, though further research is necessary. Additionally, strategies for predicting fluid responsiveness without a fluid challenge, such as ccFT and periodic waveform changes, appear promising; however, further investigation is required.

References

[1] C. K. Hofer and M. Cannesson. "Monitoring fluid responsiveness". In: *Acta anaesthesiologica Taiwanica: official journal of the Taiwan Society of Anesthesiologists* 49.2 (2011), pp. 59–65. DOI: 10.1016/j.aat.2011.05.001.

[2] P. E. Marik, M. Baram, and B. Vahid. "Does central venous pressure predict fluid responsiveness? A systematic review of the literature and the tale of seven mares". In: *Chest* 134.1 (2008), pp. 172–178. DOI: 10.1378/chest.07-2331.

[3] A. Carsetti, M. Cecconi, and A. Rhodes. "Fluid bolus therapy: monitoring and predicting fluid responsiveness". In: *Current opinion in critical care* 21.5 (2015), pp. 388–394. DOI: 10.1097/MCC.0000000000000240.

[4] X. Monnet, P. E. Marik, and J. L. Teboul. "Prediction of fluid responsiveness: an update". In: *Annals of Intensive Care* 6.1 (2016), p. 111. DOI: 10.1186/s13613-016-0216-7.

[5] J. H. Boyd and D. Sirounis. "Assessment of adequacy of volume resuscitation". In: *Current Opinion in Critical Care* 22.5 (2016), pp. 424–427. DOI: 10.1097/MCC.0000000000000344.

[6] S. J. Millington. "Ultrasound assessment of the inferior vena cava for fluid responsiveness: easy, fun, but unlikely to be helpful". In: *Canadian Journal of Anaesthesia = Journal Canadien d'Anesthésie* 66.6 (2019), pp. 633–638. DOI: 10.1007/s12630-019-01357-0.

[7] E. Kupersztych-Hagege et al. "Bioreactance is not reliable for estimating cardiac output and the effects of passive leg raising in critically ill patients". In: *British Journal of Anaesthesia* 111.6 (2013), pp. 961–966. DOI: 10.1093/bja/aet282.

[8] D. Fagnoul, J. L. Vincent, and D. De Backer. "Cardiac output measurements using the bioreactance technique in critically ill patients". In: *Critical Care (London, England)* 16.6 (2012), p. 460. DOI: 10.1186/cc11481.

[9] Harsha Kalagara et al. "Point-of-Care Ultrasound (POCUS) for the Cardiothoracic Anesthesiologist". In: *Journal of Cardiothoracic and Vascular Anesthesia* 36.4 (2022), pp. 1132–1147. DOI: 10.1053/j.jvca.2021.01.018.

[10] Xue Yang and Bin Du. "Does Pulse Pressure Variation Predict Fluid Responsiveness in Critically Ill Patients? A Systematic Review and Meta-Analysis". In: *Critical Care (London, England)* 18.6 (2014), p. 650. DOI: 10.1186/s13054-014-0650-6.

[11] Zhi Zhang et al. "Accuracy of Stroke Volume Variation in Predicting Fluid Responsiveness: A Systematic Review and Meta-Analysis". In: *Journal of Anesthesia* 25.6 (2011), pp. 904–916. DOI: 10.1007/s00540-011-1217-1.

[12] Elie Kupersztych-Hagege et al. "Bioreactance is Not Reliable for Estimating Cardiac Output and the Effects of Passive Leg Raising in Critically Ill Patients". In: *British Journal of Anaesthesia* 111.6 (2013), pp. 961–966. DOI: 10.1093/bja/aet282.

[13] Xiang Si et al. "Diagnostic Accuracy of Transthoracic Echocardiography to Predict Fluid Responsiveness by Passive Leg Raising in the Critically Ill: A Meta-Analysis". In: *Open Journal of Emergency Medicine* 4.4 (2016), pp. 98–108. DOI: 10.4236/ojem.2016.44011.

[14] J. Xie et al. "The Accuracy of Velocity-Time Integral Variation and Peak Velocity Variation of the Left Ventricular Outflow Tract in Predicting Fluid Responsiveness in Postoperative Patients Mechanically Ventilated at Low Tidal Volumes". In: *Journal of Cardiothoracic and Vascular Anesthesia* 37.6 (2023), pp. 911–918. DOI: 10.1053/j.jvca.2023.02.009.

[15] P. E. Marik et al. "The use of bioreactance and carotid Doppler to determine volume responsiveness and blood flow redistribution following passive leg raising in hemodynamically unstable patients". In: *Chest* 143.2 (2013), pp. 364–370. DOI: 10.1378/chest.12-1274.

[16] Y. Song et al. "Respirophasic carotid artery peak velocity variation as a predictor of fluid responsiveness in mechanically ventilated patients with coronary artery disease". In: *British Journal of Anaesthesia* 113.1 (2014), pp. 61–66. DOI: 10.1093/bja/aeu057.

[17] M. Á. Ibarra-Estrada et al. "Respiratory variation in carotid peak systolic velocity predicts volume responsiveness in mechanically ventilated patients with septic shock: a prospective cohort study". In: *Critical Ultrasound Journal* 7.1 (2015), p. 29. DOI: 10.1186/s13089-015-0029-1.

[18] N. Lu et al. "Exploring the best predictors of fluid responsiveness in patients with septic shock". In: *The American Journal of Emergency Medicine* 35.9 (2017), pp. 1258–1261. DOI: 10.1016/j.ajem.2017.03.052.

[19] C. Roehrig et al. "Carotid Doppler flowmetry correlates poorly with thermodilution cardiac output following cardiac surgery". In: *Acta Anaesthesiologica Scandinavica* 61.1 (2017), pp. 31–38. DOI: 10.1111/aas.12822.

[20] I. Barjaktarevic et al. "Ultrasound Assessment of the Change in Carotid Corrected Flow Time in Fluid Responsiveness in Undifferentiated Shock". In: *Critical Care Medicine* 46.11 (2018), e1040–e1046. DOI: 10.1097/CCM.0000000000003356.

[21] V. Girotto et al. "Carotid and femoral Doppler do not allow the assessment of passive leg raising effects". In: *Annals of Intensive Care* 8.1 (2018), p. 67. DOI: 10.1186/s13613-018-0413-7.

[22] B. Jalil et al. "Comparing Changes in Carotid Flow Time and Stroke Volume Induced by Passive Leg Raising". In: *The American Journal of the Medical Sciences* 355.2 (2018), pp. 168–173. DOI: 10.1016/j.amjms.2017.09.006.

[23] Q. Zhang et al. "Respiratory Variations in Peak Peripheral Artery Velocities and Waveforms for Rapid Assessment of Fluid Responsiveness in Traumatic Shock Patients". In: *Medical Science Monitor: International Medical Journal of Experimental and Clinical Research* 27 (2021), e928804. DOI: 10.12659/MSM.928804.

[24] J. Zhao et al. "Predictive value of trendelenburg position and carotid ultrasound for fluid responsiveness in patients on VV-ECMO with acute respiratory distress syndrome in the prone position". In: *Scientific Reports* 14.1 (2024), p. 31808. DOI: 10.1038/s41598-024-83038-7.

[25] L. Beier et al. "Carotid Ultrasound to Predict Fluid Responsiveness: A Systematic Review". In: *Journal of ultrasound in medicine : official journal of the American Institute of Ultrasound in Medicine* 39.10 (2020), pp. 1965–1976. DOI: 10.1002/jum.15301.

8.2 Appendix – ECG extraction from ultrasound

8.2.1 $ECG_{us,nan}$ and $ECG_{us,int}$

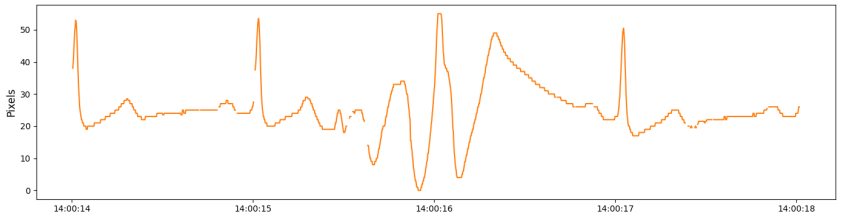

(A) $ECG_{us,nan}$

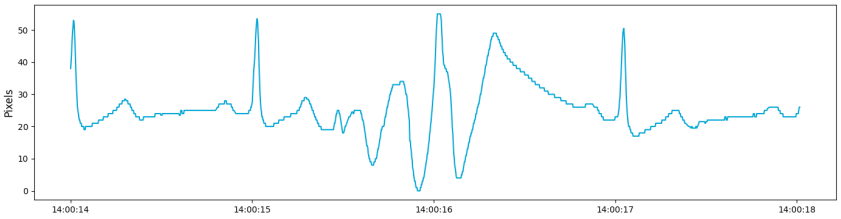

(B) $ECG_{us,int}$

Figure 14: An example of the ECG signals extracted from the ultrasound image, including **(A)** the version retaining missing values ($ECG_{us,nan}$) and **(B)** the interpolated version ($ECG_{us,int}$), is shown. In this example, an artefact is present.

8.2.2 Flatline artefact

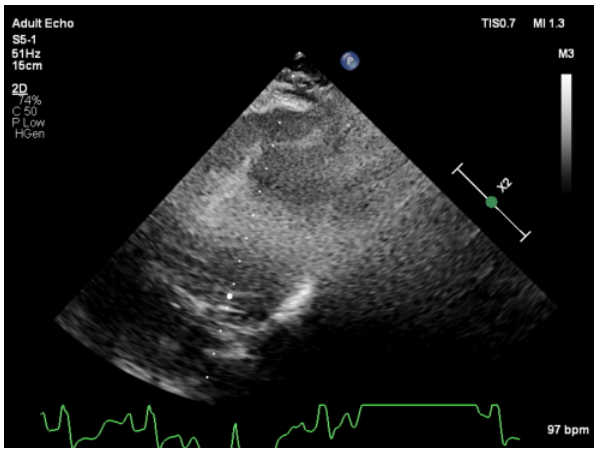

Figure 15: Example of an ECG_{us} signal within an ultrasound frame with a flatline artefact. These plateaus, which occur when the signal remains at its maximum value for a prolonged period, are treated as missing data in $ECG_{us,nan}$ to improve the quality of subsequent analyses.

8.2.3 Missing values from annotations & scale markings

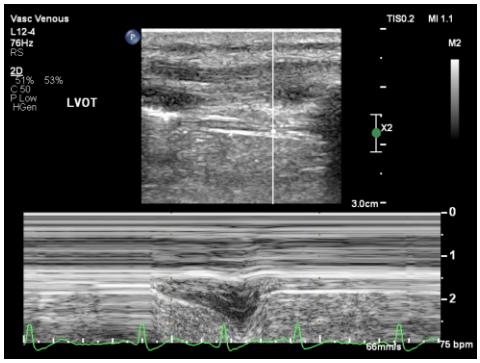

(A) Original ultrasound frame.

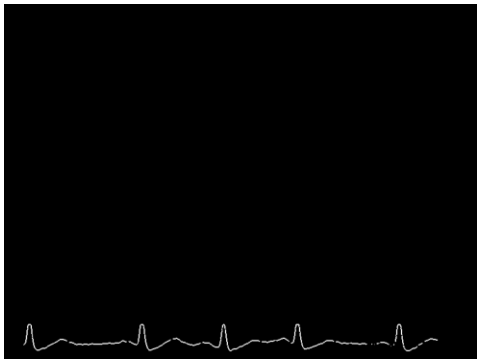

(B) Frame after green-channel filtering.

Figure 16: Example of missing values caused by annotations and scale markings: **(A)** the original ultrasound frame showing annotations and scale markings, and **(B)** the frame after green-channel filtering, where gaps appear in the ECG signal at the locations of the annotations and scale markings.

8.2.4 Green 3D-box

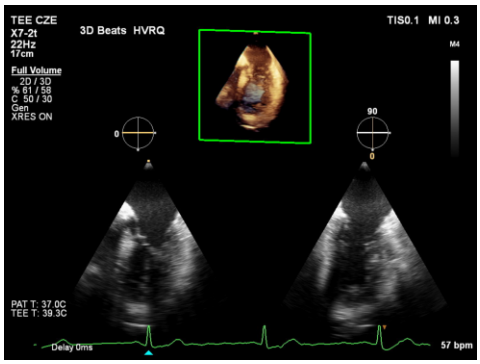

(A) Original ultrasound frame.

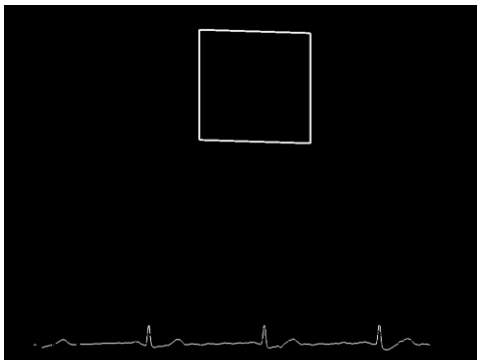

(B) Frame after green-channel filtering.

Figure 17: Example of a green 3D box in ultrasound imaging and its effect after applying green filtering.

8.2.5 End of ECG

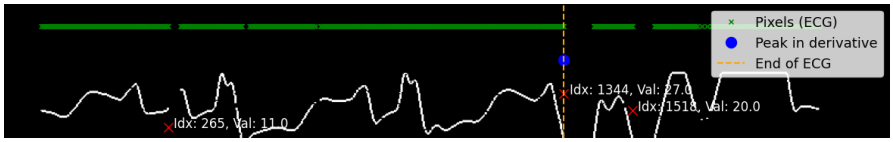

Figure 18: Visualization of the ECG endpoint detection process using signal derivative peaks. In this example, artefacts led to incorrect automatic detection, requiring manual correction. The three highest peaks, along with their indices and values, are shown. The ECG endpoint was manually adjusted to index 265.

8.3 Appendix - NeuroKit

8.3.1 Introduction of NeuroKit

NeuroKit2 is an open-source, community-driven, and user-centered Python package for neurophysiological signal processing. It provides a comprehensive suite of processing routines for a variety of bodily signals (e.g., ECG, PPG, EDA, EMG, RSP). These processing routines include high-level functions that enable data processing in a few lines of code using validated pipelines. The package also includes tools for specific processing steps such as rate extraction and filtering methods, offering a trade-off between high-level convenience and fine-tuned control. Its goal is to improve transparency and reproducibility in neurophysiological research, as well as foster exploration and innovation. Its design philosophy is centred on user-experience and accessibility to both novice and advanced users. [18]

NeuroKit2 offers a breadth of functionalities which includes, but is not limited to, signal simulation; data management (e.g., downloading existing datasets, reading and formatting files into a dataframe); event extraction from signals; epoch extraction, signal processing (e.g., filtering, resampling, rate computation using different published algorithms detailed in the package's documentation); spectral analyses; complexity and entropy analyses; and convenient statistical methods (e.g., K-means clustering, ICA or PCA). A variety of plotting functions allow for quick and expressive visualization of the signal processing and the resulting features. [18]

8.3.2 Example of Baseline Drift and High-Frequency Noise Correction

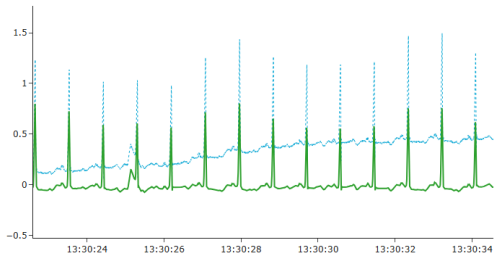

(A) Baseline Drift

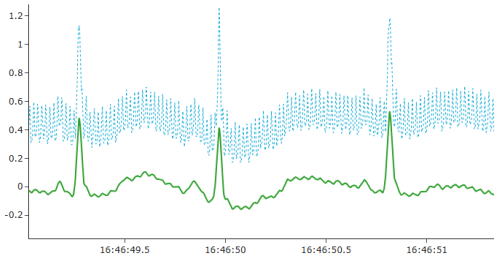

(B) High Frequency Noise

Figure 19: An example of ECG_{dwc} signals, with the raw data shown in blue and the data cleaned using `ecg_clean` shown in green, illustrating the correction of **(A)** baseline drift and **(B)** high frequency noise.

8.3.3 NeuroKit Peak Detection

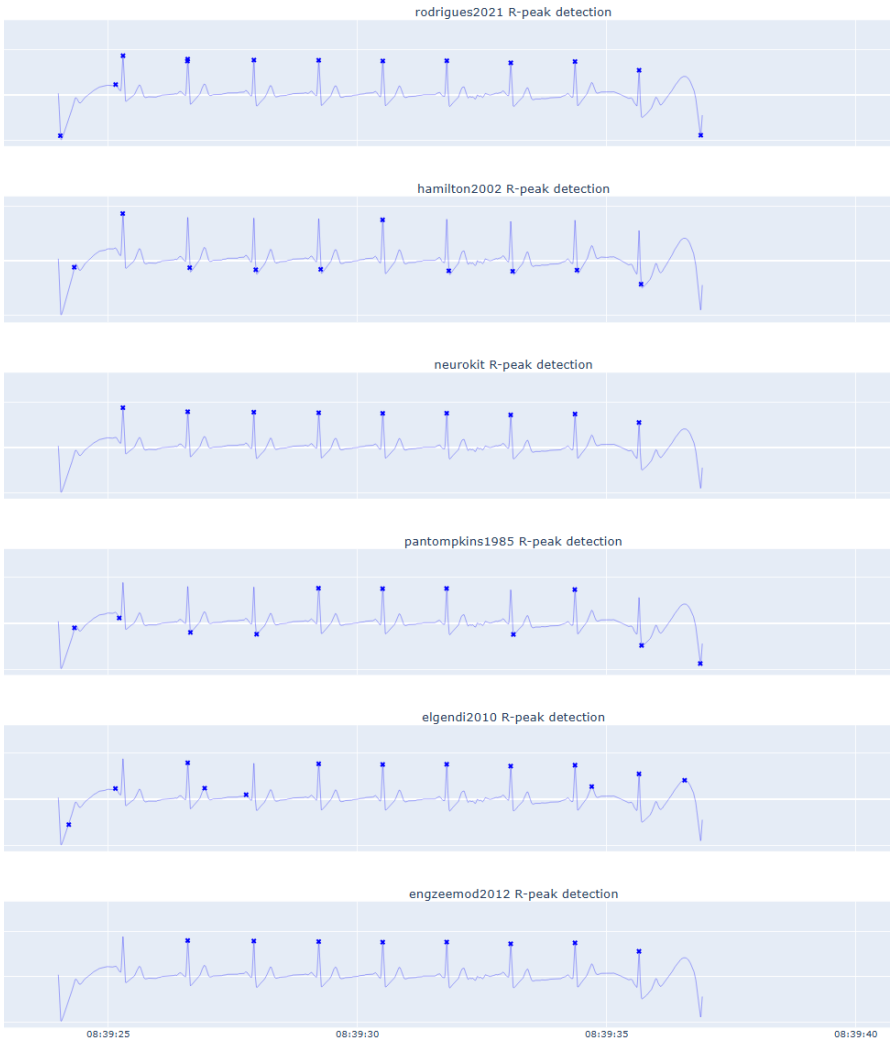

Figure 20: Comparison of R-peak detection methods applied to an $ECG_{us,int}$ signal. Each subplot displays the detected peaks for a specific algorithm, blue crosses indicate detected R-peaks in the $ECG_{us,int}$ signal. The NeuroKit method was selected based on performance.

8.4 Appendix - Timeshift results

Patient	Type	Pearson		RRIC NK		RRIC MM0.2		RRIC MM1		BPC NK		BPC MM0.2		BPC MM1	
		Timeshift (s)	Corr.	Timeshift (s)	Corr.	Timeshift (s)	Corr.	Timeshift (s)	Corr.	Timeshift (s)	Corr.	Timeshift (s)	Corr.	Timeshift (s)	Corr.
POR_01_21	Long	436,55	0,48	455,93	0,98	473,93	0,47	455,93	0,98	455,94	0,94	455,94	0,85	455,94	0,94
POR_01_23	Long	413,58	0,47	456,18	0,89	367,19	0,64	456,18	0,89	394,22	1,00	373,52	0,72	394,22	1,00
POR_01_24	Short	457,45	0,90	363,98	1,00	370,41	1,00	362,69	1,00	365,18	1,00	445,58	1,00	365,18	1,00
POR_02_33	Artefact	4121,34	0,58	4141,38	1,00	4157,62	0,84	4121,35	1,00	4092,51	1,00	4121,31	0,66	4121,31	0,71
POR_02_34	Artefact	4121,52	0,54	4121,52	1,00	4121,52	0,68	4146,74	1,00	4121,55	0,94	4121,55	0,71	4121,55	0,86
POR_02_35	Artefact	4121,94	0,52	4109,43	0,99	4184,99	0,75	4084,72	0,85	4085,65	0,64	4084,55	0,65	4084,85	0,71
POR_02_36	Artefact	4137,67	0,35	4113,02	1,00	4136,98	0,97	4121,78	1,00	4169,75	0,80	4136,85	0,53	4083,15	0,54
POR_02_38	Artefact	4080,86	0,34	4089,82	0,97	4192,12	0,47	4105,37	0,99	4081,97	0,81	4081,97	0,51	4081,97	0,71
POR_02_39	Long	4094,23	0,86	4156,51	0,84	4163,26	0,80	4156,51	0,84	4090,47	1,00	4109,97	1,00	4090,47	1,00
POR_02_9	Short	4114,66	0,54	4090,54	1,00	4126,24	1,00	4090,54	1,00	4082,51	1,00	4086,11	0,75	4084,31	1,00
POR_03_03	Artefact	-1,56	0,50	-1,56	0,93	-49,22	0,88	-9,11	0,78	3,02	1,00	20,22	0,75	3,02	0,76
POR_03_16	Artefact	-1,17	0,63	-42,10	0,98	-1,43	0,96	-1,43	1,00	-49,95	0,74	-13,35	0,70	-1,65	0,75
POR_04_05	Artefact	0,31	0,68	-28,64	1,00	9,26	0,76	-43,01	0,98	-57,50	1,00	0,30	0,84	0,30	0,76
POR_04_12	Long	6,12	0,71	1,24	0,71	-32,89	0,98	1,24	0,71	9,06	1,00	0,26	0,76	9,06	1,00
POR_04_24	Short	0,27	0,74	-59,43	1,00	-55,71	0,83	-59,43	1,00	0,26	1,00	0,26	0,81	0,26	0,84
POR_04_25	Short	0,28	0,76	-62,27	1,00	-41,98	0,84	-64,10	1,00	-52,02	1,00	-28,62	0,82	55,08	1,00
POR_04_27	Artefact	63,11	0,56	-28,64	1,00	-19,26	0,83	-62,64	1,00	-62,58	1,00	0,22	0,73	20,82	1,00
PIC_01_06	Short	4537,45	0,46	4511,46	1,00	4616,12	0,63	4589,42	1,00	4504,74	1,00	4607,64	0,83	4504,74	0,87
PIC_01_07	Short	4573,83	0,68	4586,48	1,00	4612,14	0,99	4520,35	0,93	4505,36	1,00	4508,46	0,75	4505,36	0,77
PIC_02_09	Short	4564,52	0,66	4564,54	1,00	4546,31	0,91	4564,54	1,00	4564,54	1,00	4617,04	0,58	4564,54	1,00
PIC_02_10	Long	4564,10	0,73	4564,11	0,99	4585,98	0,64	4564,11	0,99	4564,12	0,88	4593,92	0,58	4564,12	0,88
PIC_02_11	Long	4563,55	0,78	4563,56	1,00	4511,81	0,81	4563,56	1,00	4563,52	0,64	4590,22	0,42	4563,52	0,64
PIC_02_12	Long	4563,52	0,73	4563,53	1,00	4622,48	0,77	4563,53	1,00	4563,54	0,77	4545,04	0,40	4563,54	0,77
PIC_02_13	Long	4564,07	0,74	4564,08	1,00	4513,84	0,73	4580,15	0,83	4564,02	0,76	4523,82	0,39	4564,02	0,67
PIC_03_1_20	Long	-52,09	0,87	41,69	0,98	-1,25	0,96	27,19	0,48	41,71	1,00	-27,69	0,63	27,21	0,71
PIC_03_1_21	Short	39,84	0,84	10,04	1,00	14,05	0,96	44,85	0,98	-61,37	1,00	-40,87	0,85	-11,77	0,80
PIC_03_1_22	Long	43,44	0,85	-24,13	1,00	66,74	0,92	27,50	0,41	-18,21	1,00	-40,01	0,79	-31,41	0,69
PIC_03_1_24	Long	55,48	0,86	-53,41	1,00	-63,49	0,81	-48,74	0,42	-53,45	1,00	56,15	0,88	2,35	0,80
PIC_03_1_25	Artefact	-30,43	0,60	31,18	0,93	-55,64	-0,13			-4,53	0,93	-2,63	0,25	-37,13	0,36
PIC_03_1_26	Short	64,98	0,86	-63,19	1,00	-19,86	0,82			19,93	1,00	-21,57	0,41	-53,97	0,46
PIC_03_1_28	Long	36,19	0,78	-8,83	1,00	-6,14	0,93	26,96	0,55	-55,95	0,88	-37,35	0,73	53,45	0,85
PIC_03_1_29	Artefact	-4,63	0,61	-44,42	1,00	-54,98	0,68	36,49	0,47	31,79	0,80	-4,61	0,66	-4,61	0,74
PIC_03_1_30	Long	-4,03	0,82	59,74	0,72	-45,03	0,86	-17,89	0,75	-7,99	0,88	22,51	0,75	15,21	0,85
PIC_03_1_31	Artefact	-18,46	0,63	-40,31	0,77	9,42	0,74	-40,98	0,80	-4,55	0,69	52,55	0,60	-7,85	0,60
PIC_03_1_32	Short	-35,03	0,89			3,44	0,97			-53,57	1,00	31,33	0,90	-55,57	0,84
PIC_03_1_33	Long	-51,99	0,85	-53,32	0,90	-49,30	0,85	37,64	0,53	-38,73	1,00	-4,83	0,73	-42,03	0,66
PIC_03_1_34	Long	-54,41	0,82	-0,01	0,82	-45,90	0,80	12,45	0,52	-63,75	0,88	-51,75	0,70	-63,05	0,67
PIC_03_1_35	Long	54,06	0,76	-19,53	0,89	15,65	0,96	51,44	0,56	-36,11	1,00	55,39	0,63	48,09	0,94
PIC_03_1_36	Short	-42,20	0,84	-61,28	1,00	44,84	0,96	60,13	1,00	-43,53	1,00	-39,53	0,70	61,27	0,87
PIC_03_1_37	Short	-56,20	0,84	-60,67	1,00	-44,76	0,96	46,14	1,00	-57,57	1,00	34,03	0,80	47,33	0,84
PIC_03_1_38	Long	8,05	0,72	47,33	0,78	36,93	0,69	42,65	0,52	44,67	0,76	17,37	0,72	8,07	0,80
PIC_03_1_39	Long	-6,34	0,78	-40,00	1,00	40,92	0,92	34,29	0,48	-20,11	0,88	-52,01	0,58	38,09	0,66

(A) POR_01, POR_02, POR_03, POR_04, PIC_01, PIC_02, and PIC_03_1.

Patient	Type	Pearson		RRIC NK		RRIC MM0.2		RRIC MM1		BPC NK		BPC MM0.2		BPC MM1	
		Timeshift (s)	Corr.	Timeshift (s)	Corr.	Timeshift (s)	Corr.	Timeshift (s)	Corr.	Timeshift (s)	Corr.	Timeshift (s)	Corr.	Timeshift (s)	Corr.
PIC_03_2_45	Long	38,51	0,84	49,64	1,00	43,50	0,92	2,04	0,29	37,85	0,76	36,65	0,62	-61,15	0,74
PIC_03_2_46	Short	33,08	0,88	-62,16	1,00	-11,25	0,86	-61,80	1,00	-60,91	1,00	-60,41	0,89	-61,21	0,63
PIC_03_2_47	Short	-56,14	0,89	-63,45	1,00	-51,80	0,95			-62,87	1,00	-41,97	0,89	-43,17	0,72
PIC_03_2_48	Long	-63,14	0,88	-63,76	0,83	-63,12	0,94	56,54	0,54	-36,75	1,00	51,75	0,74	1,95	0,81
PIC_03_2_49	Long	66,54	0,85	-8,99	0,76	-45,80	0,93	28,52	0,49	-53,23	0,88	60,97	0,65	-57,53	0,81
PIC_03_2_50	Long	48,32	0,83	-22,29	0,93	61,96	0,87	-48,06	0,35	50,15	1,00	66,25	0,75	8,45	0,73
PIC_03_2_51	Short	32,55	0,89	-62,53	1,00	40,63	0,93			-58,89	1,00	-50,39	0,78	-60,19	0,84
PIC_03_2_52	Short	57,54	0,87	-60,82	1,00	45,81	0,94	-47,82	0,45	-60,83	1,00	-41,03	0,85	-63,93	0,67
PIC_03_2_53	Short	33,85	0,91	-64,75	1,00	41,29	0,95	-40,85	0,90	-63,49	1,00	-5,69	0,89	-62,99	0,76
PIC_03_2_55	Artefact	-8,87	0,65	-18,10	0,97	-7,50	0,57	-18,56	0,81	-16,89	0,67	-9,99	0,46	-40,99	0,51
PIC_03_2_56	Artefact	42,78	0,77	-10,13	0,89	67,66	0,51	-32,34	0,36	-3,31	0,94	50,29	0,73	-62,01	0,84
PIC_03_2_57	Artefact	60,06	0,58	-19,13	1,00	-49,34	0,76	-50,56	0,71	54,43	0,94	40,03	0,58	-2,97	0,73
PIC_03_2_59	Long	56,25	0,88	-26,43	0,96	-54,87	0,84	39,56	0,43	-28,31	0,88	35,19	0,77	-34,51	0,73
PIC_03_2_60	Short	-21,97	0,90	-57,66	1,00	-24,45	0,72	-2,16	0,69	-48,21	1,00	-25,11	0,84	-56,31	0,67
PIC_03_2_61	Long	25,11	0,88	52,89	0,77	49,34	0,75	4,09	0,07	63,61	0,88	63,61	0,87	-48,19	0,93
PIC_03_2_62	Long	52,86	0,88	-23,54	1,00	-30,33	0,77	-35,89	0,08	-61,93	0,88	45,37	0,74	27,97	0,86
PIC_03_2_63	Long	8,97	0,88	-18,99	0,89	-49,95	0,94	54,43	0,43	-41,95	1,00	2,75	0,84	8,35	0,83
PIC_03_2_64	Long	-55,92	0,88	68,58	0,75	47,28	0,88	-14,20	0,40	-63,39	1,00	-32,89	0,75	-55,29	0,80
PIC_03_2_65	Long	7,36	0,86	-57,42	1,00	1,82	0,95	-21,40	0,22	-57,39	0,83	33,31	0,71	-4,99	0,90
PIC_03_2_66	Long	14,67	0,88	24,59	0,99	-29,19	0,95	58,57	0,42	-42,97	0,88	44,43	0,81	16,53	0,83
PIC_03_2_67	Long	-34,65	0,88	-42,21	0,73	-40,20	0,95	50,11	0,43	-50,23	0,76	-9,93	0,74	-34,03	0,79
PIC_03_2_68	Long	-61,66	0,89	52,84	0,71	47,05	0,76	21,35	0,52	-14,63	0,76	-14,63	0,77	-20,83	0,76
PIC_03_2_69	Long	10,95	0,88	31,99	0,86	-54,78	0,73	-7,80	0,35	-32,51	0,81	-39,31	0,51	-39,91	0,66
PIC_03_3_01	Long	52,37	0,92	42,95	0,91	5,00	0,58	53,26	0,56	-3,40	1,00	5,50	0,68	1,30	0,88
PIC_03_3_02	Long	-35,21	0,98	-52,36	0,84	-43,00	0,44	-6,94	1,00	-57,64	0,88	-15,34	0,67	-17,44	0,84
PIC_03_3_03	Short	-7,59	0,92	-60,92	1,00	16,84	0,81	17,85	1,00	-60,40	1,00	-59,20	0,77	-59,20	1,00
PIC_03_3_04	Short	59,18	0,93	-58,95	1,00	-2,04	0,93	-29,14	0,83	-59,44	1,00	-21,34	0,88	-59,34	0,74
PIC_03_3_05	Short	-36,72	0,99			-1,15	0,75	-58,25	1,00	-57,24	1,00	-0,14	0,75	-54,64	1,00
PIC_03_3_06	Long	-48,88	0,98			16,46	0,58	-10,35	0,52	-63,12	0,60	0,28	0,68	-37,02	0,85
PIC_03_3_07	Long	63,03	0,91	-7,01	0,96	-32,58	0,71	-59,21	0,33	-58,72	1,00	53,58	0,72	-56,62	0,96
PIC_03_3_08	Short	0,01	0,92	-60,02	1,00	45,59	0,81	61,14	1,00	-60,56	1,00	-4,76	0,78	-50,46	1,00
PIC_03_3_09	Short	9,88	0,99	-57,26	1,00	-8,45	0,77	58,36	0,72	-60,46	1,00	-60,46	0,83	-60,46	0,71
PIC_03_3_10	Short	-2,12	0,99	-51,72	1,00	-53,31	0,94	41,31	0,81	-63,42	1,00	-53,32	0,91	-63,42	0,62
PIC_03_3_11	Long	-30,36	0,98	-46,89	0,82	-8,74	0,61	5,79	0,53	-59,70	0,88	65,50	0,76	65,50	0,81
PIC_03_3_12	Short	-20,16	0,92			-52,68	0,76			-63,24	1,00	-33,84	0,75	-39,24	0,62
PIC_03_3_13	Short	-3,27	0,90	-63,23	1,00	-8,53	0,85	-42,76	0,81	-63,80	1,00	-2,20	0,83	-59,20	0,62
PIC_03_3_14	Long	59,23	0,90	-26,15	0,85	42,92	0,58	-45,20	0,34	-60,02	1,00	-45,72	0,67	-52,62	0,92
PIC_03_3_15	Long	-46,45	0,79	38,25	0,97	37,21	0,69	61,84	0,57	-53,90	0,88	-47,50	0,63	-52,30	0,73
PIC_03_3_16	Long	-63,42	0,92	16,96	0,95	23,32	0,72	49,56	0,68	-62,36	1,00	-17,16	0,75	27,54	0,66
PIC_03_3_17	Short	31,36	0,92	64,17	1,00	-50,16	0,87	-15,50	0,77	-60,76	1,00	13,44	0,81	-61,26	0,82
PIC_03_3_18	Short	42,94	0,90	-3,51	1,00	-43,96	0,84	52,31	0,93	-62,44	1,00	-57,14	0,72	-61,54	0,62
PIC_03_3_20	Short	-52,41	0,92	-62,60	1,00	-2,17	0,79	3,11	0,80	-63,14	1,00	-6,44	0,88	-56,64	0,75
PIC_03_3_21	Long	-9,47	0,97	-17,00	0,79	25,42	0,61	-46,15	0,61	-48,32	1,00	47,48	0,74	-43,02	0,96
PIC_03_3_22	Short	27,20	1,00	-64,66	1,00	60,85	0,82	-50,73	1,00	-64,16	1,00	-41,06	0,88	-56,56	1,00
PIC_03_3_23	Short	4,20	1,00	-36,65	1,00	37,86	0,83	60,56	1,00	-36,66	1,00	-4,46	0,78	-22,66	1,00
PIC_03_3_24	Short	-7,81	1,00	-48,59	1,00	25,86	0,82	37,97	1,00	-48,06	1,00	-16,46	0,88	-44,76	0,87

(B) PIC_03_2, and PIC_03_3.

Figure 21: Results of the timeshift (in seconds) and correlation value (corr.) for each patient across the seven synchronization methods. Green indicates a correct timeshift, red indicates an incorrect one, and yellow represents cases that could not be validated.
RRIC: R-R Interval Correlation; **BPC**: Binned Peak Correlation; **NK**: NeuroKit; **MM0.2**: Moving Mean with an offset of 0.2; **MM1**: Moving Mean with an offset of 1.

8.5 Appendix - ECG-signals with artefacts

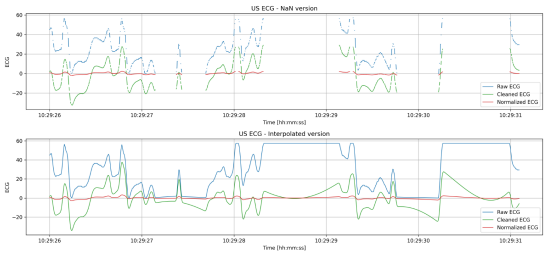

(A) PIC_03_2_55

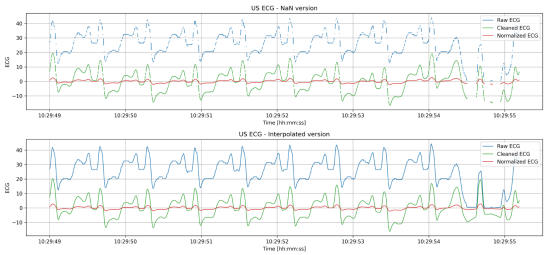

(B) PIC_03_2_56

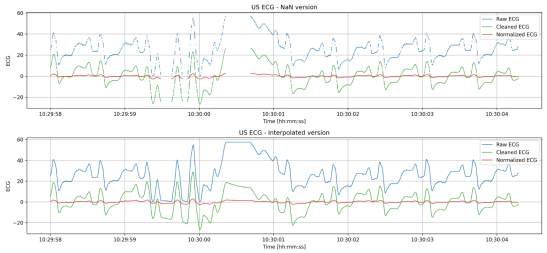

(C) PIC_03_2_57

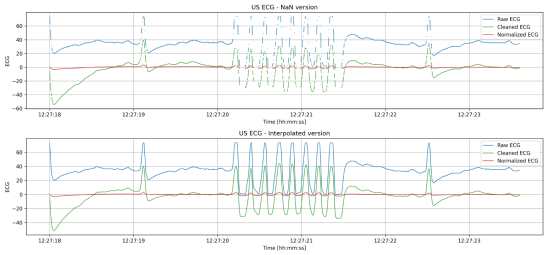

(D) POR_02_33

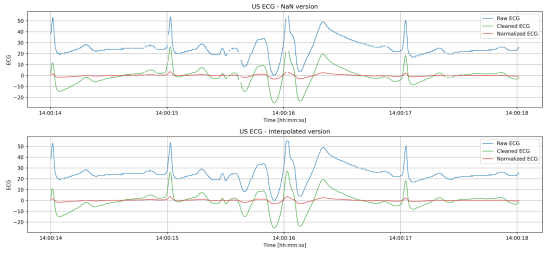

(E) PIC_04_05

Figure 22: Visualization of ECG-signals containing artefacts.

8.6 Appendix - Visualization Synchronization

8.6.1 Short

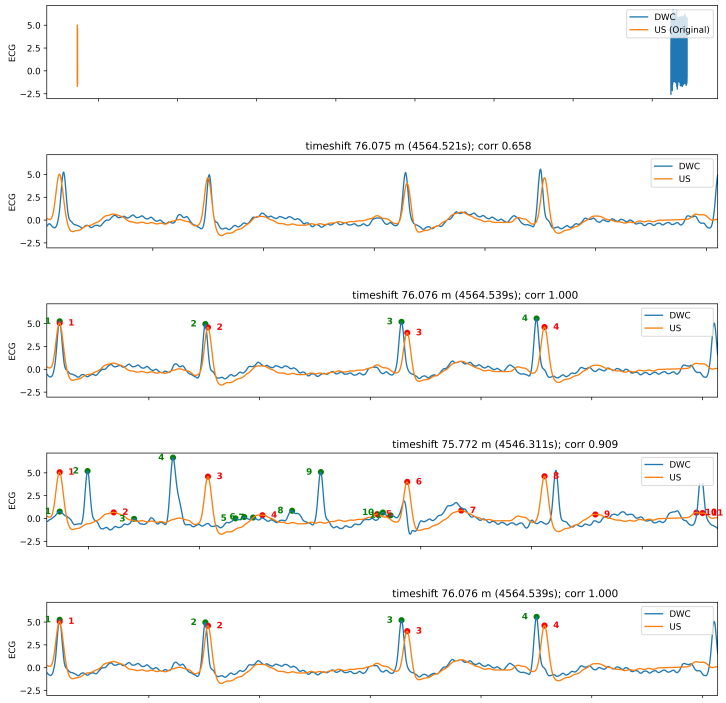

(A) Initial alignment, Pearson, RRIC NK, RRIC MM0.2, and RRIC MM1.

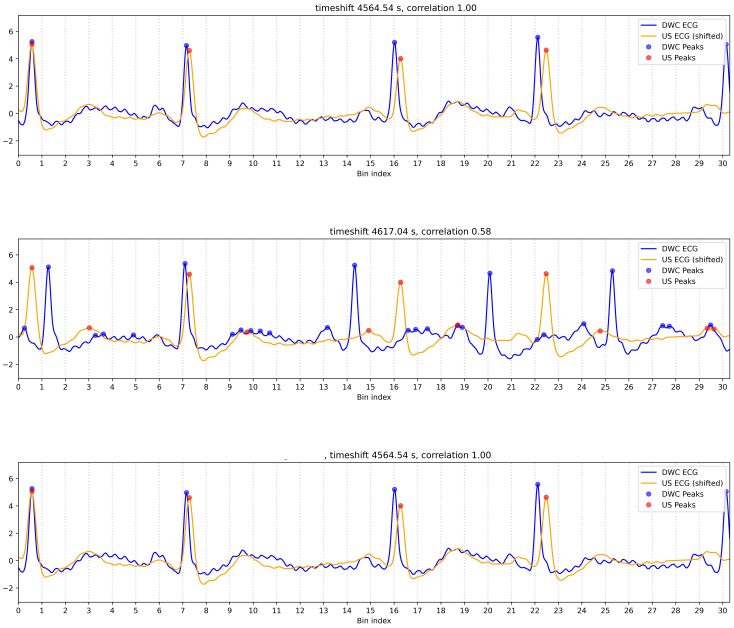

(B) BPC NK, BPC MM0.2, and BPC MM1.

Figure 23: Example of the synchronization process for a short ECG-segment. **[A] (1)** Initial alignment between ECG_{dwc} and ECG_{us}, **(2)** Pearson correlation between ECG_{dwc} and $ECG_{us,nan}$, **(3)** RRIC with NK, **(4)** RRIC with MM0.2 **(5)** RRIC with MM1. **[B] (1)** BPC with NK, **(2)** BPC with MM0.2, **(3)** BPC with MM1.
RRIC: R-R Interval Correlation; **BPC**: Binned Peak Correlation; **NK**: NeuroKit; **MM0.2**: Moving Mean with an offset of 0.2; **MM1**: Moving Mean with an offset of 1.

8.6.2 Long

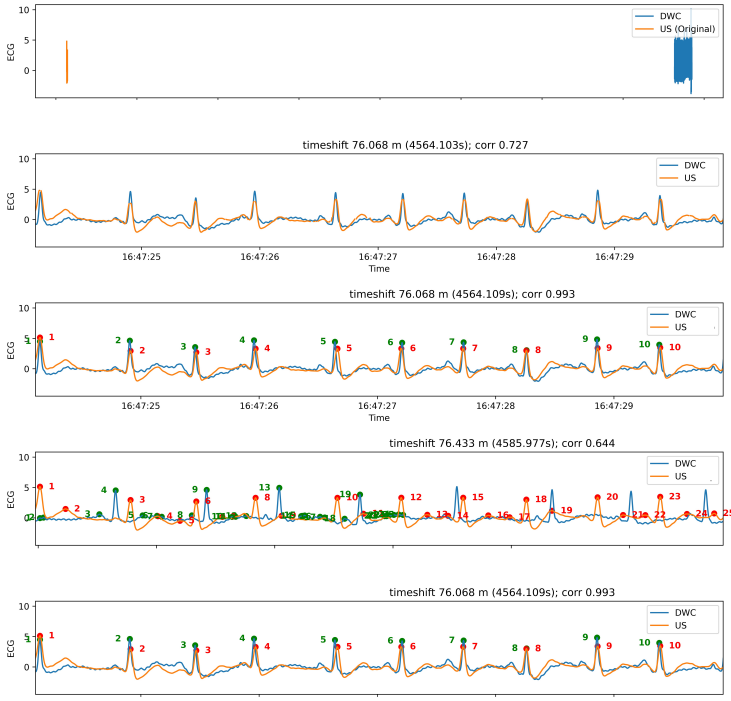

(A) Initial alignment, Pearson, RRIC NK, RRIC MM0.2, and RRIC MM1.

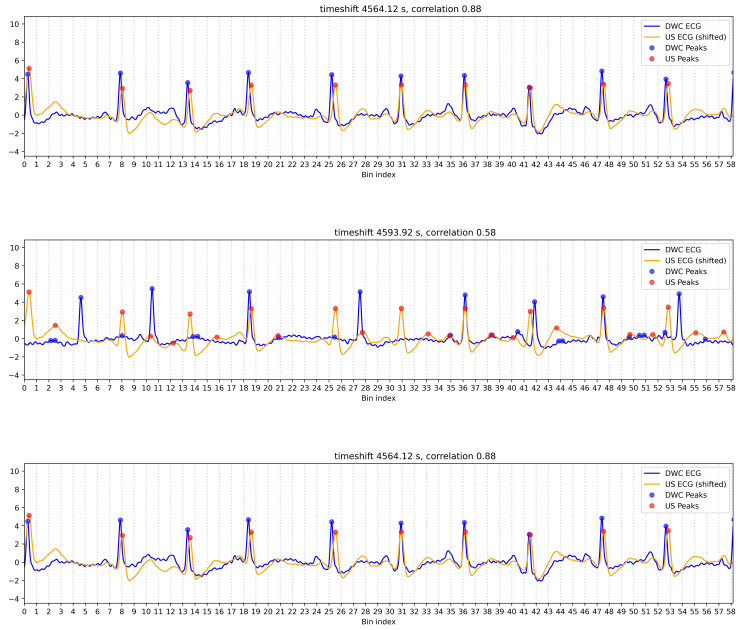

(B) BPC NK, BPC MM0.2, and BPC MM1.

Figure 24: Example of the synchronization process for a long ECG-segment. **[A]** **(1)** Initial alignment between ECG_{dwc} and ECG_{us}, **(2)** Pearson correlation between ECG_{dwc} and $ECG_{us,nan}$, **(3)** RRIC with NK, **(4)** RRIC with MM0.2 **(5)** RRIC with MM1. **[B]** **(1)** BPC with NK, **(2)** BPC with MM0.2, **(3)** BPC with MM1.
RRIC: R-R Interval Correlation; **BPC**: Binned Peak Correlation; **NK**: NeuroKit; **MM0.2**: Moving Mean with an offset of 0.2; **MM1**: Moving Mean with an offset of 1.

8.6.3 Artefact

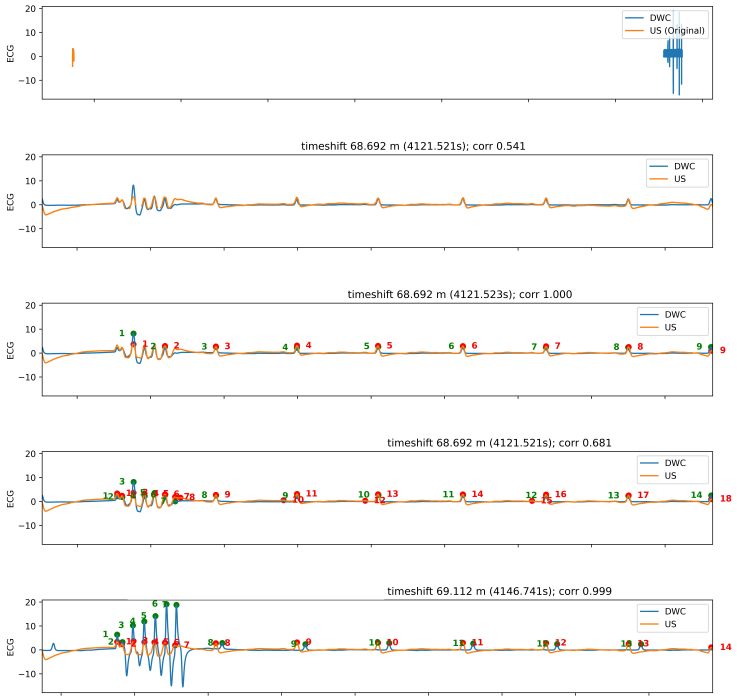

(A) Initial alignment, Pearson, RRIC NK, RRIC MM0.2, and RRIC MM1.

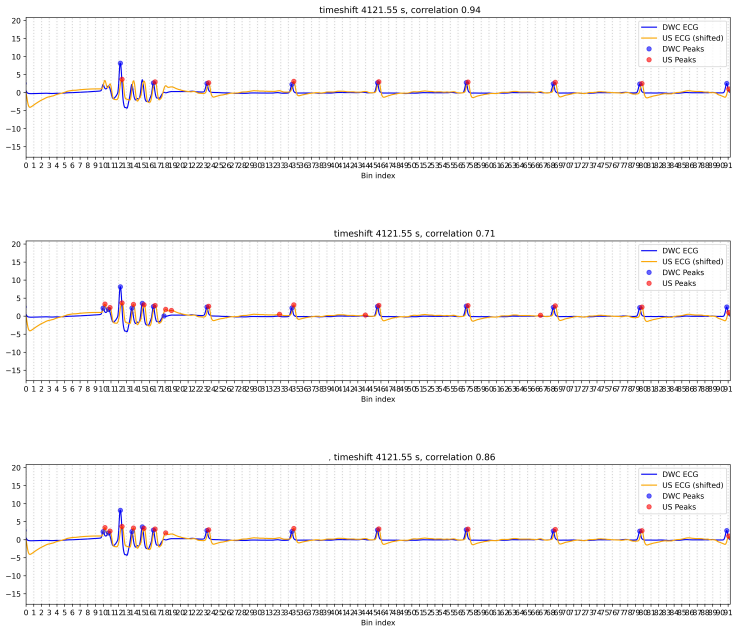

(B) BPC NK, BPC MM0.2, and BPC MM1.

Figure 25: Example of the synchronization process for a ECG-segment with artefact. **[A] (1)** Initial alignment between ECG_{dwc} and ECG_{us}, **(2)** Pearson correlation between ECG_{dwc} and $ECG_{us,nan}$, **(3)** RRIC with NK, **(4)** RRIC with MM0.2 **(5)** RRIC with MM1. **[B] (1)** BPC with NK, **(2)** BPC with MM0.2, **(3)** BPC with MM1.
RRIC: R-R Interval Correlation; **BPC**: Binned Peak Correlation; **NK**: NeuroKit; **MM0.2**: Moving Mean with an offset of 0.2; **MM1**: Moving Mean with an offset of 1.

8.7 Comparison ECG shape US and DWC

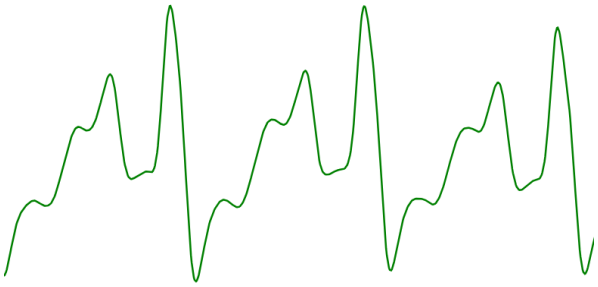

(A) ECG_{us}

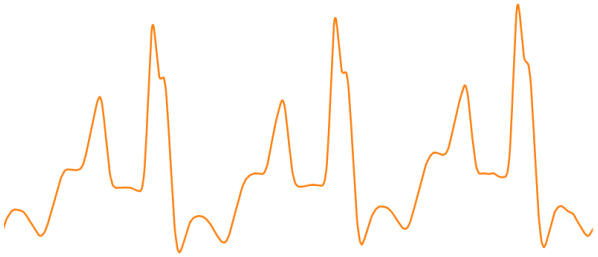

(B) ECG_{dwc}

Figure 26: Comparison of the peak morphology of patient PIC_03 between **(A)** ECG_{us}, and **(B)** ECG_{dwc}.

8.8 Appendix – Research protocol

RE-WEAN

(Respiratory Effort in Weaning Patients)

STUDY PROTOCOL

Respiratory Effort in Weaning: Evaluation and assessment of invasive and non-invasive methods quantifying respiratory effort in patients weaning from mechanical ventilation.

Protocol ID	XXXXXXXXX
Short title	RE-WEAN Respiratory Effort in Weaning: Evaluation and assessment of invasive and non-invasive methods quantifying respiratory effort in patients weaning from mechanical ventilation.
Version	V1
Date	16 July 2025
Coordinating investigator/project leader	F.D. (Femke) Bosman Masterstudent Technical Medicine Catharina Ziekenhuis Eindhoven
Principal investigator(s) (in Dutch: hoofdonderzoeker/ uitvoerder) ***<Multicenter research: per site>***	Prof. dr. R. A. (Arthur) Bouwman Anesthesiologist Catharina Ziekenhuis Eindhoven Dr. A.J.R. (Ashley) de Bie Dekker Internist-Intensivist Catharina Ziekenhuis Eindhoven Ir. I.W.F. (Igor) Paulussen Senior Clinical Research Coördinator Catharina Ziekenhuis Eindhoven
Sponsor (in Dutch: verrichter/opdrachtgever)	
Subsidising party	
Independent expert(s)	

PROTOCOL SIGNATURE SHEET

Name	**Signature**	**Date**
Sponsor or legal representative: ***<please include name and function>*** ***<For non-commercial research >*** **Head of Department:** ***<include name and function>***		
[Coordinating Investigator/Project leader/Principal Investigator]: ***<please include name and function>***		

TABLE OF CONTENTS <*After completion of the research protocol, the table of contents has to be updated. Select whole content (click left mouse button) and push F9.*>

LIST OF ABBREVIATIONS AND RELEVANT DEFINITIONS

AE	**Adverse Event**
CCMO	**Central Committee on Research Involving Human Subjects; in Dutch: Centrale Commissie Mensgebonden Onderzoek**
DSMB	**Data Safety Monitoring Board**
DTF	**Diaphragm ultrasound-derived Thickening Fraction**
GCP	**Good Clinical Practice**
GDPR	**General Data Protection Regulation; in Dutch: Algemene Verordening Gegevensbescherming (AVG)**
IB	**Investigator's Brochure**
IC	**Informed Consent**
ICU	**Intensive Care Unit**
Edi	**Diaphragm electrical activity**
IMDD	**Investigational Medical Device Dossier**
METC	**Medical research ethics committee (MREC); in Dutch: medisch-ethische toetsingscommissie (METC)**
P0.1	**Drop in airway pressure (Paw) during the first 100ms of an occluded breath**
Pocc	**Swing in airway pressure (Paw) generated by respiratory muscle effort when the airway is briefly occluded**
Paw	**Airway pressure**
Pdi	**Transdiaphragmatic pressure**
PEEP	**Positive End-Expiratory Pressure**
Pes	**Esophageal pressure**
Pga	**Gastric pressure**
Pmus	**Respiratory muscles pressure**
PS	**Pressure Support**
PTPes	**Esophageal Pressure-Time Product**
Review committee	**Medical research ethics committee (MREC) or CCMO**
(S)AE	**(Serious) Adverse Event**
Sponsor	**The sponsor is the party that commissions the organisation or performance of the research, for example a pharmaceutical company, academic hospital, scientific organisation or investigator. A party that provides funding for a study but does not commission it is not regarded as the sponsor, but referred to as a subsidising party.**

UAVG	**Dutch Act on Implementation of the General Data Protection Regulation; in Dutch: Uitvoeringswet AVG**
WMO	**Medical Research Involving Human Subjects Act; in Dutch: Wet Medisch-wetenschappelijk Onderzoek met Mensen**

SUMMARY

Rationale: Mechanical ventilation is a critical component in the treatment of critically ill patients, ensuring adequate respiratory support during episodes of severe illness and acute respiratory failure. However, prolonged mechanical ventilation can result in diaphragm dysfunction caused by both insufficient and excessive respiratory effort. This dysfunction complicates the weaning process and is associated with adverse clinical outcomes, including increased mortality and the risk of patient self-inflicted lung injury (P-SILI) (Dres et al., 2017; Goligher et al., 2018). Weaning is the process of gradually discontinuing mechanical ventilatory support and removing the endotracheal tube. Typically, this process begins with a spontaneous breathing trial (SBT) to assess the patient's readiness for weaning (Boles et al., 2007). The patient's readiness for weaning can be evaluated by measuring respiratory effort, which can be assessed using various methods.
To date, to our knowledge, no study has comprehensively evaluated and compared all available methods and their correlations in mechanical ventilated patients, including:

1) Transdiaphragmatic pressure (Pdi) and pressure-time product (PTPes)
2) Diaphragm electrical activity (Edi)
3) Ultrasound derived diaphragm thickening fraction (DTF)
4) Occlusion pressures (P0.1 & Pocc)

While prior research has primarily focused on individual techniques in isolation, a systematic comparison, particularly between invasive and non-invasive approaches, remain absent. Exploring the correlations among these methods could help determine whether certain non-invasive techniques, either alone or in combination, can serve as reliable surrogates for more invasive measurements. This could form the basis for developing a standardized, clinically feasible approach for monitoring respiratory effort.

Objective: The primary objective of this study is to assess the relationship between invasive gold standard measures of respiratory effort, using a double-balloon NutriVent catheter to measure transdiaphragmatic pressure (Pdi) and pressure-time-product (PTPes), or a Getinge catheter to measure diaphragm electrical activity (Edi), and non-invasive techniques, including the ultrasound derived diaphragm thickening fraction (DTF), along with occlusion pressure measurements (such as P0.1 and Pocc), in patients weaning from mechanical ventilation.

Study design: A prospective observational study with additional diagnostic interventions, conducted in two separate cohorts.

Study population: This prospective observational study will include a total of 46 patients: 15 post-operative cardiac surgery patients admitted to the ICU (cohort 1) and 31 ICU patients mechanically ventilated for more than 24 hours (cohort 2). Based on the power analysis, in cohort 1, 5 patients will receive the Pdi catheter and 10 the Edi catheter; in cohort 2, 21 patients will receive the Pdi catheter and 10 the Edi catheter.

Intervention (if applicable): Each patient in the study will receive standard care according to their cardiac surgery or ICU treatment plan. Additionally, if catheter use is not part of their standard care, patients will be assigned to receive either a double-balloon NutriVent catheter to measure Pdi and PTPes, or a Getinge catheter to access Edi. Pre-expiratory occlusion maneuvers will be performed using the ventilator, and diaphragm ultrasound assessments will be conducted. All measurements will be performed six times under varying ventilator settings.

Main study parameters/endpoints: The primary endpoint of this study is to assess the correlations between invasive and non-invasive methods of respiratory effort quantification, expressed as Pearson's or Spearman's correlation coefficients, depending on the distribution and linearity of the data. A correlation matrix will be used to visualize these relationships, and scatter plots will further help in examining their patterns. Furthermore, Bland-Altman plots will be utilized to evaluate agreement and identify any potential systematic bias between the measurement techniques.

Nature and extent of the burden and risks associated with participation, benefit and group relatedness:

Patients included in this study are on mechanical ventilation as part of standard care. Respiratory effort is assessed six times using diaphragm ultrasound, the end-expiratory occlusion maneuver, and either a Pdi or Edi catheter. Ultrasound examination is non-invasive. Since patients remain under a level of sedation and are closely monitored, the discomfort associated with the end-expiratory occlusion maneuver and catheter insertion is considered low risk and acceptable, particularly because both procedures are routinely performed in the ICU.

Given the low risk profile and the potential for this study to significantly improve future respiratory monitoring strategies, the overall risk for participants is considered justified and proportionate.

1. INTRODUCTION AND RATIONALE

In 2024, there were 70,108 admissions to intensive care units (ICUs) in the Netherlands. On average, patients required mechanical ventilation for 9.6 hours per admission (Stichting NICE, 2024). Mechanical ventilation is a critical component in the treatment of critically ill ICU patients, ensuring adequate respiratory support during episodes of severe illness and acute respiratory failure. However, prolonged mechanical ventilation can result in diaphragm dysfunction caused by both insufficient and excessive respiratory effort. This dysfunction complicates the weaning process and is associated with adverse clinical outcomes, including increased mortality and the risk of patient self-inflicted lung injury (P-SILI) (Dres et al., 2017; Goligher et al., 2018). Weaning is the process of gradually discontinuing mechanical ventilatory support and removing the endotracheal tube. Typically, this process begins with a spontaneous breathing trial (SBT) to assess the patient's readiness for weaning (Boles et al., 2007). The patient's readiness for weaning can be evaluated by measuring respiratory effort, which can be assessed using various methods.

Transdiaphragmatic pressure

The measurement of transdiaphragmatic pressure (Pdi) via an esophageal catheter is considered the reference standard (Jonkman et al., 2023). Pdi is calculated as the difference between gastric pressure (Pga) and esophageal pressure (Pes), requiring the placement of a catheter capable of measuring both pressures. Limitations of assessing the pressure swings is the neglect of contraction duration and frequency, lack of correction for chest wall recoil pressure, and its weak association with energy expenditure (de Vries et al., 2018). The pressure-time product (PTPes) represents the area under the inspiration curve of the respiratory muscles pressure (Pmus) during the inspiration phase, providing an integrated measure of inspiratory effort (Cornejo et al.,2024; Mauri et al., 2016). Compared to Pdi, PTPes better reflects muscle activity and energy expenditure (de Vries et al., 2018). A significant limitation of both Pdi and PTPes is the invasive approach.

Diaphragm electrical activity

An alternative catheter-based method to assess respiratory effort is the measurement of diaphragm electrical activity (Edi) through a nasogastric (feeding) catheter. Edi provides a reliable estimate of respiratory drive by measuring neuromuscular transmission and has shown good correlation with Pdi (Jonkman et al., 2020). Some limitations of Edi include its inability to reflect the activation of accessory respiratory muscles, which reduces its suitability for assessing breathing effort at high workloads. Additionally, Edi measures neural drive rather than direct breathing effort, and it remains an invasive technique (de Vries et al., 2018).

Diaphragm ultrasound

One promising non-invasive method for assessing respiratory effort is ultrasound evaluation of the diaphragm. The diaphragm thickening fraction (DTF), measured in M-mode, quantifies the change in diaphragm thickness between inspiration and expiration. It has demonstrated a strong correlation with Edi (Sklar et al., 2021). However, its accuracy decreases in patients with diaphragmatic dysfunction, and it does not capture the duration or frequency of diaphragm excursions (Umbrello et al., 2020). Despite these limitations, it remains a valuable non-invasive tool.

Occlusion pressures

Lastly, occlusion pressure measurements from modern ventilators, obtained through an end-expiratory occlusion maneuver, provide another method for evaluating respiratory effort. Pocc represents the swing in airway pressure (Paw) generated by respiratory muscle effort when the airway is briefly occluded, while P0.1 reflects the drop in Paw during the first 100 milliseconds of an occluded breath (Cornejo et al., 2024). However, this technique lacks standardization across ventilator models, with some providing an estimate of P0.1 without requiring a maneuver. Furthermore, P0.1 tends to underestimate respiratory drive, particularly in patients with high levels of effort (Jonkman et al., 2020).

To our knowledge, no study to date has evaluated all of these methods and their interrelationships in assessing respiratory effort in patients weaning from mechanical ventilation:

1) Transdiaphragmatic pressure (Pdi) and pressure-time product (PTPes)
2) Diaphragm electrical activity (Edi)
3) Ultrasound derived diaphragm thickening fraction (DTF)
4) Occlusion pressures (P0.1 & Pocc)

While previous studies have largely examined individual techniques in isolation, there is still a lack of systematic comparison, especially between invasive and non-invasive methods. No clear consensus has emerged on the most accurate or practical approach. Understanding how these methods correlate may help determine whether certain non-invasive techniques, either alone or in combination, could serve as reliable surrogates for more invasive measurements. This could lay the foundation for developing a standardized, clinically feasible strategy for monitoring respiratory effort. Ultimately, such standardization could lead to more personalized weaning protocols based on patient-specific respiratory effort.

The selection of the study population aims to assess respiratory effort in a real-world ICU setting, using two distinct cohorts. The inclusion of post-operative cardiac surgery patients allows for the quantification of respiratory effort during weaning from mechanical ventilation following general anesthesia in a homogeneous group, free from known underlying respiratory complications. Additionally, the inclusion of ICU patients who have been on mechanical ventilation for more than 24 hours ensures a diverse representation of individuals at risk for diaphragm dysfunction.

By exploring the relationships between different respiratory effort parameters, including both invasive and non-invasive techniques, this study could provide evidence to support more individualized weaning and ventilation strategies. If non-invasive techniques, alone or combined, can reliably serve as alternatives to invasive standards, it could streamline monitoring practices. The findings may contribute to refining clinical guidelines, reducing diaphragm dysfunction, and ultimately improving weaning outcomes for ICU patients.

2. OBJECTIVES

2.1 Primary Objective

The primary objective of this study is to assess the relationship between invasive gold standard measures of respiratory effort, using a double-balloon NutriVent catheter to measure transdiaphragmatic pressure (Pdi) and pressure-time-product (PTPes), or a Getinge catheter to measure diaphragm electrical activity (Edi), and non-invasive techniques, including the ultrasound derived diaphragm thickening fraction (DTF), along with occlusion pressure measurements (such as P0.1 and Pocc), in patients weaning from mechanical ventilation.

2.2 Secondary Objectives

The following are the secondary objectives of this study:

- Breath-to-breath variability: Evaluate the breath-to-breath variability in respiratory effort measurements obtained using Pdi, PTPes, Edi, DTF, P0.1 and Pocc within individual patients.
    - *Hypothesis: Since ultrasound is highly operator-dependent, it is expected to show the greatest breath-to-breath variability, whereas the other techniques will be more consistent.*

- Influence of ventilator settings and other confounders: Determine the potential influence of ventilator settings, support mode, medication, and RASS sedation scores on each of the respiratory effort measures.
    - *Hypothesis: Variability in ventilator settings, support mode, medication, and sedation level is expected to affect respiratory effort measurements. Deeper sedation and higher support levels are likely to introduce more variability in non-invasive methods, leading to a lower correlation with invasive reference measures.*

- Combining non-invasive measures: Assess the combined accuracy of non-invasive measures, DTF, P0.1, and Pocc, with the gold standard Pdi, PTPes and Edi.
    - *Hypothesis: Combining multiple non-invasive measures may capture different aspects of respiratory effort, potentially improving their combined accuracy with respect to the invasive reference methods.*

- Feasibility, practicality, and patient experience: Assess the feasibility and practicality of invasive vs non-invasive techniques in a clinical ICU setting by assessing factors such as preparation time, measurement duration, time required for data analysis, operator expertise, invasiveness and patient tolerance, as well as associated costs.
    - *Hypothesis: Occlusion pressure measurements can be performed using standard ventilators, and ultrasound systems are readily available. Therefore, the non-invasive approach is expected to offer better feasibility, practicality, and patient experience compared to invasive techniques.*

3. STUDY DESIGN

This is a prospective observational study that incorporates additional non-invasive and minimally invasive measurements, conducted at the intensive care unit (ICU). The study includes two separate patient cohorts.

3.1 First cohort – post-operative cardiac surgery patients

The first cohort includes post-operative cardiac surgery patients. Informed consent (IC) will be obtained either during the pre-operative screening (PPOS) or at least one day prior to surgery, upon the patient's admission to the hospital. Patients will receive standard care according to their cardiac surgery protocol.

For anesthesia monitoring, transesophageal echocardiography (TEE) will be used. Since both the NutriVent Pdi- and Getinge Edi catheter occupy the same anatomical space as the TEE probe, there is a potential risk of catheter shearing, tip displacement, or impaired TEE image quality (Mathur & Singh, 2009). To mitigate this, catheter insertion will take place either during chest closure, when the TEE probe has typically already been removed and time permits, or upon admission to the ICU.

As part of standard care, these patients will be admitted to the ICU post-surgery, still ventilated due to general anesthesia for surgery. This provides an opportunity to quantify respiratory effort during weaning in a homogeneous group, free from known underlying respiratory complications.

3.2 Second cohort – ICU patients mechanically ventilated for more than 24 hours

The second cohort of this observational study includes ICU patients who have been mechanically ventilated for more than 24 hours and are in the weaning phase from supportive ventilation mode. This cohort is included to ensure a diverse representation of individuals at risk of diaphragmatic dysfunction. Informed consent will be obtained in consultation with a family member.

3.3 Measurements

Given the possibility that the placement of both catheters could complicate correct positioning and potentially interfere with each other's measurements, both cohorts will be divided into two groups: half will receive the double-balloon NutriVent Pdi-catheter, while the other half will receive the Getinge Edi-catheter. Catheter assignment will be determined by randomization, unless one of the catheters is already in place, in which case that catheter will be used for the measurements.

Three respiratory effort techniques will be assessed for each patient, diaphragm ultrasound, occlusion pressures or either the Pdi- or Edi-catheter. To analyze both breath-to-breath variability and the influence of ventilator settings, measurements will be performed six times: two consecutive breaths per measurement, with approximately five spontaneous breaths in between. The six distinct measurement moments, along with their corresponding ventilator settings, Pressure Support (PS) and Positive End-Expiratory Pressure (PEEP), are outlined below:

1) Original ventilator settings
2) Original ventilator settings
3) PS = 5 cmH_2O, PEEP = 5 cmH_2O
4) PS = 5 cmH_2O, PEEP = 12 cmH_2O
5) PS = 12 cmH_2O, PEEP = 5 cmH_2O
6) PS = 12 cmH_2O, PEEP = 12 cmH_2O

For the original ventilator settings, it is essential that the patient is on pressure support mode in order to measure respiratory effort. This requirement is also included in the inclusion criteria described in *Section 4.2*.

All measurements will be performed six times, each over two consecutive breaths. The first breath will be used to measure the ultrasound-derived diaphragm thickening fraction (DTF), as well as the invasive parameters, either the Pdi and PTPes, or Edi. For the measurement of Pocc and P0.1, an end-expiratory occlusion maneuver will be performed during the second breath. This setup ensures that the occlusion does not influence the spontaneous respiratory effort measurements obtained from the first breath. The measurement sequence is illustrated in *Table 1*.

Original							Original							PS = 5, PEEP = 5							PS = 5, PEEP = 12							PS = 12, PEEP = 5							PS = 12, PEEP = 12						
1	2	3	4	5	6	7	1	2	3	4	5	6	7	1	2	3	4	5	6	7	1	2	3	4	5	6	7	1	2	3	4	5	6	7	1	2	3	4	5	6	7

Table 1. *The measurement sequence: white indicates the ventilator settings with parameters shown in cmH_2O, green indicates the five spontaneous breaths, blue indicates the sixth breath with the ultrasound measurement, and red indicates the seventh breath with the end-expiratory occlusion maneuver.*

The Pdi and PTPes, or Edi, will be recorded continuously across all six measurement moments. The ultrasound images will be acquired for offline analysis of the ultrasound derived diaphragm thickening fraction. After data collection, all parameters will be analyzed and aligned to the same breath for accurate comparison, with the Pocc and P0.1 measurements obtained one breath after the other parameters. In total, six values per parameter will be obtained for each patient.

Following the completion of all measurements, the catheter will be removed in consultation with a physician, and standard care will resume.

4. STUDY POPULATION

4.1 Population (base)

This study includes two cohorts. The first cohort includes post-operative cardiac surgery patients who are admitted to the ICU following surgery. The second cohort includes ICU-patients who have been on mechanical ventilation for more than 24 hours.

4.2 Inclusion criteria

To be eligible for participation in this study, participants must meet all of the following criteria:

- Be 18 years of age or older.
- Be admitted to the ICU at Catharina Hospital Eindhoven following cardiac surgery, OR be on mechanical ventilation for more than 24 hours at the ICU.
- Be in the weaning phase of mechanical ventilation on a supportive mode.
- Be willing and able to provide informed consent, OR informed consent may be provided by a family member (deferred informed consent).

4.3 Exclusion criteria

A potential participant will be excluded from this study if they meet any of the following criteria:

- Contraindications for Pdi or Edi catheter placement, such as history of esophageal, nose or stomach surgery or recent nose bleedings
- Use of intravenous or systemic muscle relaxants (neuromuscular blocking agents), as these directly affect diaphragmatic function
- Be hemodynamically unstable at the time of measurement, defined as being supported by mechanical circulatory support device (ECMO, IABP or Impella) or noradrenaline dose above 1mu.
- Have sustained a surgical diaphragmatic injury.
- Have active air leakage (e.g., pneumothorax).
- Be pregnant.
- Have a neuromuscular disorder affecting respiration.
- Have a body mass index (BMI) greater than 40 kg/m², as excessive adipose tissue may impair ultrasound image quality and alter respiratory mechanics, potentially affecting the accuracy and interpretability of study measurements.

4.4 Sample size calculation

For the sample size calculation, the *G*Power* tool version 3.1.9.7 was used, with the settings as outlined in *Table 2.*

Parameter	**Value**
Test family	Exact
Statistical test	Correlation: Bivariate normal model
Type of power analysis	A priori: Compute required sample size – given α, power and effect size
Tail(s)	Two
Significance level (α)	0.05
Power	0.8

Table 2. *Settings for the sample size calculation in G*Power-tool.*

For each patient, a total of six measurements per parameter will be obtained. However, since assessing breath-to-breath variability and the influence of confounders are secondary objectives, the sample size calculation will determine the number of patients, rather than the number of measurements needed.

Diaphragm ultrasound

DTF showed only a weak correlation with PTPes (R^2 = 0.326, r ≈ 0.571, p < 0.001), after excluding patients with diaphragmatic dysfunction, the correlation became markedly stronger (R^2 = 0.887, r ≈ 0.942, p < 0.001). As diaphragm dysfunction is not expected in cohort 1 (post-operative cardiac surgery patients), the sample size calculation is shown in *Figure 1A* using r = 0.942, resulting in a required sample size of 5 patients. In contrast, for cohort 2 (ICU patients ventilated for more than 24 hours), where diaphragm dysfunction is more likely, the calculation is shown in *Figure 1B* using r = 0.571, resulting in a required sample size of 21 patients.
High correlations were observed between Edi and DTF (R^2 = 0.623, r ≈ 0.789, p < 0.001) (Sklar et al. 2021). This results in a sample size calculation of 10, see *Figure 1C*.

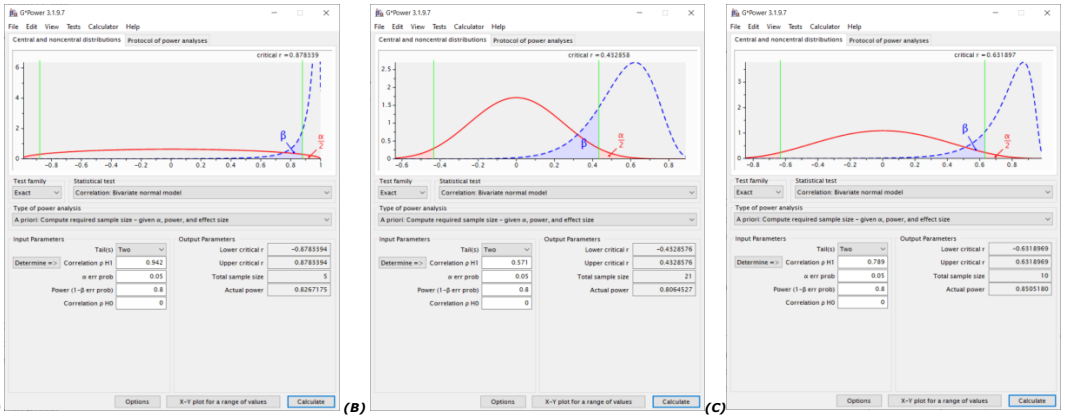

(A) (B) (C)

Figure 1. *Sample size calculation in G*Power for the correlation between: (A) PTPes and DTF in cohort 1 (post-operative cardiac surgery patients); and (B) PTPes and DTF in cohort 2 (ICU patients on mechanical ventilation for more than 24 hours); (C) Edi and DTF.*

Occlusion pressure measures

Conti et al. found a strong correlation and clinically acceptable agreement between P0.1 measured at the mouth and the drop in esophageal pressure during the first 0.1 seconds of inspiratory effort (r = 0.92, bias 0.3 ± 0.5 cmH_2O) (Conti et al., 1996). Therefore, P0.1 can be considered a valuable index for estimating respiratory drive.

Given the high correlation of occlusion pressures, sample size calculations will rely on ultrasound measurements to ensure adequate power.

The sample size calculation indicated that 5 patients were required in cohort 1 and 21 patients in cohort 2 for the Pdi catheter. For the Edi catheter, 10 patients were needed in both cohorts. This results in a total of 46 patients (5 + 21 + 10 + 10).

5. TREATMENT OF RESEARCH PARTICIPANTS

5.1 Investigational product/treatment

Several measurements will be performed during this study. The investigational products are the non-invasive techniques, specifically the Philips affinity ultrasound and the Getinge Servo-u ventilator. The non-investigational products are the invasive techniques, particularly the double-balloon NutriVent Pdi-catheter and the Getinge Edi-catheter. For more information, please refer to Chapter 6 and 7.

5.2 Use of co-intervention (if applicable)

N.A.

5.3 Escape medication (if applicable)

N.A.

6. INVESTIGATIONAL PRODUCT

6.1 Name and description of investigational product(s)

The investigational products are non-invasive techniques for quantifying respiratory effort, including diaphragm ultrasound and occlusion pressures with the ventilator.

Diaphragm ultrasound

For the diaphragm ultrasound measurements, the Affiniti ultrasound system of Philips will be used, which is a Class IIa CE-marked device. All measurements will be performed over two consecutive breaths, with the ultrasound measures from the first breath. A linear transducer will be placed along the right anterior axillary line, oriented longitudinally relative to the body axis. This longitudinal approach is preferred over imaging at individual intercostal spaces to minimize the angle dependence of the measurements. In this position, the hemidiaphragm appears above the liver as a central, less echogenic layer situated between the echogenic peritoneal and pleural layers (Oppersma et al., 2017).

Diaphragmatic thickness will be measured using M-mode at end-expiration ($T_{di,ee}$) and at peak inspiration ($T_{di,pi}$; i.e. peak thickness during inspiration) by measuring the distance between the diaphragmatic pleura and the peritoneum. Diaphragm thickening during inspiration (ΔT_{di}) will be calculated as the difference between $T_{di,pi}$ and $T_{di,ee}$. Diaphragm thickening fraction (DTF) will be expressed as the percentage change in diaphragm thickness during inspiration with formula $DTF = 100\% * (T_{di,pi} - T_{di,ee})/T_{di,ee}$ (Goligher et al., 2015).

Occlusion pressures

Patients will receive mechanical ventilation via the Servo-U system (Getinge, version 4.5), which is a Class IIb CE-marked device. This ventilator enables an end-expiratory occlusion maneuver, which will be performed during the second breath of each measurement moment. During this maneuver, the airway pressure (Paw) signal will be analyzed to determine P0.1 and Pocc. P0.1 is defined as the negative airway pressure generated during the first 100 ms of the occlusion. Pocc represents the pressure swing caused by respiratory muscle effort during the brief occlusion. This value can be used to estimate muscular pressure (Pmus) using the formula:

$Pmus = -0.75 \times Pocc$ (Cornejo et al., 2024).

6.2 Summary of findings from non-clinical studies

Diaphragm ultrasound

Non-clinical studies evaluating respiratory effort parameters using diaphragm ultrasound have shown that the diaphragm thickening fraction, although assessed in healthy individuals, correlates poorly with the gold standard measurement of transdiaphragmatic pressure (Poulard et al., 2022).

Occlusion pressures

The Getinge Servo-U system is widely used in intensive care units for mechanically ventilated patients. Since occlusion pressure measurements are well established in clinical practice and

validated through extensive clinical studies, reporting outcomes from non-clinical studies is not considered relevant in this context.

6.3 Summary of findings from clinical studies

Diaphragm ultrasound

In a cohort of 21 patients, DTF was moderately correlated with Edi ($R^2 = 0.623$, $p < 0.001$) (Sklar et al., 2021). Another study found that DTF had a weak overall correlation with PTPes ($R^2 = 0.326$, $p < 0.001$), which improved substantially ($R^2 = 0.887$, $p < 0.001$) after excluding patients with diaphragm dysfunction (Umbrello et al., 2020).

Occlusion pressures

Conti et al. demonstrated a strong correlation and clinically acceptable agreement between P0.1 measured at the mouth and the decrease in esophageal pressure (Pes) during the first 100 ms of inspiratory effort ($r = 0.92$, bias 0.3 ± 0.5 cmH_2O) (Conti et al., 1996). These findings support the use of P0.1 as a reliable index for estimating respiratory drive.

6.4 Summary of known and potential risks and benefits

Diaphragm ultrasound

Diaphragm ultrasound measurements will be performed using the Philips Affiniti ultrasound system. This technique uses high-frequency sound waves to visualize internal structures, such as the diaphragm. Ultrasound is a non-invasive imaging method and is widely regarded as safe, with no harmful effects associated with its use.

Occlusion pressures

The end-expiratory occlusion maneuver briefly interrupts the airflow, which may cause mild patient discomfort. However, as this procedure is routinely performed in ICUs, it is generally well accepted and considered a non-invasive technique.

A more comprehensive risk analysis for both the diaphragm ultrasound measurements and occlusion pressure assessments will be provided in Chapter 13.

6.5 Description and justification of route of administration and dosage

N.A.

6.6 Dosages, dosage modifications and method of administration

N.A.

7. NON-INVESTIGATIONAL PRODUCT

7.1 Name and description of non-investigational product(s)

The investigational products are invasive techniques for quantifying respiratory effort, including measuring both the esophageal pressure (Pes) and the gastric pressure (Pga) with the double-balloon NutriVent catheter and measuring the diaphragm electrical activity (Edi) with the Getinge catheter.

Transdiaphragmatic pressure (Pdi) and pressure-time product (PTPes)

The Pdi and PTPes will be measured using the double-balloon NutriVent Pdi-catheter, a nasogastric catheter for simultaneous measurement of gastric pressure (Pga) and esophageal pressure (Pes). This catheter is considered the reference standard for assessing respiratory effort and is visualized in *Figure 2*. The transdiaphragmatic pressure (Pdi) is calculated as the difference between Pga and Pes, reflecting diaphragm-specific effort, while Pes also captures the contribution of accessory inspiratory muscles (Jonkman et al., 2023). Both pressures are measured continuously to allow for offline alignment with the corresponding non-invasive measurements.

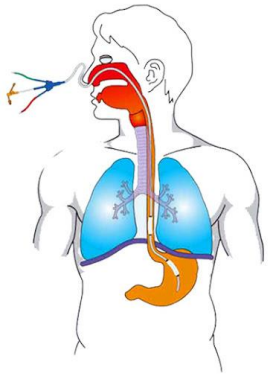

Figure 2. *Illustration of the double-balloon nasogastric NutriVent catheter with gastric and esophageal balloons for the measurement of Pga and Pes. (Illustration from NutriVent.)*

The pressure-time product (PTPes) can be determined from the Pes curve, illustrated in *Figure 3*. The PTPes is a gold standard method for estimating respiratory muscle effort. PTPes represents the integral of muscular pressure (Pmus) over the inspiratory phase, where Pmus is defined as the pressure generated by all respiratory muscles. Pmus is calculated as the difference between Pes and the elastic recoil pressure of the chest wall (Pcw) during inspiration. (Cornejo et al., 2024)

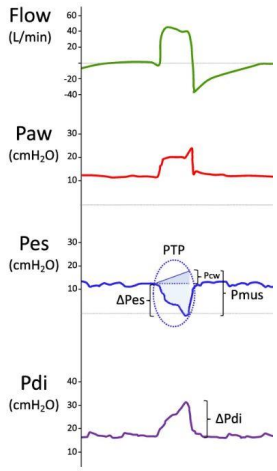

Figure 3. *Illustration of the pressure-time product (PTPes) derived from the esophageal pressure (Pes) curve, with Pmus representing respiratory muscle pressure, and Pcw representing chest wall recoil pressure. (Illustration adapted from Cornejo et al. (2024))*

Diaphragm electrical activity (Edi)

The Getinge Edi-catheter enables measuring the diaphragm electrical activity. Neural signals originating from the respiratory center travel via the phrenic nerve, triggering electrical activity in the diaphragm. This activity is detected by electrodes on the Edi catheter, which is placed in the esophagus at the level of the diaphragm. The electrical activity will be measured continuously to allow for offline alignment with the corresponding non-invasive measurements.

7.2 Summary of findings from non-clinical studies

As both the double-balloon NutriVent Pdi-catheter and the Getinge Edi-catheter have both obtained CE marking, indicating their compliance with European Union (EU) regulations for medical devices and underscore their status as state-of-art technology in healthcare. Both techniques are seen as gold-standard references for respiratory effort measurements (Cornejo et al., 2024, Jonkman et al., 2023). Therefore, a summary of findings from non-clinical studies is not relevant here.

7.3 Summary of findings from clinical studies

As both the double-balloon NutriVent Pdi-catheter and the Getinge Edi-catheter have both obtained CE marking, indicating their compliance with European Union (EU) regulations for medical devices and underscore their status as state-of-art technology in healthcare. Both techniques are seen as gold-standard references for respiratory effort measurements (Cornejo et al., 2024, Jonkman et al., 2023). Therefore, a summary of findings from clinical studies is also not relevant here.

7.4 Summary of known and potential risks and benefits

Both the NutriVent and Getinge catheters are inserted through the nose, which may pose a risk of nasal bleeding caused by possible trauma to the nasal mucosa during insertion. A more comprehensive risk analysis will be outlined in Chapter 13.

7.5 Description and justification of route of administration and dosage

N.A.

7.6 Dosages, dosage modifications and method of administration

N.A.

7.7 Preparation and labelling of Non Investigational Medicinal Product

N.A.

7.8 Drug accountability

N.A.

8. METHODS

8.1 Study parameters/endpoints

8.1.1 Main study parameter/endpoint

For each patient included in the study, the following parameters will be collected during six measurement moments, each separated by five spontaneous breaths, see *Table 1* (*Section 3.3*). Each measurement moment consists of two consecutive breaths, resulting in six values per parameter per patient.

Device	**Parameters**	**Method**
Servo-U Ventilator (Getinge)	Pocc [cmH_2O], P0.1 [cmH_2O]	The end-expiratory maneuver will be performed during the second breath.
Affiniti Ultrasound (Philips)	DTF [%] DTF = diaphragm thickening fraction	Diaphragm ultrasound imaging will be performed during the first breath.
Double-balloon NutriVent Catheter **OR** Getinge Catheter	Pga [cmH_2O], Pes [cmH_2O], PTPes [cmH_2O*s], Pdi [cmH_2O] (difference between Pga & Pes) Pga = gastric pressure, Pes = esophageal pressure, Pdi = transdiaphragmatic pressure **OR** Edi [µV] Edi = diaphragm electrical activity	Both the Pdi and Edi are automatically and continuously monitored. The corresponding measures will be time-matched to correlate with the non-invasive measures.

The main study endpoints are correlations between the invasive and non-invasive techniques for assessing respiratory effort:

- Pocc with Pdi/PTPes
- P0.1 with Pdi/PTPes
- DTF with Pdi/PTPes
- Pocc with Edi
- P0.1 with Edi
- DTF with Edi

Correlations will be analyzed using either Pearson or Spearman correlation coefficients (r), depending on data distribution and linearity. Correlation coefficients and corresponding p-values will be reported with the statistical significance set at $p<0.05$.

8.1.2 Secondary study parameters/endpoints (if applicable)

Breath-to-breath variability

To assess breath-to-breath variability in respiratory effort measurements within individual patients, the first two of the six total measurements will be performed using the original ventilator settings. This enables the evaluation of breath-to-breath variability over two separate measurement moments, with five spontaneous breaths in between, see *Table 1 (Section 3.3)*. This design will minimize the influence of external changes. Given that only two breaths will be measured under identical conditions, breath-to-breath variability will be assessed descriptively by calculating the absolute and relative (percentage) difference between the two measurements for each parameter. The results will serve as an exploratory indication of intra-individual variability.

Influence of ventilator settings and other confounders

To assess the influence of ventilator settings and support mode on each parameter, four of the six measurements will be performed using predefined pressure support (PS) mode and positive end-expiratory pressure (PEEP), as outlined in *Table 1 (Section 3.3)*. In addition, intravenous medications administered at the time of measurement will be documented, along with the Richmond Agitation-Sedation Scale (RASS) score to assess sedation level, as outlined in *Appendix 1* (Sessler et al., 2002).

A multivariable linear regression analysis will be conducted in SPSS to quantify the individual effects of the four confounding variables on each measurement outcome. In these models, the dependent variables will consist of both invasive and non-invasive measures of respiratory effort (Pdi, PTPes, Edi, DTF, P0.1, and Pocc). The independent variables will include PEEP level (set at either 5 or 12 cmH_2O), ventilator support mode (set at either 5 or 12 cmH_2O), sedation level (RASS score), and the presence or absence of specific intravenous medications. This statistical approach will allow for the assessment of the individual contribution of each factor.

Combining non-invasive measures

In addition to analyzing individual correlations, multiple linear regression analyses will be conducted to assess whether combinations of non-invasive measures (Pocc, P0.1, and DTF) correlate more strongly with the invasive reference values (Pdi, PTPes, and Edi) than any single parameter alone. These analyses will be conducted in SPSS, with Pdi, PTPes, or Edi as the dependent variable and combinations of non-invasive parameters as independent variables. The strength of these associations will be assessed using the coefficient of determination (R^2), and the individual contribution of each predictor will be evaluated using standardized regression coefficients and significance testing.

Feasibility, practicality, and patient experience

For each measurement technique, the following practical aspects will be evaluated:

- Preparation time: Time (in seconds) from the start of preparation until the initiation of the measurement procedure.
- Measurement duration: Time (in seconds) required to complete the measurement over a single breath.
- Time required for data analysis: Time (in seconds) from completion of the measurement until the parameter values are obtained. For offline analyses, such as ultrasound-based measures, this includes the time taken to start the computer and run the required software for parameter calculation.
- Operator expertise: The level of operator expertise required to perform each respiratory effort technique will be assessed using a 5-point scale:
    1) No training required – procedure is intuitive or self-explanatory.
    2) Minimal training needed – approximately 1 hour; most ICU staff are generally familiar with the technique.
    3) Basic training required – 1 to 3 hours of additional instruction needed.
    4) Advanced expertise needed – typically performed by trained specialists due to complexity.
    5) Specialist level – requires extensive training or certification beyond standard ICU competencies.
- Invasiveness and patient tolerance: The level of invasiveness and expected patient tolerance for each respiratory effort measurement technique will be evaluated using a 5-point scale:
    1) Non-invasive with no discomfort
    2) Non-invasive with mild discomfort
    3) Minimally invasive with mild discomfort
    4) Invasive with discomfort
    5) Invasive with patient intolerance
- Associated costs: The cost assessment will include only the purchase of single-use materials. Expenses related to durable equipment, such as ultrasound machines or ventilators, will be excluded.

8.1.3 Other study parameters (if applicable)

Additional study parameters collected for analysis will include gender, age, height, body weight, body mass index (BMI), smoking status, COPD severity, primary ICU admission diagnosis, hours since intubation, and duration of mechanical ventilation prior to the measurement. Ventilator

settings such as tidal volume, respiratory rate, and inspiratory time will also be recorded. Relevant comorbidities, including heart failure, kidney disease, and diabetes, will be documented as well.

8.2 Randomization, blinding and treatment allocation

Patients will be assigned to receive either a double-balloon NutriVent catheter or a Getinge catheter, with the aim of enrolling the target sample size as calculated in *Section 4.4*. Since both devices are invasive, randomization will only apply when neither catheter is already in place. If a patient has an existing catheter (either NutriVent or Getinge), that catheter will be used for the study to avoid unnecessary additional procedures.
For patients without a pre-inserted catheter, randomization will be performed using a computer-generated allocation sequence. The allocation sequence will be managed by an independent researcher not involved in data collection or analysis, to minimize selection bias.
Blinding is not required for this study.

8.3 Study procedures

Two different cohorts will be included in this study. For the first cohort, the post-operative cardiac surgery patients, informed consent will be obtained either during the pre-operative screening or on the day of hospital admission, one day prior to surgery. The latter is the preferred approach, as it is logistically more practical, reduces the burden on patients during the pre-operative phase and because this study only involves procedures that are part of standard care, it is not expected to cause significant distress.

For the second cohort, ICU patients who have been on mechanical ventilation for more than 24 hours, informed consent will be obtained from a family member. If a patient is subsequently weaned off the ventilator, they will have the option to withdraw from the study, and any data collected from them will be deleted.

The researcher will inform the patients (first cohort) or patients family (second cohort), about the study and provide the opportunity to ask questions or request additional information, which will be addressed by the researcher. Patients who are able to provide consent will sign the informed consent form prior to surgery. For the second cohort, a legally authorized representative or family member will provide consent on their behalf.

Patients will receive standard care according to their cardiac surgery or ICU treatment plan. Post-operative cardiac surgery patients will be admitted to the ICU following surgery. Study measurements will be conducted in the ICU while patients are in the weaning phase from mechanical ventilation. Patients will receive either a double-balloon NutriVent catheter or a Getinge Edi catheter. If one of these catheters is already in place, this one will be used. Otherwise, catheter allocation will be determined by randomization. The catheter insertion will be performed by a physician. The catheter will automatically and continuously measure either the Pga & Pes or the Edi. For each patient, six measurements will be performed as illustrated in *Table 1* (*Section 3.3*). Five spontaneous breaths under the defined ventilator settings will be followed by an ultrasound measurement during the sixth breath and an end-expiratory occlusion maneuver during the seventh breath. Subsequently, the ventilator settings will be adjusted as specified in *Table 1* (*Section 3.3*), followed by five spontaneous breaths and a repetition of the measurements. After completing the six measurements, the inserted catheter will be removed in consultation with a physician, as it is already in place and may still be medically relevant.

8.4 Withdrawal of individual research participants

Participants can leave the study at any time for any reason without any consequences if they wish to do so. The investigator can decide to withdraw a participant from the study for urgent medical reasons. Collected data until the withdrawal will be used for analysis.

8.4.1 Specific criteria for withdrawal (if applicable)

N.A.

8.5 Replacement of individual research participants after withdrawal

In case of withdrawal of a patient, the patient will be replaced until the targeted sample size has been reached.

8.6 Follow-up of research participants withdrawn from treatment

N.A.

8.7 Premature termination of the study

The inclusion of patients will stop after the targeted sample size has been reached.

9. SAFETY REPORTING

9.1 Temporary halt for reasons of research participant safety

In accordance to section 10, subsection 4, of the WMO, the sponsor will suspend the study if there is sufficient ground that continuation of the study will jeopardise participant health or safety. The sponsor will notify the review committee without undue delay of a temporary halt including the reason for such an action. The study will be suspended pending a further positive decision by the review committee. The investigator will take care that all participants are kept informed.

9.2 AEs, SAEs

9.2.1 Adverse events (AEs)

Adverse events are defined as any undesirable experience occurring to a participant during the study, whether considered related to the investigational product. All adverse events reported spontaneously by the participant or observed by the investigator or his staff will be recorded.

9.2.2 Serious adverse events (SAEs)

A serious adverse event is any untoward medical occurrence or effect that

- results in death;
- is life threatening (at the time of the event);
- requires hospitalisation or prolongation of existing inpatients' hospitalisation;
- results in persistent or significant disability or incapacity;
- is a congenital anomaly or birth defect; or
- any other important medical event that did not result in any of the outcomes listed above due to medical or surgical intervention but could have been based upon appropriate judgement by the investigator.

An elective hospital admission will not be considered as a serious adverse event.

The investigator will report all SAEs to the sponsor without undue delay after obtaining knowledge of the events, only if they are related to the respiratory measurements of the investigational products.
The sponsor will report these study-related SAEs through the web portal *Research Portal* to the review committee that approved the protocol, within 7 days of first knowledge for SAEs that result in death or are life threatening followed by a period of maximum 8 days to complete the initial preliminary report. All other SAEs will be reported within a period of maximum 15 days after the sponsor has first knowledge of the serious adverse events.

9.3 Follow-up of adverse events

All AEs will be followed until they have abated, or until a stable situation has been reached. Depending on the event, follow up may require additional tests or medical procedures as indicated, and/or referral to the general physician or a medical specialist. SAEs need to be reported till end of study within the Netherlands, as defined in the protocol.

9.4 [Data Safety Monitoring Board (DSMB) / Safety Committee]

N.A.

10. STATISTICAL ANALYSIS

All parameters collected in this study will be presented as discrete values derived from a single breath. For the non-invasive parameters, one value per parameter will be determined for each measurement during a single breath, resulting in six values per patient. The diaphragm thickening fraction (DTF) will be derived through offline analysis of the ultrasound images taken during the first breath, while Pocc and P0.1 will be obtained from the end-expiratory occlusion maneuvers performed at the second breath, which could otherwise affect the ultrasound and invasive measurements.

The invasive parameters will be collected continuously and automatically, with either Pdi or Edi being recorded depending on the randomization group. After data acquisition, they will be matched offline to the corresponding breaths during which the ultrasound measurements were performed. For each matched measurement, the pressure waveforms from the gastric (Pga) and esophageal (Pes) catheters will be visualized. From these curves, the transdiaphragmatic pressure (Pdi = Pga – Pes) and the esophageal pressure–time product (PTPes) will be calculated.
For the electrical activity of the diaphragm (Edi), a continuous waveform will be recorded per measurement. From this waveform, the peak Edi will be extracted for each breath, resulting in six parameter values per patient.

Per patient, six values per parameter will be obtained: one for each of the five ventilator settings, plus one additional repeated measurement to assess breath-to-breath variability.

All statistical analyses will be performed using SPSS. Statistical significance will be defined as a two-tailed p-value < 0.05. Normality will be evaluated using the Shapiro-Wilk test in combination with visual inspection of histograms, Q-Q plots, and scatterplots. Assessments will be conducted individually per patient and for each ventilator setting.

Missing data will be documented. However, the other parameters from that patient will still be included for analysis if complete.

10.1 Primary study parameter(s)

The primary analysis will focus on assessing the strength of association between non-invasive and invasive measures of respiratory effort. This will be done through correlation analyses between the following parameter pairs:

- Pocc with Pdi/PTPes
- P0.1 with Pdi/PTPes
- DTF with Pdi/PTPes
- Pocc with Edi
- P0.1 with Edi
- DTF with Edi

For each patient, six values per parameter will be collected under five different ventilator settings, with two measurements performed under identical settings to evaluate breath-to-breath variability. To avoid subjective decisions during analysis, all six predefined measurement time points (outlined in *Section 3.3*) will be included in the primary analysis without exclusion. Measurements will be aligned per breath and time-matched between the invasive and non-invasive parameters. Only the first breath of each measurement moment will be used for diaphragm ultrasound and invasive respiratory effort measurements to ensure consistency. The second breath will be reserved for the end-expiratory occlusion maneuver, which could otherwise affect the ultrasound and invasive measurements.

Normality of data distribution will be assessed per parameter using the Shapiro-Wilk test and visual inspection of histograms and Q-Q plots. Based on data distribution and visual assessment of linearity in scatterplots, either Pearson (for normally distributed, linear relationships) or Spearman (for non-normal or non-linear relationships) correlation coefficients will be calculated. Two-tailed p-values < 0.05 will be considered statistically significant.

10.2 Secondary study parameter(s)

Breath-to-breath variability

Breath-to-breath variability will be assessed using the first and second measurements obtained under the original, identical ventilator settings. Absolute and relative differences between the two measurements per parameter will be calculated and reported descriptively to provide insight into intra-individual variability.

Influence of ventilator settings and other confounders

A multivariable linear regression analysis will be conducted in SPSS to quantify the individual effects of the four confounding variables on each measurement outcome. The dependent variables will include both invasive (Pdi, PTPes, Edi) and non-invasive (Pocc, P0.1, and DTF) measures. Independent variables will include:

- PEEP level (5 or 12 cmH_2O)
- Pressure support level (5 or 12 cmH_2O)
- Sedation level (RASS score, see *Appendix 1* (Sessler et al., 2002))
- Use of intravenous medications (categorized by type, e.g., sedatives, pain medication; recorded as yes/no for each type)

This statistical approach will allow for the assessment of the individual contribution of each factor.

Combining non-invasive measures

In addition, multivariate analysis will be conducted using multiple linear regression models to explore whether combinations of non-invasive parameters provide a stronger association with the invasive reference standards (Pdi, PTPes and Edi). These models will be performed in SPSS, with either Pdi, PTPes or Edi as the dependent variable and combinations of Pocc, P0.1, and DTF as independent variables. Model strength will be assessed by the coefficient of determination (R^2), and the contribution of individual predictors will be evaluated using standardized regression coefficients and p-values.

Feasibility, practicality, and patient experience

Descriptive statistics will be used to summarize the practical aspects of each respiratory effort measurement technique. Continuous variables, including preparation time, measurement duration, and time required for data analysis (all measured in seconds), will be reported as means with standard deviations or medians with interquartile ranges, depending on data distribution assessed by Shapiro-Wilk tests and visual inspection of histograms and Q-Q plots.

Variables, such as operator expertise and invasiveness/patient tolerance ratings (both assessed on 5-point scales), will be described using medians and interquartile ranges, and frequencies for each category will be presented.

Associated costs (purchase price of single-use materials) will be presented descriptively.

10.3 Other study parameters

Other study parameters such as gender (male/female), age (years), height (cm), body weight (kg), BMI (kg/m²), smoking status (yes/no/history), COPD severity (GOLD stage), primary ICU admission diagnosis, time since intubation (hours), and duration of mechanical ventilation (hours) will be summarized using descriptive statistics. Continuous variables will be reported as mean ± standard deviation or median with interquartile range, depending on data distribution. Categorical variables will be presented as frequencies and percentages.

Ventilator settings at the time of measurement (e.g. tidal volume, respiratory rate, inspiratory time), as well as comorbidities such as heart failure, kidney disease, and diabetes, will also be included in the descriptive statistics.

10.4 Interim analysis (if applicable)

N.A.

11. ETHICAL CONSIDERATIONS

11.1 Regulation statement

Study involving human subjects will be conducted in the respect of the following codes:

- The study will be conducted in accordance with the principles of the Declaration of Helsinki (latest version, 75th WMA General Assembly, Oslo, Norway, October 2024), Directive 2001/20/EC of the European Parliament and of the Council of 4 April 2001 on the approximation of the laws, regulations and administrative provisions of the Member States relating to the implementation of good clinical practice (GCP).
- The Medical Research Involving Human Subjects Act (WMO)
- ICH E6, International Conference of Harmonization (ICH) guideline for Good Clinical Practice
- EN ISO 14155:2011(E)
- Medical Device Regulation, no 2017/745, dated May 26, 2021
- All investigators including the PI are GCP (by passing the GCP or BROK exam) certified.
- No benefit is expected upon participation with this study.

11.2 Recruitment and consent

Two different cohorts will be included in this study, each with specific recruitment and informed consent procedures:

Cohort 1: Post-operative cardiac surgery patients
Eligible patients will be identified during their pre-operative screening or on the day of hospital admission, one day prior to surgery. The preferred approach is to obtain informed consent on the day of admission, as this is logistically more practical and reduces patient burden during the pre-operative phase. The study involves only procedures that are part of standard care at ICU-departments and is therefore not expected to cause significant distress. Patients will be informed about the study by the investigator or a qualified research team member, who will explain the study purpose, procedures, and risks in detail. Patients will have until the morning of surgery to consider participation and ask any questions before providing written informed consent.

Cohort 2: ICU patients on mechanical ventilation for more than 24 hours
Since these patients may be unable to provide consent themselves, informed consent will be sought from a legally authorized representative or family member. The investigator or a qualified research team member will approach the family to explain the study, answer questions, and provide written information. If a patient is weaned off mechanical ventilation and regains decision-making capacity, they will be informed about the study and given the option to withdraw consent. In such cases, any previously collected data will be deleted.

In both cohorts, the investigator or a qualified member of the research team will be responsible for providing information and obtaining consent. Participants or their representatives will be given sufficient time to consider their decision and ask questions to ensure fully informed voluntary participation.

11.3 Objection by minors or incapacitated research participants (if applicable)

N.A.

11.4 Benefits and risks assessment, group relatedness

This study includes capacitated adults, inclusion of post-operative cardiac surgery patients and ICU patients receiving mechanical ventilation for more than 24 hours. For the latter group, informed consent will be obtained from a legally authorized representative.

Although the study focuses on measuring and comparing different techniques for assessing respiratory effort, all procedures are part of standard clinical care in ICU departments and are routinely used in patients undergoing weaning. For post-operative cardiac surgery patients, these procedures are not usually part of their standard care. However, since the invasive techniques are frequently employed in ICU settings, involve minimal additional risk, and are performed while patients are sedated or otherwise unaware, they are not expected to cause significant discomfort or distress. Therefore, their use is considered proportionate to the potential future benefits for both patient groups.

The minimal risks and burden are justified by the potential value of the study, namely improving the accuracy and usability of non-invasive techniques for measuring respiratory effort. This may lead to less invasive monitoring and better care for mechanically ventilated patients in the future.

This study cannot be conducted without including the specified patient groups. Post-operative cardiac surgery patients are valuable due to their homogenous profile without underlying respiratory issues, while mechanically ventilated ICU patients represent a broader, more clinically diverse population that reflects real-world use of the techniques.

11.5 Compensation for injury

The investigator has a liability insurance which is in accordance with article 7 of the WMO.

The Catharina hospital (initiator/investigator) has an insurance which is in accordance with the legal requirements in the Netherlands (Article 7 WMO). This insurance provides cover for damage to research subjects through injury or death caused by the study.
The insurance applies to the damage that becomes apparent during the study or within 4 years after the end of the study.

11.6 Incentives (if applicable)

No incentives or compensation will be given to the subjects through participation in the study.

12. ADMINISTRATIVE ASPECTS, MONITORING AND PUBLICATION

12.1 Handling and storage of data and documents

Each participant will be assigned a unique study identification code to ensure anonymity. Personal identifying information (such as name, date of birth, and medical record number) will be stored separately from the coded research data in a secure and access-restricted environment. The key linking the unique study codes to personal identifiers will be securely password-protected and maintained solely by the principal investigator.

All raw measurement data, will be stored in an encrypted, access-controlled database located within the Catharina Hospital's secure IT infrastructure. Access to this database will be limited to the principal investigator and authorized research team members involved in data processing.

Data processing, such as parameter extraction and transformation into anonymized formats, will take place within the hospital's secure environment. The processed data, in which individual participants cannot be identified, will be shared with research team members involved in data analysis and scientific reporting. The shared data will be used exclusively for the purpose of scientific analysis and publication in peer-reviewed journals.

All data, including coded raw and processed datasets, will be retained for a period of 15 years in accordance with institutional and legal requirements. Physical and digital security measures, including encrypted storage and controlled user access, will be maintained throughout the storage period.

To facilitate research documentation and monitoring, anonymized participant information and study-related data will be entered and managed in a secure electronic case report form (eCRF) system, accessible only to authorized study staff.

These measures collectively ensure the privacy of study participants is protected and that data integrity and security are upheld throughout the research process.

12.2 Monitoring and Quality Assurance

A monitor from Catharina Hospital will oversee the study to ensure it is conducted in accordance with the clinical investigation plan, the principles of good clinical practice (ISO 14155:2020), and the Medical Device Regulation (MDR). The monitor will also verify patient safety and ensure that the reported data are accurate and complete.

Prior to study initiation, the monitor will visit the site to confirm that the principal investigator and the study team have all necessary information to begin the clinical investigation. Throughout the study, the monitor will perform ongoing oversight, either on-site or remotely, according to the monitoring plan to ensure compliance with the clinical investigation plan and maintain study quality. This may include reviewing the collected data. Upon study completion, the monitor will carry out close-out activities.

12.3 Amendments

Amendments are changes made to the research after a favorable opinion by the review committee has been given. All amendments will be notified to the review committee that gave a favorable opinion.

Non-substantial amendments will not be notified to the review committee, but will be recorded and filed by the sponsor. Examples of non-substantial amendments include typographical errors and administrative updates, such as changes to names, telephone numbers, or other contact details of individuals listed in the study documentation.

12.4 Annual progress report

The sponsor/investigator will submit a summary of the progress of the trial to the review committee once a year. Information will be provided on the date of inclusion of the first participant, numbers of participants included and numbers of participants that have completed the trial, serious adverse events, other problems, and amendments.

12.5 Temporary halt and (prematurely) end of study report

The investigator/sponsor will notify the review committee of the end of the study within a period of 8 weeks. The end of the study is defined as the moment when the final measurements from the last patient have been collected. The sponsor will notify the review committee immediately of a temporary halt of the study, including the reason of such an action.
In case the study is ended prematurely, the sponsor will notify the review committee within 15 days, including the reasons for the premature termination.
Within one year after the end of the study, the investigator/sponsor will submit a final study report with the results of the study, including any publications/abstracts of the study, to the review committee.

12.6 Public disclosure and publication policy

- The clinical trial will be registered in a public clinical trial registry (clinicaltrials.gov) prior to enrolling the first patient.
- The scientific findings of this study will be published in peer-reviewed journals and presented at scientific conferences.

13. STRUCTURED RISK ANALYSIS

The investigational products are the non-invasive techniques, specifically the Philips affinity ultrasound and the Getinge Servo-u ventilator, and the non-investigational products are the invasive techniques, particularly the double-balloon NutriVent Pdi-catheter and the Getinge Edi-catheter. For these four products, the structured risk analysis is outlined below.

13.1 Potential issues of concern

a. Level of knowledge about mechanism of action

The investigational products (Philips Affiniti ultrasound and Getinge Servo-u ventilator) and non-investigational products (NutriVent double-balloon Pdi-catheter and Getinge Edi-catheter) are all well-established medical devices with clearly understood mechanisms of action.

- Philips Affiniti ultrasound operates using conventional ultrasound imaging principles to visualize diaphragmatic motion. It is non-invasive and widely used in clinical practice, with no known systemic effects.
- Getinge Servo-u ventilator is a standard ICU ventilator. The investigational aspect lies in the software-based estimation of respiratory effort, which is enabled by performing a pre-expiratory occlusion maneuver.
- NutriVent double-balloon catheter is used for esophageal pressure measurements and gastric pressure measurement to determine the transdiaphragmatic pressure. This method is well-established in intensive care settings and is used worldwide in both clinical and research contexts.
- Getinge Edi-catheter measures diaphragm electrical activity via sensors on a nasogastric tube. The technology is well understood and used in the clinical setting to optimize patient-ventilator interaction.

All techniques rely on local mechanical or electrical measurements and do not introduce pharmacologic agents or systemic biological effects. Based on current clinical and physiological knowledge, no plausible self-amplifying mechanisms (e.g., immunologic, psychiatric, or coagulatory pathways) are expected to be triggered by any of these techniques.

Therefore, the mechanism of action of all four devices is adequately known, and the risk of unintended activation of systemic pathways is considered negligible.

b. Previous exposure of human beings with the test product(s) and/or products with a similar biological mechanism

Philips Affiniti ultrasound system is routinely used for bedside monitoring of patients in the ICU, including applications such as point-of-care ultrasound (POCUS). It uses non-ionizing ultrasound waves, making it a non-invasive and safe imaging technique.

Getinge Servo-u ventilator is a standard ICU ventilator. The investigational aspect relates to the use of a software-supported estimation of respiratory effort via a pre-expiratory occlusion maneuver, which is a well-described and safe method used in both research and clinical practice to estimate patient effort during mechanical ventilation.

NutriVent double-balloon catheter has been used in various studies for invasive measurement of transdiaphragmatic pressure (Pdi) and is considered the gold standard for quantifying respiratory effort. The technique is invasive but has been demonstrated to be safe in sedated, intubated patients, which is applicable to the population in this study.

Getinge Edi-catheter is routinely used in clinical practice to measure diaphragmatic activity as part of neurally adjusted ventilatory assist (NAVA). Its safety and functionality have been well-established.

c. Can the primary or secondary mechanism be induced in animals and/or in *ex-vivo* human cell material?

The primary and secondary mechanisms involved in the investigational techniques are based on physiological measurements of respiratory muscle activity and pressure dynamics, rather than pharmacological or receptor-mediated pathways. Therefore, traditional approaches such as inducing mechanisms in animal models or using ex-vivo human cell material are not applicable.

d. Selectivity of the mechanism to target tissue in animals and/or human beings

The investigational techniques do not involve pharmacological mechanisms, receptor binding, or tissue-specific toxicity. Instead, they rely on physiological monitoring of respiratory effort using mechanical or electrical signal detection. As no drugs or biological agents are administered, general pharmacological or toxicological studies are not applicable.

- Philips Affiniti ultrasound targets the diaphragm through imaging, using non-ionizing ultrasound waves. It is non-invasive, routinely used, and does not interact with tissues chemically or biologically. Selectivity is based on the anatomical focus of the ultrasound probe rather than biochemical specificity.
- Getinge Servo-u ventilator assesses with the pre-expiratory occlusion maneuver the respiratory effort via airway pressure changes. The target is the mechanical output of the respiratory system.
- NutriVent double-balloon catheter is an invasive device designed to monitor esophageal and gastric pressure. Its double-balloon configuration ensures accurate anatomical positioning and specificity in relation to the diaphragm. No other mechanisms are involved.
- Getinge Edi-catheter is an invasive device intended to selectively measure diaphragmatic electrical activity. Proper positioning ensures anatomical specificity, and no other mechanisms are involved.

e. Analysis of potential effect

All four techniques have well-established safety records in ICU settings. Adverse effects are unlikely and, if present, are expected to be minor (e.g., discomfort due to catheter placement). No vital organ systems are directly affected, and no systemic adverse effects are anticipated.

f. Pharmacokinetic considerations

N.A.

g. Study population

The study population consists of two patient cohorts admitted to the ICU. The first cohort includes post-operative cardiac surgery patients, who are generally clinically stable but recovering from major surgery and are in the weaning phase from mechanical ventilation. The second cohort includes ICU patients of mechanical ventilation for more than 24 hours with varied underlying conditions, some of whom may have unstable health statuses due to their critical illness.

h. Interaction with other products

This study uses monitoring devices, including the invasive Edi- and Pdi-catheters, alongside standard ICU equipment such as endotracheal tubes for mechanical ventilation. While no pharmacokinetic interactions are expected due to the absence of investigational drugs, potential physical or mechanical interactions may occur between the catheters and the

endotracheal tube or other airway devices. These interactions will be carefully monitored and managed according to clinical protocols to minimize patient risk. The monitoring techniques themselves do not pharmacologically affect the patient or interact with administered medications.

i. Predictability of effect

The techniques generate physiological parameters related to respiratory effort. This study will investigate the correlation between these parameters to evaluate their accuracy and clinical relevance.

j. Can effects be managed?

The insertion of the Pdi and Edi catheters involves certain procedural risks, such as discomfort, bleeding, or infection, which are well-recognized and managed according to standard ICU protocols. Additionally, the pre-expiratory occlusion maneuver enabled by the Servo-u ventilator may cause temporary discomfort for the patient. However, since patients are sedated during these procedures, they are unlikely to be consciously aware of any discomfort.

Throughout the study, patients will be closely monitored by experienced ICU staff, ensuring immediate access to appropriate medical support to manage any adverse effects or discomfort. There are no specific antidotes needed for these interventions.

13.2 Synthesis

This study investigates relationship between the invasive and non-invasive techniques for assessing respiratory effort in ICU patients. While the investigational procedures carry some procedural risks, such as discomfort or minor complications from catheter insertion, or transient discomfort from ventilator maneuvers, these are well-documented, routinely used in clinical practice, and are applied under strict ICU protocols.
Several measures have been taken to reduce risks for study participants:

- Study population: Participants are ICU patients who are already sedated and mechanically ventilated, meaning they are unlikely to experience or remember procedural discomfort.
- Inclusion criteria: Only stable, sedated patients are included. Patients in acute distress, with contraindications for catheter placement, or with known risk factors for complications are excluded.
- Standard procedures: All interventions, including the insertion of the NutriVent Pdi catheter and Getinge Edi catheter, and use of the pre-expiratory occlusion maneuver, are standard or clinically validated ICU procedures.
- Trained staff: All procedures are performed by the investigator under supervision of trained ICU staff, ensuring proper technique and response to any unexpected complications.
- Data protection: Privacy-related risks are mitigated through strict data pseudonymization, secure storage, and limited access protocols.

Remaining risks, primarily related to minor procedural complications, are considered low and acceptable, especially given the level of sedation and close clinical monitoring in the ICU setting. No additional medication or unapproved medical devices are introduced in the study.

Given the low risk profile and the potential for this study to significantly improve future respiratory monitoring strategies, the overall risk for participants is considered justified and proportionate.

14. REFERENCES

Boles, J. M., Bion, J., Connors, A., Herridge, M., Marsh, B., Melot, C., Pearl, R., Silverman, H., Stanchina, M., Vieillard-Baron, A., & Welte, T. (2007). Weaning from mechanical ventilation. The European respiratory journal, 29(5), 1033–1056. https://doi.org/10.1183/09031936.00010206

Conti, G., Cinnella, G., Barboni, E., Lemaire, F., Harf, A., & Brochard, L. (1996). Estimation of occlusion pressure during assisted ventilation in patients with intrinsic PEEP. American journal of respiratory and critical care medicine, 154(4 Pt 1), 907–912. https://doi.org/10.1164/ajrccm.154.4.8887584

Cornejo, R., Telias, I., & Brochard, L. (2024). Measuring patient's effort on the ventilator. Intensive care medicine, 50(4), 573–576. https://doi.org/10.1007/s00134-024-07352-4

Dres, M., Dubé, B. P., Mayaux, J., Delemazure, J., Reuter, D., Brochard, L., Similowski, T., & Demoule, A. (2017). Coexistence and Impact of Limb Muscle and Diaphragm Weakness at Time of Liberation from Mechanical Ventilation in Medical Intensive Care Unit Patients. American journal of respiratory and critical care medicine, 195(1), 57–66. https://doi.org/10.1164/rccm.201602-0367OC

Fritsch, S. J., Hatam, N., Goetzenich, A., Marx, G., Autschbach, R., Heunks, L., Bickenbach, J., & Bruells, C. S. (2022). Speckle tracking ultrasonography as a new tool to assess diaphragmatic function: a feasibility study. Ultrasonography (Seoul, Korea), 41(2), 403–415. https://doi.org/10.14366/usg.21044

Goligher, E. C., Dres, M., Fan, E., Rubenfeld, G. D., Scales, D. C., Herridge, M. S., Vorona, S., Sklar, M. C., Rittayamai, N., Lanys, A., Murray, A., Brace, D., Urrea, C., Reid, W. D., Tomlinson, G., Slutsky, A. S., Kavanagh, B. P., Brochard, L. J., & Ferguson, N. D. (2018). Mechanical Ventilation-induced Diaphragm Atrophy Strongly Impacts Clinical Outcomes. American journal of respiratory and critical care medicine, 197(2), 204–213. https://doi.org/10.1164/rccm.201703-0536OC

Goligher, E. C., Laghi, F., Detsky, M. E., Farias, P., Murray, A., Brace, D., Brochard, L. J., Bolz, S. S., Rubenfeld, G. D., Kavanagh, B. P., & Ferguson, N. D. (2015). Measuring diaphragm thickness with ultrasound in mechanically ventilated patients: feasibility, reproducibility and validity. Intensive care medicine, 41(4), 642–649. https://doi.org/10.1007/s00134-015-3687-3

Jonkman, A. H., Telias, I., Spinelli, E., Akoumianaki, E., & Piquilloud, L. (2023). The oesophageal balloon for respiratory monitoring in ventilated patients: updated clinical review and practical aspects. European respiratory review : an official journal of the European Respiratory Society, 32(168), 220186. https://doi.org/10.1183/16000617.0186-2022

Jonkman, A. H., de Vries, H. J., & Heunks, L. M. A. (2020). Physiology of the Respiratory Drive in ICU Patients: Implications for Diagnosis and Treatment. Critical care (London, England), 24(1), 104. https://doi.org/10.1186/s13054-020-2776-z

Mathur, S. K., & Singh, P. (2009). Transoesophageal echocardiography related complications. Indian journal of anaesthesia, 53(5), 567–574.

Mauri, T., Yoshida, T., Bellani, G., Goligher, E. C., Carteaux, G., Rittayamai, N., Mojoli, F., Chiumello, D., Piquilloud, L., Grasso, S., Jubran, A., Laghi, F., Magder, S., Pesenti, A., Loring, S., Gattinoni, L., Talmor, D., Blanch, L., Amato, M., Chen, L., … PLeUral pressure working Group (PLUG—Acute Respiratory Failure section of the European Society of Intensive Care Medicine) (2016). Esophageal and transpulmonary pressure in the clinical setting: meaning, usefulness and perspectives. Intensive care medicine, 42(9), 1360–1373. https://doi.org/10.1007/s00134-016-4400-x

NutriVent (n.d.). Indications for use. http://www.nutrivent.eu/en/indications.php

Oppersma, E., Hatam, N., Doorduin, J., van der Hoeven, J. G., Marx, G., Goetzenich, A., Fritsch, S., Heunks, L. M. A., & Bruells, C. S. (2017). Functional assessment of the diaphragm by speckle tracking ultrasound during inspiratory loading. Journal of applied physiology (Bethesda, Md. : 1985), 123(5), 1063–1070. https://doi.org/10.1152/japplphysiol.00095.2017

Poulard, T., Bachasson, D., Fossé, Q., Niérat, M. C., Hogrel, J. Y., Demoule, A., Gennisson, J. L., & Dres, M. (2022). Poor Correlation between Diaphragm Thickening Fraction and Transdiaphragmatic Pressure in Mechanically Ventilated Patients and Healthy Subjects. Anesthesiology, 136(1), 162–175. https://doi.org/10.1097/ALN.0000000000004042

Sessler, C. N., Gosnell, M. S., Grap, M. J., Brophy, G. M., O'Neal, P. V., Keane, K. A., Tesoro, E. P., & Elswick, R. K. (2002). The Richmond Agitation-Sedation Scale: validity and reliability in adult intensive care unit patients. American journal of respiratory and critical care medicine, 166(10), 1338–1344. https://doi.org/10.1164/rccm.2107138

Sklar, M. C., Madotto, F., Jonkman, A. H., & others. (2021). Duration of diaphragmatic inactivity after endotracheal intubation of critically ill patients. Critical Care, 25(1), 26. https://doi.org/10.1186/s13054-020-03435-y

Stichting NICE. (2024). Basisgegevens IC-units 2024 [Dataset]. Data in Beeld. Retrieved July 16, 2025, from https://www.stichting-nice.nl/datainbeeld/public?year=2024&subject=BASIC&hospital=-1&icno=0

Umbrello, M., Formenti, P., Lusardi, A. C., Guanziroli, M., Caccioppola, A., Coppola, S., & Chiumello, D. (2020). Oesophageal pressure and respiratory muscle ultrasonographic measurements indicate inspiratory effort during pressure support ventilation. British journal of anaesthesia, 125(1), e148–e157. https://doi.org/10.1016/j.bja.2020.02.026

de Vries, H., Jonkman, A., Shi, Z. H., Spoelstra-de Man, A., & Heunks, L. (2018). Assessing breathing effort in mechanical ventilation: physiology and clinical implications. Annals of translational medicine, 6(19), 387. https://doi.org/10.21037/atm.2018.05.53

15. Appendix

15.1 Appendix 1 – RASS-Score

Score	Term	Description
+4	Combative	Overtly combative or violent; immediate danger to staff
+3	Very agitation	Pulls on or removes tube(s) or catheter(s) or has aggressive behavior toward staff
+2	Agitated	Frequent nonpurposeful movement or patient–ventilator dyssynchrony
+1	Restless	Anxious or apprehensive but movements not aggressive or vigorous
0	Alert and calm	
−1	Drowsy	Not fully alert, but has sustained (more than 10 seconds) awakening, with eye contact, to voice
−2	Light sedation	Briefly (less than 10 seconds) awakens with eye contact to voice
−3	Moderate sedation	Any movement (but no eye contact) to voice
−4	Deep sedation	No response to voice, but any movement to physical stimulation
−5	Unarousable	No response to voice or physical stimulation

Procedure

1. Observe patient. Is patient alert and calm (score 0)?
   Does patient have behavior that is consistent with restlessness or agitation (score +1 to +4 using the criteria listed above, under DESCRIPTION)?
2. If patient is not alert, in a loud speaking voice state patient's name and direct patient to open eyes and look at speaker. Repeat once if necessary. Can prompt patient to continue looking at speaker.
   Patient has eye opening and eye contact, which is sustained for more than 10 seconds (score −1).
   Patient has eye opening and eye contact, but this is not sustained for 10 seconds (score −2).
   Patient has any movement in response to voice, excluding eye contact (score −3).
3. If patient does not respond to voice, physically stimulate patient by shaking shoulder and then rubbing sternum if there is no response to shaking shoulder.
   Patient has any movement to physical stimulation (score −4).
   Patient has no response to voice or physical stimulation (score −5).

The Richmond Agitation-Sedation Scale (Sessler et al., 2002).